LABYRINTH SEAL LEAKAGE ANALYSIS

A Thesis

by

GAURAV CHAUDHARY

Submitted to the Office of Graduate Studies of
Texas A&M University
in partial fulfillment of the requirements for the degree of

MASTER OF SCIENCE

August 2011

Major Subject: Mechanical Engineering

LABYRINTH SEAL LEAKAGE ANALYSIS

A Thesis

by

GAURAV CHAUDHARY

Submitted to the Office of Graduate Studies of
Texas A&M University
in partial fulfillment of the requirements for the degree of

MASTER OF SCIENCE

Approved by:

Chair of Committee,	Gerald Morrison
Committee Members,	J.C. Han
	H.C. Chen
Head of Department,	Dennis O'Neal

August 2011

Major Subject: Mechanical Engineering

ABSTRACT

Labyrinth Seal Leakage Analysis.

(August 2011)

Gaurav Chaudhary, B.E., Panjab University

Chair of Advisory Committee: Dr. Gerald L. Morrison

Seals are basic mechanical devices used in machinery to avoid undesired flow losses of working fluids. Particularly Annular seals are one of the most widely used in rotating machinery comprising turbines, compressors and pumps. Among all annular seals straight through rectangular labyrinth seals are the most commonly used ones. These seals provide resistance to the fluid flow through tortuous path comprising of series of cavities and clearances. The sharp tooth converts the pressure energy to the kinetic which is dissipated through turbulence viscosity interaction in the cavity. To understand the accurate amount of leakage the flow a matrix of fluid flow simulations carried out using commercially available CFD software Fluent® where all parameters effecting the flow field has been studied.

The carry over coefficient is found to be a function of the geometry and non-dimensional flow parameters of the labyrinth seal tooth configuration. Carry over coefficient increases with tooth clearance, tooth width and Reynolds Number. The variation with shaft speed does not follow a certain pattern always and varies with shaft speed.

The discharge coefficient of the first tooth has been found to be lower and varying in a different manner as compared to a tooth from a multiple cavity seal. The discharge coefficient of is found to be increasing with increasing tooth width. Rest of the variation is similar to carry over coefficient variation.

Further the compressibility factor has been defined to incorporate the deviation of the performance of seals with compressible fluid to that with the incompressible flow. Its dependence upon pressure ratio and shaft speed has also been established. Using all the above the mentioned relations it would be easy decide upon the tooth configuration for a given rotating machinery or understand the behavior of the seal currently in use.

DEDICATION

To Spiritual Leader Asaram Bapuji

ACKNOWLEDGEMENTS

I would like to express my sincere thanks to my committee chair, Dr. Gerald L. Morrison, for the wonderful opportunity of working under his guidance. His exhaustive knowledge and insight in the field of seals has been a constant source of inspiration and has provided invaluable assistance during the course of research. I would also like to express my gratitude to Dr. J. C. Han and Dr. H.C. Chen for being on my thesis committee and their support.

Special thanks to the Turbo Machinery Research Consortium for partially funding this research. I am proud to be a part of the Turbo Machinery Laboratory at Texas A&M University and would like to extend my warm regards to the faculty, staff and fellow researchers of the Turbo lab.

I thank my parents, sister and uncle for their unfettered support and encouragement during the entire course of my study. Individual thanks to the department faculty for making my time at Texas A&M University a wonderful experience.

I've also been fortunate to have a great group of friends at Texas A&M. This includes my office mates, Anand, Milind, Orcun, Ekene, Vamshi, Shankar, Abhay and Pranitha. Special thanks go to my many other friends, Vishal, Mohit, Navjit, Ankush, Aashish, Manish, Narottam and Praveen.

NOMENCLATURE

A - Clearance area, πDc

c - Radial clearance, m

C_d - Discharge coefficient for a given tooth

C_d^{1tooth} - Discharge coefficient for first tooth

D – Shaft diameter, m

h – Tooth height, m

L - Axial length of the seal, m

$\dot{m}$ - Mass flow rate of leakage flow (kg/s)

P_i – Tooth inlet pressure, Pa

P_e - Tooth exit pressure, Pa

Pr – Pressure ratio, p_e/p_i

Re – Reynolds number based on clearance, $\frac{\dot{m}}{\pi D\mu}$

s - Tooth pitch

w - Tooth width

x - Axial distance along seal, m

α - Flow coefficient

β – Divergence angle of jet, radians

γ - Kinetic energy carry over coefficient

ε – Dissipation of turbulent kinetic energy

κ –	Turbulent kinetic energy
μ–	Dynamic viscosity, Pa/s
ρ_i –	Fluid density at seal inlet, kg/m^3
ρ –	Fluid density at tooth inlet, kg/m^3
χ-	Percentage of kinetic energy carried over
ψ -	Expansion factor

TABLE OF CONTENTS

Page

Page

LIST OF FIGURES

Page

Page

Page

Page

LIST OF TABLES

Page

1. INTRODUCTION

High Speed Turbo-machinery is a major source for power production from high pressure and temperature fluid flow. Consequently sealing of these machines to decrease the flow losses has been a major engineering challenge since the inception of steam turbines by C.J. Parsons [1]. Currently, various kinds of seals are in use including lip seals, alternative elastomer and plastic seals, mechanical seals, clearance seals, magnetic fluid seals etc. Each seal has its own unique advantages and disadvantages.

From engineering viewpoint seals are used to introduce the friction in the fluid flow path to reduce the flow leakage. They do so in two ways on the basis of which seals can be subdivided into contact and non-contact seals. Though contact seals are always engineers preferable choice as they fully constrict the losses between two parts and thus increase the efficiency of the machine effectively as desired. However these seals are not suitable for relative high speed moving parts where contact forces not only degrade the rubbing parts but also possess excessive heat generation problem. Here non-contacting seals come in to play which help to create a resistance to fluid flow by extensive turbulence generation through tortuous flow paths as described by C.J. Parsons [1]. Among various non-contacting seals available, honeycomb and labyrinth seals are most commonly used seals.

This thesis follows the style and format of *Journal of Turbomachinery.*

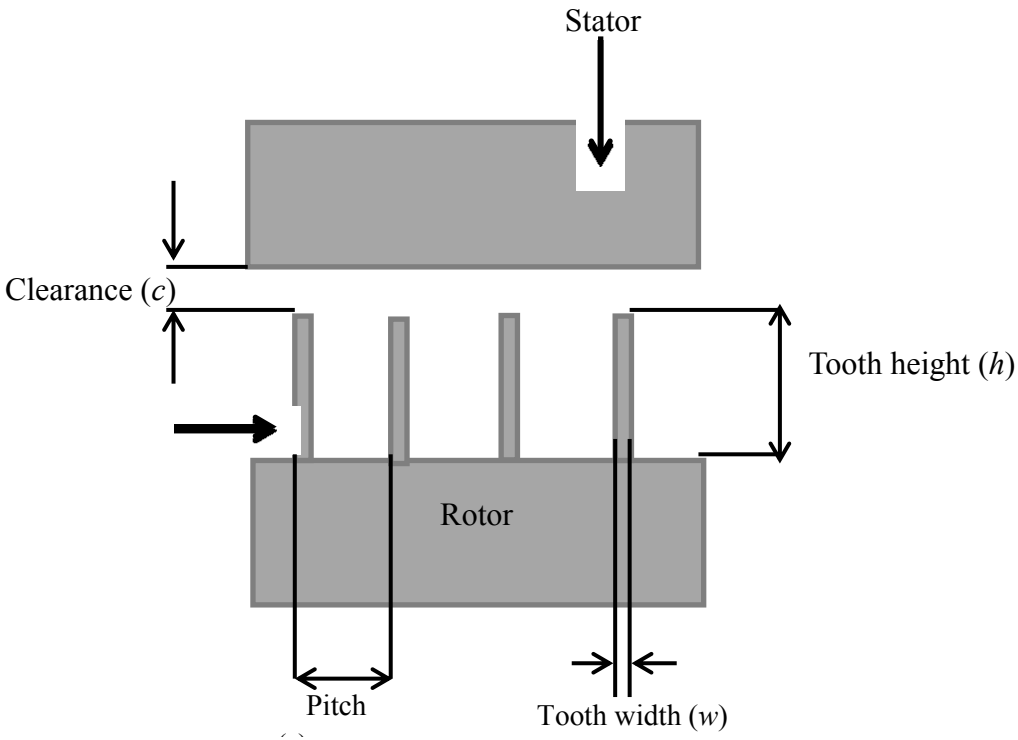

Fig 1.1 Labyrinth seal with tooth on rotor

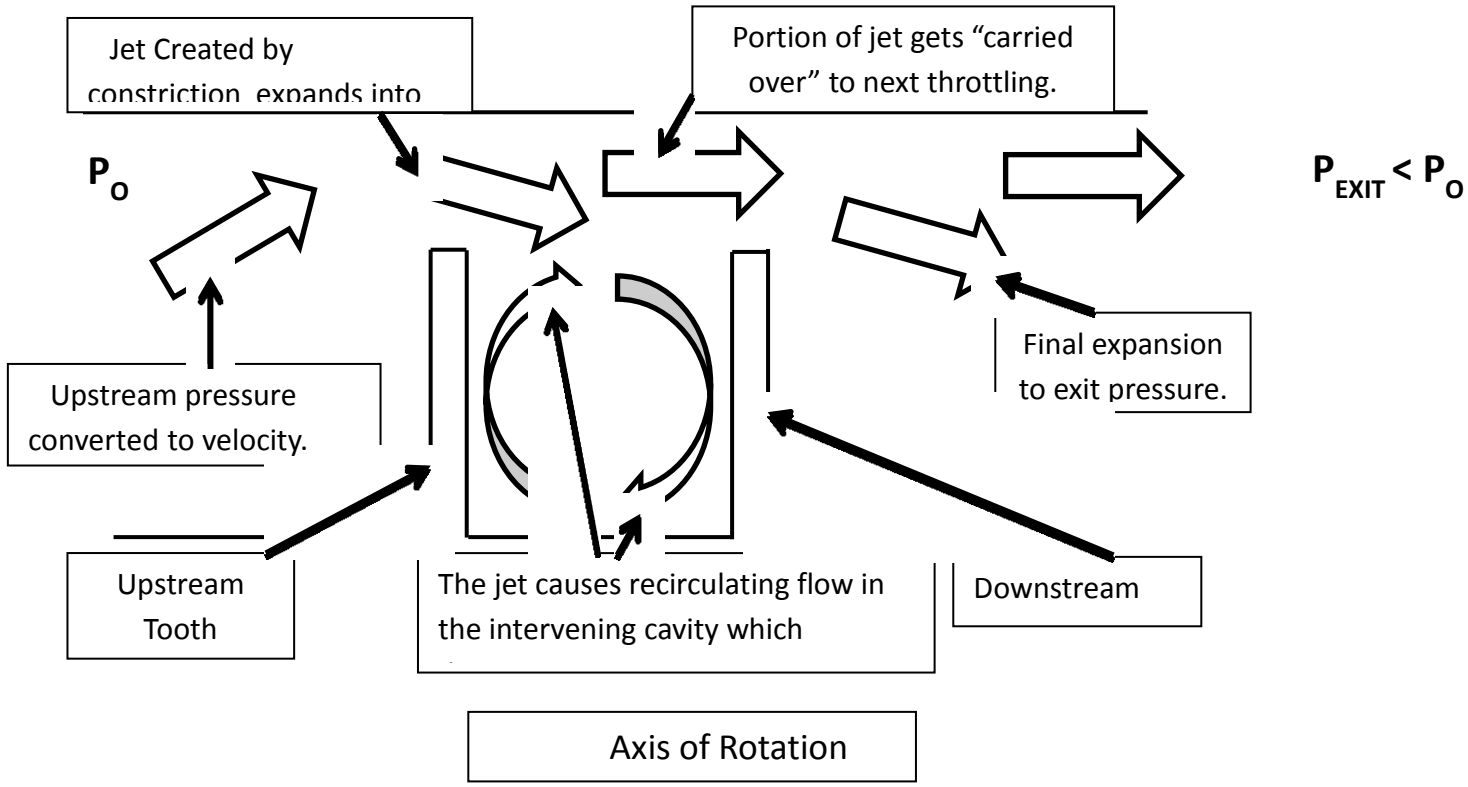

Fig 1.2 Figure sowing energy conversion of energy in labyrinth seal

Further labyrinth seals could be subdivided in to straight, stepped and staggered seals. On the basis of the tooth profile another sub-division could be done. Among all the above discussed seals straight through rectangular tooth labyrinth seals are the most popular type due to the ease manufacturing and effective sealing properties. These seals consist of a series of rectangular teeth over the length of a span of turbine blades or on the rotating shaft with cavities in between to dissipate the energy of fluid flow leakage as is shown in Figure 1.1. The sharp tooth clearance in geometry helps to increase the kinetic energy of the fluid flow by throttling and converting pressure energy to kinetic energy. Additionally it also create losses by generation of eddies and vena contracta effect. Further in the cavities fluid dissipate kinetic energy through turbulence-viscosity interaction. This has been shown in Figure 1.2. Thus effectively a labyrinth creates 3-D vortices in each chamber between two constrictions going all around the circumference of the rotating machinery.

Mathematically for the steady state operation of a Turbine (fixed RPM) the governing equations produce an elliptic problem with the governing equations described by basic conservation laws from thermal and fluid flow sciences. Due to this nature of the problem, various factors (geometry, flow and operating conditions) which constitute the boundary conditions need to be studied to determine the effect of each on the fluid flow leakage. The geometry of the labyrinth seal flow being one of those prominent parameters. Among various other factors affecting the labyrinth seal leakage are the fluid flow boundary conditions and the relative movement of the shaft.

During the last few years, the increasing demand for energy has fostered the development of more efficient turbo-machinery running at higher RPM's. This resulted with ever-tightening tooth clearances in labyrinth seals. The labyrinths currently in use have the ratio of the order of 1:100 (as compared to that of 1:1000 for fluid film bearings). On the other hand due to their undesirable rotor-dynamic characteristics they have raised concerns about rotor-dynamic stability of the rotating machinery. Since the better prediction of fluid leakage corresponds to improvement in determining fluid forces damping coefficients for rotor-dynamic calculation of a Turbine, labyrinth seals leakage flow needs to be determined more precisely. Additionally Childs and Thorat [2] have shown that the inertia of the fluid generally neglected in low speed rotor-dynamic calculation up to now, could no longer be done due to the inertia of the fluid flow at high speed of shaft rotation. This further emphasizes the need of accurate empirical formula for labyrinth seals leakage so as to improve bulk flow models used to better estimate the fluid damping coefficients in the study of rotor dynamics.

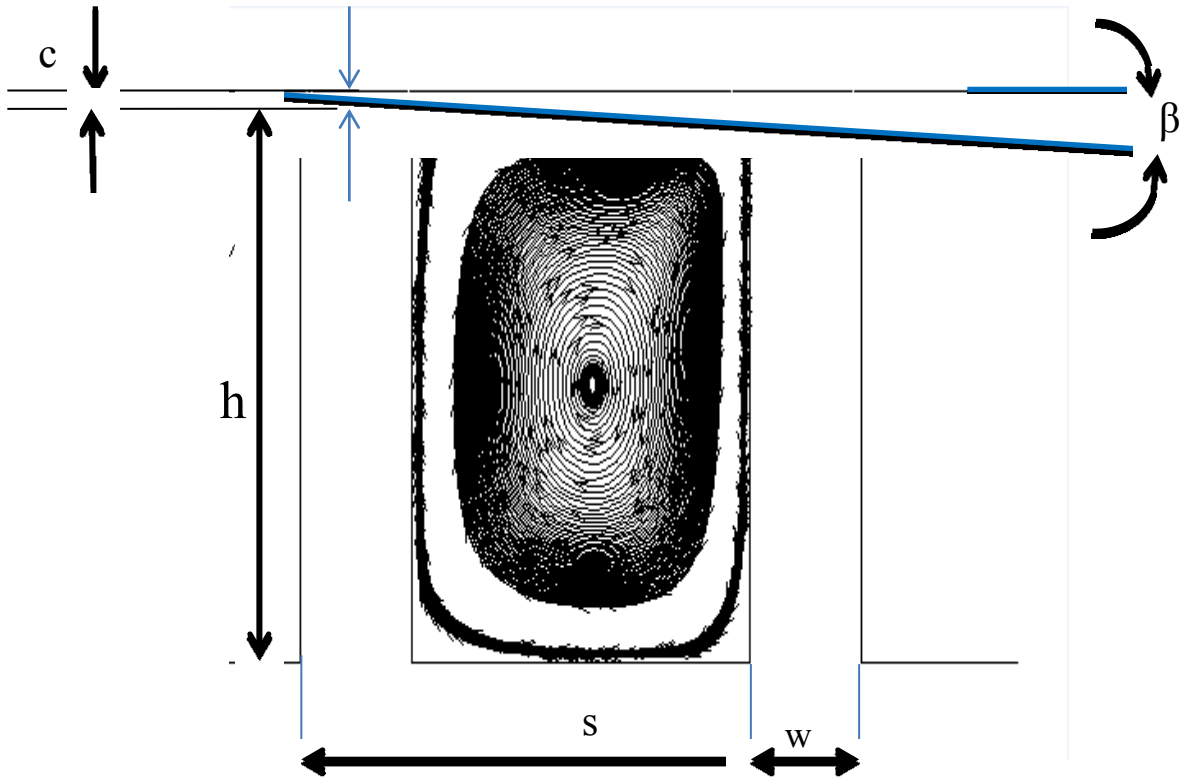

Fig 1.3 Flow pattern in a labyrinth seal cavity

Fluid flow pattern though a typical labyrinth seal has been shown above in Figure 1.3 using the streamlines. We could observe that a portion of fluid flows directly through the next constriction without involved in energy dissipation through eddy viscosity interaction while the other part goes for recirculation. This portion is further quantitatively defined by the terminology of angle β coined by Hodkinson [3].

The main parameters used to define the fluid flow loss characteristics through labyrinth seals are carry over coefficient and discharge coefficient. The carry over coefficient stands for energy dissipation in the cavity. It is related to the percentage of kinetic energy carried over to the next cavity by the following relation:

$$\gamma^2 = \frac{1}{1-\chi}$$

where the angle beta is defined by the relation:

$$\tan(\beta) = c\frac{1-\chi}{\chi\, s}$$

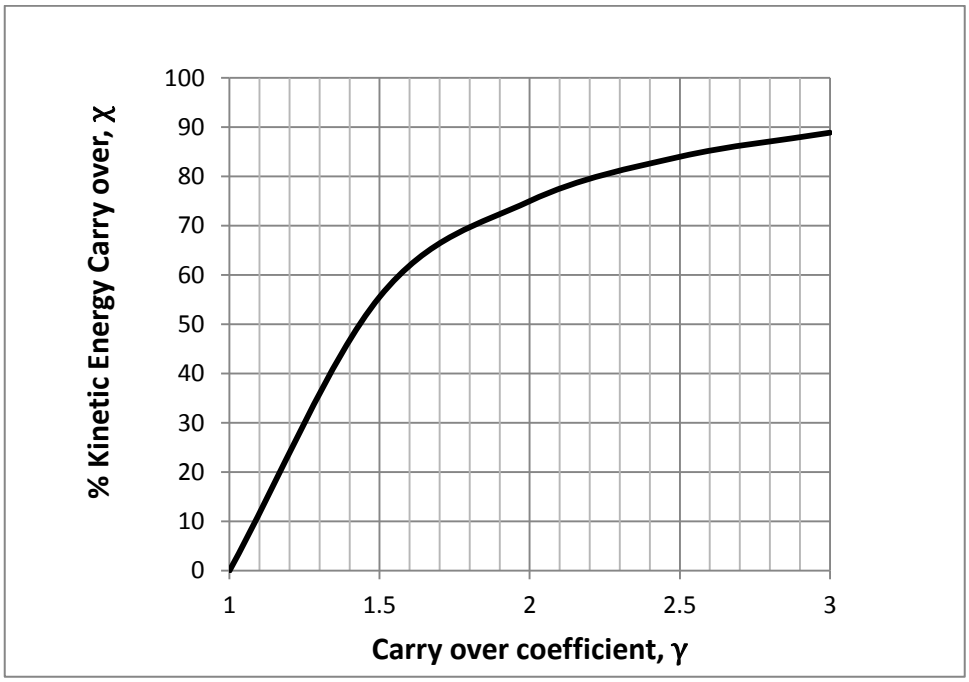

Fig 1.4 Figure showing the relationship between γ and χ

From the Figure 1.4 it is clear that the ideal value of carry over coefficient should be 1 which denoted the complete dissipation of the energy in the cavity. As the value of the angle beta goes higher than lesser is the dissipation of the energy. The discharge coefficient as usually denoted defines the flow losses through each constriction. It is somehow similar to the flow losses through the orifice plate but not exactly same due to the flow conditions being much different.

2. REVIEW OF CURRENTLY EXISTING LEAKAGE MODELS

The first paper to describe the labyrinth fluid flow was by Becker [4]. He modeled the fluid flow through labyrinth seals as Poiseuille flow with an attempt to find a coefficient of friction as to treat the flow as a simple annular flow. He observed that smaller decrease in clearance has a greater effect rather than changing the fluid flow path by varying tooth and cavity geometry.

Shortly after Becker [4] in another pioneering paper in 1908, Martin [5] proposed to treat the problem in an entirely different manner by considering labyrinth seals as a series of throttling process similar to the flow through a series of orifices. His approach was purely analytical with various false assumptions. He treated the pressure drop to be linearly varying and flow to be isothermal. Additionally he assumed the pressure across each constriction (tooth) to be very small or treated that the flow was always in sub-critical state throughout the labyrinth seal. He did not compare his equations against any experimental data. In the subsequent papers mostly all authors tried to address the wrong assumptions made by Martin [5] and improved his formulae.

Stodola [6] in his book on steam and gas turbines considered flow leakage through staggered and radial seals. He presented two separate equations to calculate flow leakage one each for subsonic and sonic respectively. He presented the experimental results on interlocking seals with clearances varying from 0.14 mm to 0.38 mm and pressure ranging from 43 to 143 psi. He carried out his experiments with a non-rotating shaft and thus neglected effects of shaft rotation on fluid flow leakage. He also assumed

that kinetic energy gets completely dissipated in the cavity and neglected the kinetic energy carry over coefficient. This leaded to a variation of about 14% in his formulas for calculating flow leakages. Additionally he also developed a graphical method for analyzing seals with varying areas those found in radial labyrinths.

Dollin and Brown [7] derived the Martin [5] analytical formulae for calculating the flow through labyrinth seals. They assumed the thermodynamic path function to be polytrophic (pv^k = constant) rather than isothermal and derived more general formula for fluid flow leakage. Martin leakage equation was a special case of their formula with k=1 and for the incompressible flow its value reduced to be k=∞. They also neglected the kinetic energy carry over coefficient.

Gercke [8] derived his equation by considering the variable area. He gave importance to kinetic energy carry over between throttling. He assumed that the flow through flow through each throttling was adiabatic and that through each cavity is isothermal with constant pressure process. He also took into consideration the occurrence of vena contracta and defined discharge coefficient but neglected the shaft rotation.

Elgi [9] made another major contribution to the fluid flow through labyrinth seals through his paper on labyrinth seals in 1935. He examined both staggered and see-through configuration of labyrinth seals theoretically and experimentally. His experiments included study for clearances in range of 15 to 40 mils. He used the same formula as stated by Martin [5] but used took in to consideration the occurrence of vena contract as the fluid goes through tooth clearances. He also considered the kinetic energy

carry over coefficient by defining a “carry-over” factor which he determined experimentally. Through experimental results and analytical study he also noticed that kinetic energy carry over coefficient decreases with increasing pitch between constrictions or by decreasing clearances. This effect could be attributed to the increases in the expansion of the jet emerging from tooth clearance in the subsequent cavity due to the above two factors. In non-dimensional he mentioned the result as a ratio clearance–to-pitch ratio. The variation of discharge coefficient with the variation of pressure ratio was also observed.

Keller [10] through his experiments analyzed the leakage quantitatively. He did experiments on flow of water and air through labyrinth seals. His results showed how the interlocking blade configuration has much better sealing properties as compared to see through seals. He neglected the effect of shaft rotation on the fluid flow and conducted tests in a non-rotating test rig having rectangular and rounded shape blades with clearances in the form of long rectangular strips rather than annuli.

Hodkinson [3] analyzed the leakage problem analytically rather than experimentally. He stated that a portion of jet leaving the clearances was intercepted by the next clearance without any energy loss. He defined this portion of fluid by using a parameter beta (β). He took this effect in to consideration in the Stodola equation for orifice coefficient. He also discussed the effects of eccentricity and rotational speed on seal leakage. From the results of his experiments he showed that eccentricity is more pronounces in laminar flow than in case of turbulent flow where flow could increase up to 2.5 times. His study included low RPM (not true for modern turbo machinery realm

where shaft speed could go up to supersonic) of machines where he showed that rotating shaft has nominal difference on leakage of fluid as compared to a stationary shaft from viewpoint of labyrinth seal leakage.

Bell and Bergin [11] assumed that the labyrinth seal constrictions to follow the flow field as through annular orifices. They mentioned few interesting observations made during experiments done on orifice meter. They mainly divided the fluid flow in two main categories based on the Reynolds number. For the lower Reynolds molecular viscosity is the main cause of losses for fluid flow. While for the high Reynolds number turbulent viscosity is the major factor to be considered responsible for fluid flow losses. An equation to take into consideration the eccentricity of the shaft is also mentioned by them. It was also observed that undesirable recovery of kinetic energy to pressure energy (reverse of throttling process) occurs for turbulent flow through thicker orifices but it does not occur smooth orifices. Further for higher Reynolds number flow wall friction factor also comes into play for thick orifices or wider tooth of labyrinth constriction. From the experimental readings for high Reynolds number it was claimed that undesirable pressure recovery due to the occurence of vena contracta starts from thickness-to-clearance (w/c) ratio of 1 and increases up to 6. Further increasing thickness makes wall friction to be more dominant and which reduces the flow leakage by creating pressure losses through shear stress losses at the boundaries of labyrinth tooth clearance flow field. Contrastingly for low *Re* flow pressure recovery does and occurs and only wall helps to create a pressure loss.

Kearton and Keh [12] performed experiments on single orifice with zero initial velocity. They determined the effects of pressure ratios on discharge coefficient. They also accounted for the compressibility of the fluid flow and used that in the correction for the for the leakage flow developed by Martin. However they neglected the kinetic energy carry over coefficients and avoided the rotation effect of the shaft on the fluid flow leakage. They did performed tests on a 14 throttle staggered labyrinth seals where their analytical formulae performed predicted flow leakage with a fair accuracy.

Zabriskie and Sternlicht [13] performed investigation on straight tooth labyrinth seals. They did not perform any experiments but used data gathered from previous studies. Their basic approach was to determine a friction factor and later correlate it with the seal geometry, mass flow rate and pressure ratio.

Heffener [14] use the formula given by Martin [5] and found the value of empirical data for Coefficient of discharge to take in to consideration the effects of wall losses and flow contraction at the throttling of the constriction. His neglected the kinetic energy carry over coefficient and the rotation effect of the shaft.

Komotri and Mori [15] treated the flow through constriction as adiabatic and entire leakage as isoenthalpic. They had n equations for n constrictions. These equations were solved together for finding the final function which is a function of carryover coefficient, number of teeth and thermodynamic process coefficient.

Rao and Narayanamurthi [16] took in to account the rotation of the shaft in their study of labyrinth seals. They performed experiments on two geometries: (1) 40 teeth seal with a pitch of 5 mm, (2) 20 teeth seal with pitch of 10 mm on a see through

labyrinth seals. The results from their experiments indicated that for a pressure ration in the range of 0.15 to 0.6 the leakage increases till the speed of 1100 rpm and decreases afterwards. This increment in the leakage was 4% for the 40 teeth as compared to the 10% increase for 20 teeth geometry.

From his investigations on labyrinth seals Stocker revealed the following facts about labyrinth seals. The data from his studies indicate that leakage decreased up to certain limit of surface roughness further roughness would tend to increase the flow leakage. Also he noticed that rotation of the shaft could affect the leakage up to 10%. Further he concluded that somewhere in between 50 to 70 degrees tooth angle leakage was minimum and pitch decreases for minimum leakage decreases with increasing tooth angle.

Deych [17] studied seals for steam turbine turbines. He conducted two experimental studies. In the first study he calculated leakage through seals as a function of pressure ratio and quality of steam. He did not consider the carry over coefficient for kinetic energy and for the kinetic energy carried over the next cavity.

Vermes [18] covered all the issues that were either missing or lacking in the previous papers discussed above. Martin's formula was adjusted for non-isothermal fluid flow with flow coefficients adopted from Bell and Berglein [11]. A further major correction was derived by considering boundary layer theory of Schiliting [19] in the kinetic energy carry over coefficient. His flow coefficient is a function of pitch, tooth width and clearance. His equations varied from experimental results by 5%.

Ahmed Gamal [20] further analyzed the above mentioned models and showed the variation of kinetic energy carry over coefficient. These results showed the fundamental dependence of the leakage problem upon factors other than geometry of labyrinth seals as expected from the elliptic nature of the governing equations for steady state flow.

Saikishan [21] discussed in his thesis how the variations of flow defining parameters are related to changing fluid flow characteristics. He did not consider the tooth on the rotating shaft seal nor the effect of that on the kinetic energy carry over coefficient.

3. COMPUTATIONAL FLUID DYNAMICS

3.1 Computational Method

The current research work is done using CFD simulations of fluid flow through labyrinth seals. The effect of rotation of shaft on the flow pattern through seals is studied by varying the shaft surface velocity from zero to slightly above Mach 1. Apart from this the effect of geometric shapes of the labyrinth seal geometry is also being studied while keeping tooth height to pitch ratio as 1 and varying another geometrical parameters. There are few assumptions made which have helped to reduce the computational effort in terms of time for the current research. These assumptions are:

1) The flow is axisymmetric which have helped to reduce the flow from three dimensional to two dimensional.

2) The variations in the shapes of the geometry of metal (due to thermal and fatigue stress) defining the fluid flow path is negligible compared to the length of the tooth clearances.

3) Fluid Surface interaction (FSI) has not been taken in to consideration to take into account the surface roughness of the seal geometry. Also impact of lateral surface vibrations due to dynamics of rotating shaft have not been considered to do negligible contribution to fluid turbulence intensity.

For the current turbulent flow simulations commercial solver FLUENT® has been employed to solve the fundamental governing equations of thermo-fluid sciences. The partial differential equation have been discretized using Finite-Volume Method and

turbulence flow modeled using standard k-ε turbulence model along with enhanced wall function in the near wall region flow to resolve viscous sub-layer without additional effort in terms of more refined mesh. The choices of current turbulence model to simulate the current fluid flow have been verified by Morrison and Al-Ghasem [22] by comparison with experimental LDA data by Morrison and Johnson [23]. More mathematical details about these models and wall function could be found in the following subsections.

Grid independence study was performed was using refined mesh till the outlet pressure difference value across the seal value stabilizes with increasing grid resolution for a given mass inlet flow rate and pressure at the inlet. Adaption of grid was based on pressure gradient set to a maximum value of 1 and Y^+ set as 5.

3.2 Governing Equations of Fluid Mechanics

The governing equations of fluid mechanics include the conservation laws for mass, momentum, and energy, which are usually, expressed using the Eulerian description. Mechanical and thermodynamic property constitutive equations are needed to close the close these system of equations. The momentum conservation law for Newtonian fluids is also known as the Navier–Stokes equations, where the stress tensor **T** is given by:

$$\mathbf{T} = -\left(\mathrm{p} + \frac{2}{3}\mu\,\nabla.\mathrm{v}\right)\mathbf{I} + 2\mu\,\mathbf{D}$$

where **μ** denotes the dynamic viscosity, **v** represents the velocity, **I** is the identity tensor, and D is the strain rate tensor

$$\mathbf{D} = \frac{1}{2}\left[\nabla \mathrm{v} + (\nabla \mathrm{v})^{\mathrm{T}}\right]$$

In the Navier–Stokes equations, the symmetric stress tensor T could be further decomposed into a volumetric stress tensor (−p**I**) representing the isotropic hydrostatic pressure and a deviatoric stress tensor τ which describes the anisotropic viscous forces

$$\tau = 2\mu\mathbf{D} - \frac{2}{3}\mu(\nabla . \mathrm{v})\mathbf{I}$$

The unsteady equations of mass, momentum, and energy conservation are given in equations below with the densityρ, body force per unit mass **g**, thermal conductivityλ, and energy source S_E. The energy conservation law is expressed in the form of total enthalpy h_{tot} to describe compressible flows.

$$\frac{\partial \rho}{\partial t} + \nabla . (\rho \mathbf{v}) = 0$$

$$\frac{\partial (\rho \mathbf{v})}{\partial t} + \nabla . (\rho\, \mathbf{v}\mathbf{v}) = -\nabla p + \nabla . \boldsymbol{\tau} + \rho\, \boldsymbol{g}$$

$$\frac{\partial (\rho h_{tot})}{\partial t} - \frac{\partial p}{\partial t} + \nabla . (\rho \mathbf{v} h_{tot}) = \nabla . (\lambda\, \nabla\, T) + \nabla . (\mathbf{v} . \tau) + \mathbf{v} . \rho \mathbf{g} + \mathrm{S_E}$$

These system of equations need to be solved for v, *p*, and h_{tot}. Further for calculation of *h* (Static enthalpy) we need to use the relation h = h_{tot} − (**v. v**)/2 where the kinetic energy contribution to total enthalpy is subtracted. Finally static temperature *T* can be computed using the caloric constitutive relation of *h = h (p, T)* which further simplifies to

$dh = c_p(T)dT$ for ideal gas behavior. Similarly, total temperature T_{tot} is calculated from h_{tot} using the similar relation, $dh_{tot} = c_p(T)dT_{tot}$. In addition, total pressure p_{tot} of ideal gas is evaluated with:

$$p_{tot} = p \exp\left[\frac{1}{R}\int_{T}^{T_{tot}} \frac{c_p(T)}{T}\, dT\right]$$

Finally to determine the density equation of state is required. For an ideal gas, this relationship is described by the ideal gas law

$$\rho = \frac{p}{RT}$$

3.3 Statistical Turbulence Models

Turbulent flow is characterized with random variation in temperature and velocity fields. These fluctuations cause further mixing of transport quantities such as momentum, energy etc. led to the fluctuations of these quantities. Alternatively these flows are often characterized with broad range of time and length scales fluctuating at high frequency which are computationally very expensive to simulate. Currently these kinds of flows are being commonly simulated with the following major turbulence models:

1) Reynolds Averaged Navier-Stokes Equations (RANS) equations.
2) Large Eddy Simulation (LES)
3) Direct Numerical Simulation (DNS)

The computational effort for these kinds of flows is increases from top to bottom. For the current research work we are using RANS equations which are derived from

perturbation method. In this approach all the flow variables are considered to be constituting of average and variable quantity.

$$u_i(x_i, t) = \overline{u_i}(x_i) + u_i'(x_i, t)$$

where $$\overline{u_i}(x_i) = \lim_{T \to \infty} \frac{1}{T} \int_0^T u_i(x_i, t)\, dt$$

here T is the time period over which the flow variable is averaged. Due to the unsteady flow ensemble averaging is used. The basic idea behind ensemble averaging is to consider set of flows where all the variables such as energy, velocity are identical but initial conditions are varied. The mathematical definition for this kind of averaging is:

$$\overline{u_i}(x_i, t) = \frac{1}{N} \sum_{n=1}^{N} u_{ni}(x_i, t)$$

where N stands for number of observations considered to accomplish the average. By decomposing the fluid variables into averaged and fluctuating components, for example, velocity v = v + v′ , the original Navier–Stokes equations are modified, resulting in the Reynolds Averaged Navier–Stokes (RANS) equations. The momentum and enthalpy transport equations thus contain turbulent flux terms adding to the molecular diffusive terms. These additional turbulent fluxes are called Reynolds stress ρ v′ v′ and Reynolds flux ρ v′ h′ , respectively. Turbulence models based on the RANS equations are known as statistical turbulence models due to the statistical averaging procedure. The equations used to model the Reynolds stresses and Reynolds fluxes define the type of turbulence model.

Eddy viscosity turbulence models are used in the current work. The eddy viscosity hypothesis assumes that the Reynolds stresses can be related to the mean flow

and turbulent viscosity μ_t in a manner analogous to molecular viscosity μ in laminar flows. In other words, the turbulent effect can be represented as an increased viscosity with the effective viscosity $\mu eff = \mu+\mu_t$.

3.3.1 K-ε Turbulence Model

It is a type of eddy viscosity model based on analogy between laminar and turbulent flows based on Boussinesq hypothesis. The central idea of this model is that turbulent flow stresses behave similar to laminar fluid stresses which follow stokes law. Mathematically it could be written as:

$$laminar \begin{cases} \tau_{ij} = \mu \left(\frac{\partial u_i}{\partial x_j} + \frac{\partial u_j}{\partial x_i}\right) - \frac{2}{3}\,\mu\,\delta_{ij}\frac{\partial u_j}{\partial x_j} \\ q_i = \frac{k}{c_p}\,\frac{\partial T}{\partial x_i} \end{cases}$$

$$turbulent \begin{cases} \tau_{ij}^t = \overline{\rho u_\iota u_j} = \mu_t \left(\frac{\partial U_i}{\partial x_j} + \frac{\partial U_j}{\partial x_i}\right) - \frac{2}{3}\,\delta_{ij}\rho k \\ q_i^t = -\overline{\rho u_\iota T} = \frac{k_t}{c_p}\,\frac{\partial T}{\partial x_i} \end{cases}$$

Here:

1) μ_t = Turbulent Viscosity

2) k = Turbulent Kinetic Energy

3) k_t = Turbulent conduction effect

All the above enlisted quantities are not inherent fluid properties but defined by fluid flow. In the k-ε turbulence model these properties are calculated by using by two transport equations one each for Turbulent Kinetic Energy (k) and turbulent kinetic energy dissipation rate (ε). The former transport equation is derived analytically from momentum equation with the velocity and using Reynolds Averaging Technique as described above, while the latter is an empirically derived equation as suggested by Pope [27].

$$\frac{\partial(\rho\kappa)}{\partial t} + \frac{\partial(\rho\kappa u_j)}{\partial x_j} = \frac{\partial}{\partial x_j}\left[\left(\mu + \frac{\mu_t}{\sigma_k}\right)\frac{\partial\kappa}{\partial x_j}\right] + G_k + G_b - \rho\varepsilon - Y_M + S_k$$

$$\frac{\partial(\rho\varepsilon)}{\partial t} + \frac{\partial(\rho\varepsilon u_j)}{\partial x_j} = \frac{\partial}{\partial x_j}\left[\left(\mu + \frac{\mu_t}{\sigma_\varepsilon}\right)\frac{\partial\varepsilon}{\partial x_j}\right] + C_{1\varepsilon}\frac{\varepsilon}{k}(G_k + C_{3\varepsilon}G_b) - C_{2\varepsilon}\,\rho\frac{\varepsilon^2}{k} + S_\varepsilon$$

where:

1) G_k denotes the generation of turbulence kinetic energy from main flow field due to mean velocity gradients. It is defined as:

$$G_k = -\overline{\rho u_i' u_j'}\,\frac{\partial u_j}{\partial x_i}$$

2) G_b defines the generation of turbulence due to buoyancy. It is calculated using the expression mentioned below:

$$G_b = \beta\, g_i\, \frac{\mu_t}{Pr_t}\,\frac{\partial T}{\partial x_i}$$

3) Y_M represents the contribution by dilation to the overall dissipation rate in compressible fluid flow. It is calculated using the expression below:

$$Y_M = 2\rho\epsilon M_t^2$$

4) σ_k and σ_ε are the turbulent Prandtl numbers for κ andε , and have default values of 1.0 and 1.3 respectively. $C_{1\varepsilon}$ and $C_{2\varepsilon}$ are constants with default values of 1.44 and 1.92. For this research these default values have been used.

4. RESEARCH OBJECTIVES

This work is aimed at understanding the effect of different parameters on the fluid flow leakage through labyrinth seals with the tooth mounted on the rotor. As mentioned earlier in this study we will explore the labyrinth tooth rectangular in shape and mounted on rotor. This study deals with exploring the effect of all the variables (including the flow parameters, geometry dimensions and moving boundaries) suspected to determine the carry over coefficients and discharge coefficients of a given labyrinth seal under consideration. Broadly it could be said that it comprises of the following main three tasks.

Firstly effect of flow parameters on the carry over coefficient was studied. This is done in a procedural manner starting from the effect of non-dimensional flow field parameter i.e. Reynolds Number. It is calculated for the current research study using the formulae mentioned below.

$$Re = \frac{\dot{m}}{\pi D \mu}$$

Further from this relation we conclude that, for a give shaft diameter

$$Re \sim \dot{m}$$

Also since $$\dot{m} = \rho \, \pi \, D \, c \, u_{axial}$$

So from using the above mentioned two equations we deduce that:

$$Re = \frac{\rho c \, u_{axial}}{\mu}$$

or $$Re \sim c \, u_{axial}$$

To explore the effect of Reynolds number same geometry (at a given shaft RPM) is considered at different Reynolds Numbers. After that, the effect of geometrical parameters including the tooth clearance to the pitch (c/s) ratio and the effect of tooth width to pitch (w/s) is studied. Both these calculations are achieved by choosing different cases with same geometrical lengths (except clearances and tooth width) are studied for different Reynolds Numbers. Finally, effect of shaft RPM on the carry over coefficient was studied by varying the shaft speed for fixed Reynolds number and geometry.

Secondly, the effect of various parameters on discharge coefficient was evaluated using the same procedure as above. Here, the study mainly bifurcated into two different cases 1) for the first tooth of labyrinth seal 2) for the tooth having cavity prior to them. This division was done after considering the difference in the discharge coefficient of first teeth from the rest of the labyrinth seal tooth.

The third task comprised of determining the effect of various conditions considered above on the expansion factor. This factor is introduced to predict the deviation in the behavior of seals with compressible fluid as compared to the one with incompressible fluids.

5. COMPUTATIONAL METHOD

The current research work has chosen the path of CFD methodology to study the Labyrinth seal fluid flow. Further, in the present study the flow field has been simplified from three dimensional to axisymmetric two dimensional. This replication of 3D leakage characteristics from 2D turbulent flow within acceptable accuracy has been proven by various other research studies including that by Stoff [24] on labyrinth seals. This saves considerable time and effort required for expensive experimental methods. These simulations are used primarily to study the factors affecting kinetic energy carry over coefficient and discharge coefficient for the fluid flow leakage through labyrinth seals. Furthermore, various others factors have been studied to show their variance with the changing geometrical and fluid conditions.

Fluent® is finite volume discretization based CFD solver used lot solve the Navier Stokes simulation. For this study, standard k-ε turbulence model has been used to solve the turbulent fluid flow field. The applicability of this model to accurately simulate the flow field has been studied by Morrison and Al-Ghasem [22]. The study mentions the similarity between labyrinth seal flow patterns obtained using k-ε modeling and the experimental data from Laser Doppler Anemometry (LDA) performed by Morrison and Johnson [23]. More details about the turbulence modeling have been mentioned in the previous section.

Gambit has been used as a preprocessor to generate the meshes required for the current simulations. Rectangular grid cells have been used for the current flow field as

shown in the Figure 5.1. It has been ensured in each simulation that the Y^+ value remains below 5 to resolve the laminar sub layer as shown by Al-Ghasem [22]. This has been accomplished through further refinement in the near wall region as shown in the Figure 5.1 below.

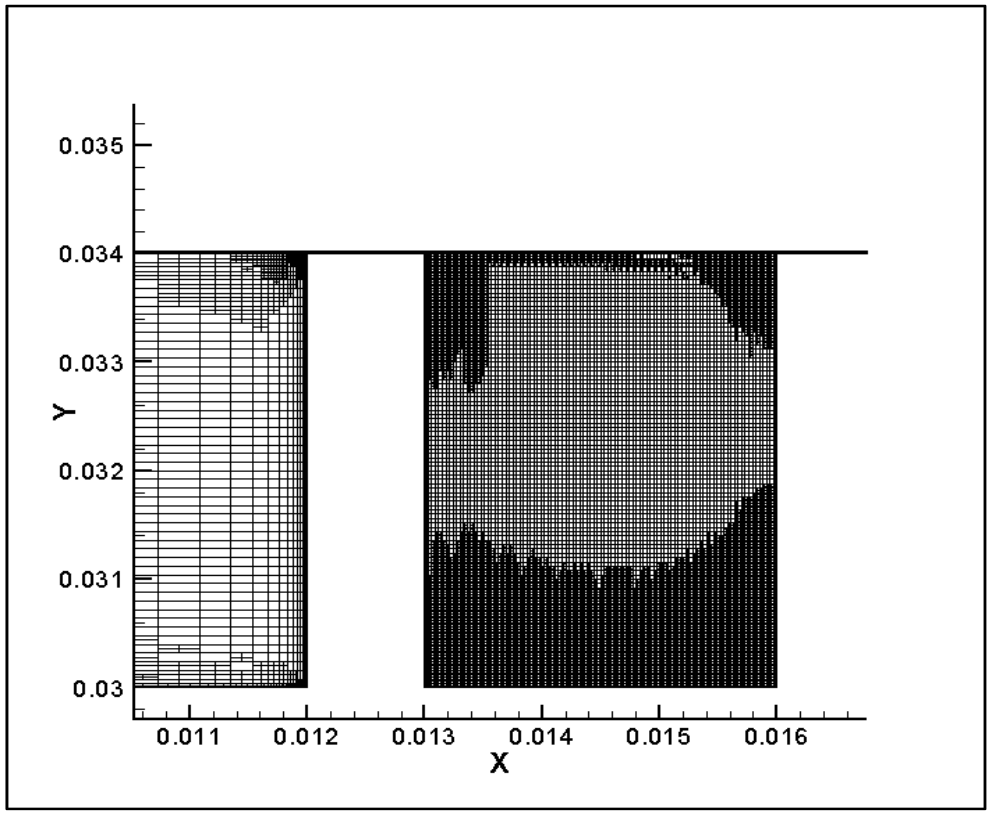

Fig 5.1 Meshed labyrinth seal geometry

Regarding the modeling in the near wall region in conjugation with k-ε model (which has been developed for free turbulence) a separate model needs to be defined. The standard wall function does not sufficiently resolve the viscous sub-layer, and is not very effective when the wall is moving rapidly or when there are high pressure gradient effects. Ideally the wall Y+ values should be below 1. Furthermore it has been suggested by Morrison-Al Ghasem [22] to use enhanced wall treatment in conjugation with standard k-ε model to accurately simulate the boundary layer flow with pressure gradients into consideration. The enhanced wall treatment is necessary to capture flow characteristics accurately in the viscous sub-layer next to the wall with lesser grid nodes. For this model Fluent allows wall y+ values as large as 5 given the first layer of the mesh lie in the viscous sub-layer.

Grid independency of the results has been confirmed using adaption based on pressure gradients. The pressure difference along a generic labyrinth is calculated by decreasing the pressure gradients value in the Adaptive Gridding Algorithm in each successive simulation till the pressure becomes independent of further refinement. In this process pressure gradient has sometimes even been reduced to 1 for some of the cases of incompressible fluid flow. A sample of the variation of checking grid independency in a simulation has been shown in the Figure 5.2 below. Here the grid refinement has been stopped after the pressure difference becomes constant for a given mass flow rate.

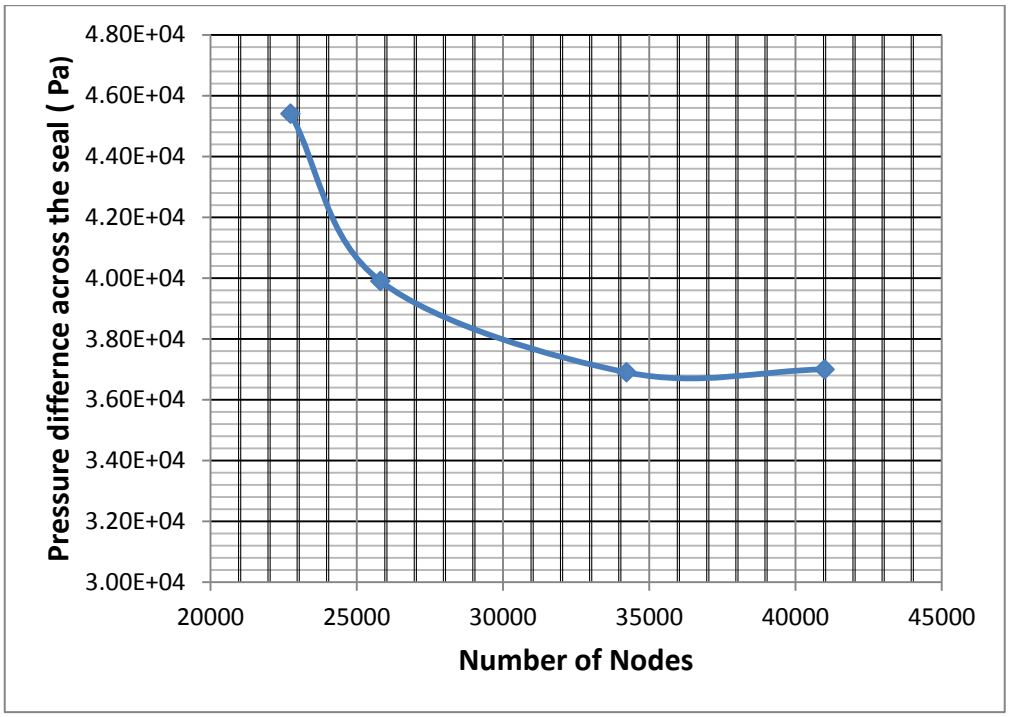

Fig 5.2 Convergence of the simulation with decreasing pressure gradient

6. CARRY OVER COEFFICIENT

6.1 Introduction

The carry over coefficient is used to measure the effectiveness of the cavity in terms of flow losses. This factor is used to measure how much of the actual amount of the kinetic energy before the start of the cavity is actually dissipated through turbulence dissipation. The lower the carry over coefficient is the more effective is the seal. Ideally the desired value of the coefficient is one but it cannot be achieved due to the presence of the energy spectrum in of turbulent flow field. More details about this can be studied in a book on turbulent flow. The current work uses the definition proposed by Hodkinson [3] to calculate the carry over coefficient. The relationships provided are as mentioned below:

$$\gamma^2 = \frac{1}{1-\chi}$$

$$\tan(\beta) = c\frac{1-\chi}{\chi\, s}$$

The angle beta (β) is used to define the mean streamline separating the recirculation zone from the fluid that passes over directly to the next clearance. In other words, this streamline is virtually acting as mass and energy transfer boundary between the recirculation zone and the mean flow field. This angle is calculated in the study using the post processing software Tec plot 360®. The required point is found by examining the point of zero velocity inside the cavity on the downstream tooth. However, in cases where the Taylor number to Reynolds number ratio is large, it is relatively hard the find

the point where the flow velocity becomes zero before the cavity wall as shown in the Figures 6.1 and 6.2 below. These conditions are particularly present for the cases with

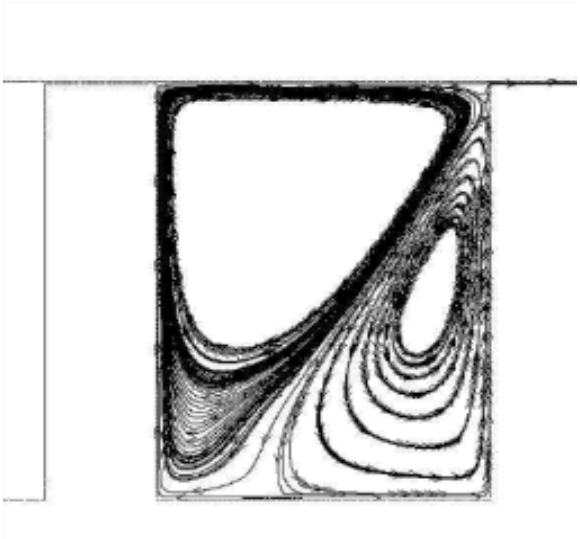

Fig 6.1 Streamlines for case with high (Ta/Re) ratio

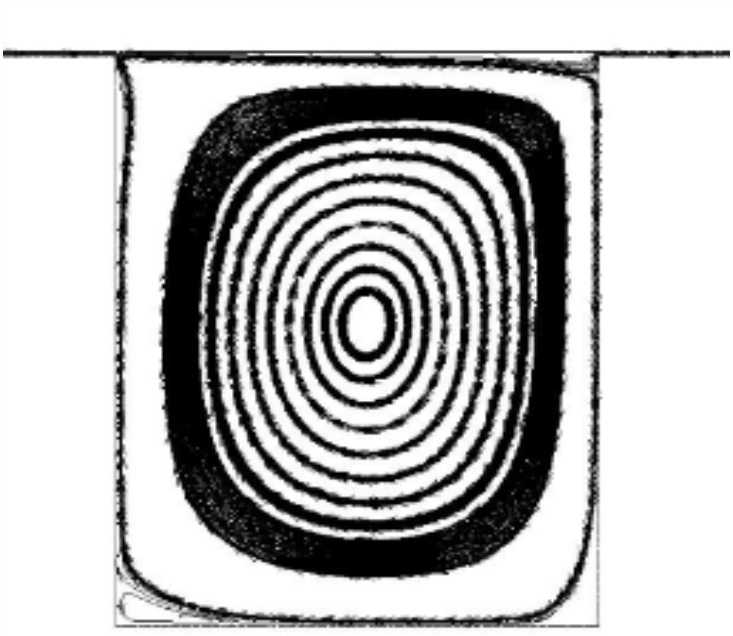

Fig 6.2 Streamlines for case with low (Ta/Re) ratio

high Taylor numbers. This occurrence of two vortices is confirmed by Demko [25] in his thesis on Labyrinth seals with the tooth on rotor configuration.

The labyrinth seal flow in the current study is an elliptic problem as mentioned in the introduction. Thus all the flow parameters used to characterize the given flow field under consideration are in general effected by both boundary conditions of the flow field and the geometry of the labyrinth tooth. The effect of both these parameters on the carry over coefficient has been investigated in a systematic manner. Firstly, the flow conditions are varied for the fixed geometry and later the geometry has been varied with different geometrical ratios. Finally, the shaft RPM has been varied in steps to increase the surface velocity from no rotation to slightly higher than Mach1.

6.2 Effect of Flow Parameters

In this subsection the effect of flow parameters on the kinetic energy carry over coefficient are studied. To study this effect, all other geometric conditions are kept the same or in other words, the same the geometry is used throughout this study. Further, the water and air case are being considered separately to observe the effect of compressibility on all the carry over coefficients. In this subsection we will present all the results using water as the fluid flowing through the seal geometry. To evaluate the effect of compressibility in the results obtained, we will introduce another factor compressibility, which will show the difference between behaviors of seal for two different fluids.

6.2.1 Reynolds Number Variation Effect on the Carry over Coefficient

Once the seal geometry has been set, the Reynolds number is varied to study its effect on the carry over coefficients. To investigate this effect, geometry G4 (s=4, h=4, c=0.15, w=0.03) (all dimensions in mm) is chosen. This choice is purely random and any other geometry could be considered but their results won't be necessarily the same which will be considered in later subsections where the effects of geometry on carry over coefficient are analyzed.

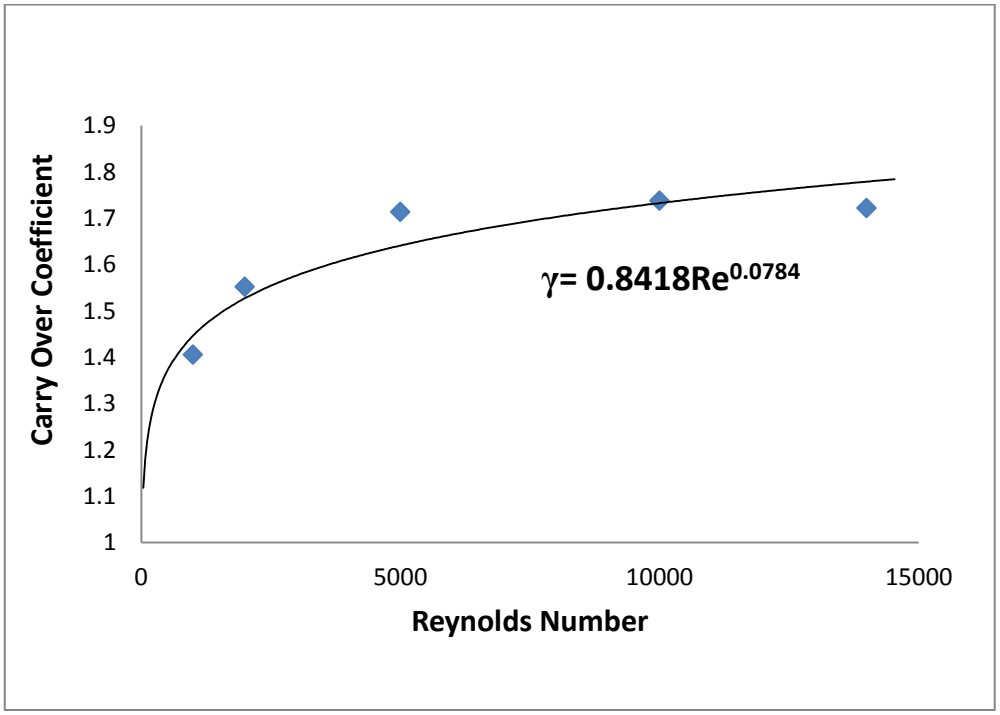

Fig 6.3 Variation of γ with Re for G4 (W_{sh} =0, water)

From the Figure 6.3, it is observed that the variation of the carry over coefficient varies with the value of Reynolds number. This result confirms that the carry over coefficient is a function of Reynolds Number (which was neglected in many previous studies on labyrinth seals, including that of Hodkinson [3] and Gamal [20]). Additionally, this variation seems to be similar to the case of tooth on stator as studied by Saikishan [21] and can be explained as follows. At high Reynolds number, the inertia of the fluid flow coming from the wall jet, generated by seal tooth does not have much time before it encounters the next clearance. In other words, given two fluid particles moving at different axial speeds but similar radial velocities, the one moving slowly will have more time to traverse downwards into the cavity than the other having more velocity. This leads to a larger beta angle (β) as shown in the Figures 6.4 and 6.5 below.

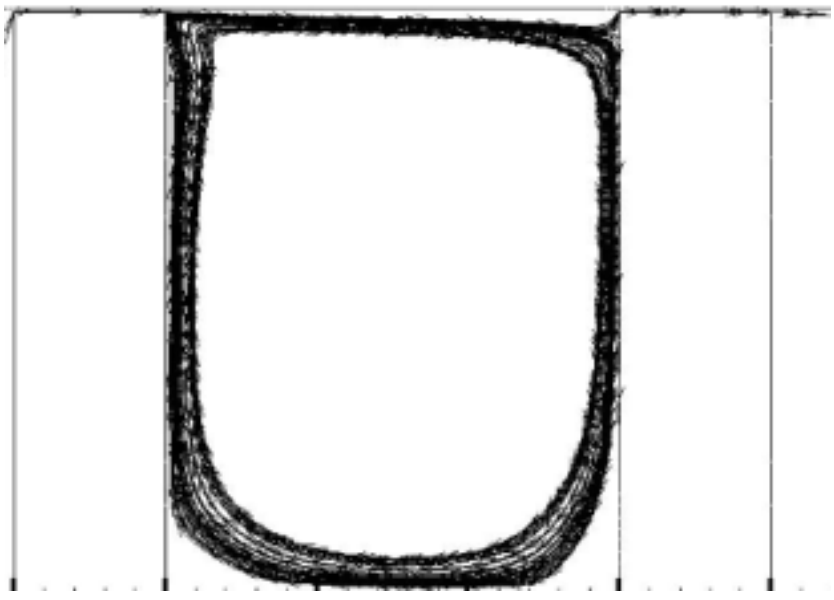

Fig 6.4 Water case with Re=1000 (G2, W_{sh} =0)

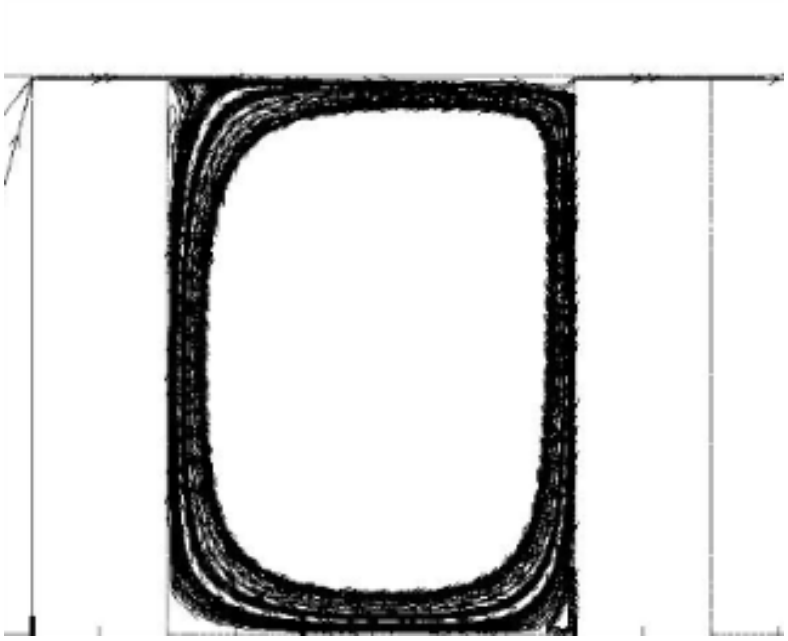

Fig 6.5 Water case with Re= 2500 (G2, W_{sh} =0)

The results are quite obvious since this case has been presented for zero shaft speed. Moreover, a sharp variation in the carry over coefficient as the Reynolds number increases from 1000 to 2000 is observed and after that the changes become more gradual because of the change of fluid flow field with increasing Reynolds number is lesser where other factors also comes into consideration. This shows that the there is a need to study the effect of changing other parameters such as the shaft speed once a geometry and Reynolds Number has been fixed upon.

6.3 Effect of Geometrical Parameters on the Carry over Coefficient

6.3.1 Effect of Clearance on Carry over Coefficient

From the literature review it has been established that clearance has a major effect on the labyrinth seal leakage. Since Hodkinson [3], Saikishan [21] and Gamal [20] had used the non- dimensional form of this clearance as c/s to analyze its effect, the same parameter will be used in the current research work Furthermore, this non-dimensional parameter makes it easier to compare and evaluate the results. In this study, we will compare different seals with the same pitch but different clearances.

The results of the comparison can be seen in the Figure 6.6. A power law has been generated in the Figure 6.6 for each set of the different clearance to pitch ratios. From the Figure 6.6 it is can be seen that there is a great jump in the carry over coefficient with the corresponding changes in the clearances. The carry over coefficient reduces 1.6 times (from 1.8 to 1.1) by decreasing the clearance to pitch ratio by 80% (from c/s = 0.0375 to c/s = 0.0075) at a Reynolds number of 16000. Further, this decrease in carry over coefficient is fully dependent on the Reynolds number as is seen from graph. The value of γ increases by 21% by increasing the value of clearance by a factor of 2.5 at the Reynolds number of 15000. The observation of increasing carry over coefficient with increasing c/s ratio can also be explained from the hypothesis of Hodkinson [3]. In his theory, Hodkinson [3] has stated “For a given divergence angle a higher value of pitch results in a higher impingement point of the jet on the downstream tooth”. This results in a small portion of fluid flowing to the next clearance resulting in

decrease of γ. Therefore an increase of c increases γ or in other words increment in c/s ratio increases the carry over coefficient. Note that as γ increases, the amount of kinetic energy dissipated in the seal cavity decreases indicating a seal design that is less effective at reducing leakage. It has to be noted that, in order to make physical significance the carry over coefficient should approach 1 as Re approaches 0. This has been further confirmed by the Figure 6.6.

6.3.2 Effect of Tooth Width on the Carry over Coefficient

In the earlier subsections, the variation of the carry over coefficient with the clearance to pitch ratio and Reynolds Number for incompressible flow was examined. However, the other geometrical constants including the tooth width had been fixed. This is not always true in the real applications of the labyrinth seals. Here the effect of this parameter on the carry over coefficient will be analyzed which will provide a better insight in the variation of flow field while changing tooth width. The current study

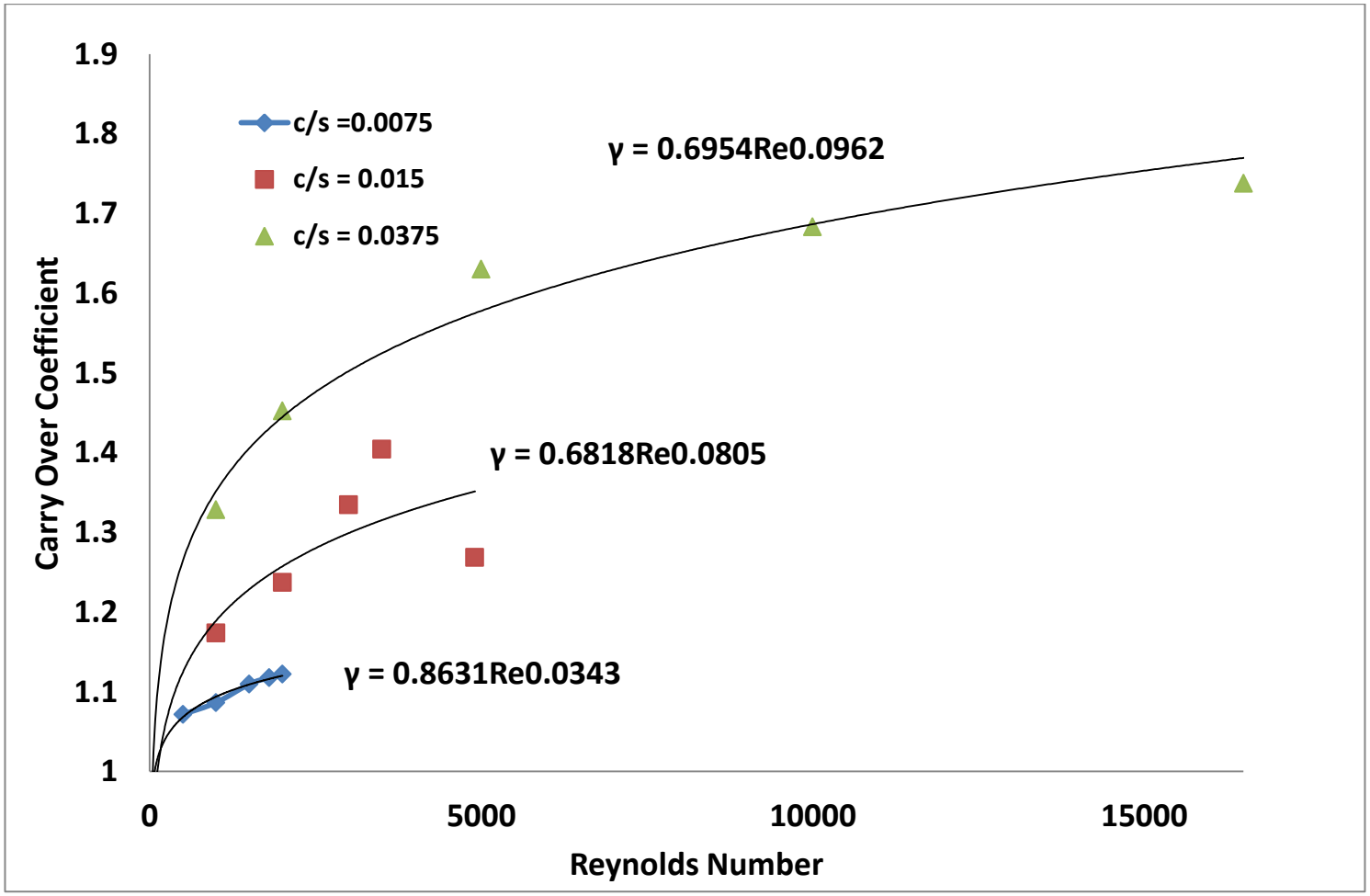

Fig 6.6 Variation of γ with Re for different c/s ratios, water

includes comparison between two flow fields having the same Reynolds Number and geometrical parameters (except the tooth width) for the flow field. The cases chosen for the current evaluation are from geometry G1 and G2 with c/s ratio of 0.0075 and tooth width increment from 0.03 mm to 1 mm using water as the working fluid.

It can be observed from the Figure 6.7 that the variation of the carry over coefficient with the tooth width is almost negligible until the Reynolds number is below 700 but increases exponentially after that. This increment could be attributed to the fact that the axial distance to be travelled by the fluid element in the cavity is less for the geometry with a thicker tooth than those flowing in a comparatively less tooth width. Therefore the corresponding changes in the carry over are in the reverse order of the increment in tooth width. This becomes clear referring back to the following formulation of the Hodkinson [3] for the carry over coefficient. The formula he used for the carry over coefficient formulae is as mentioned below.

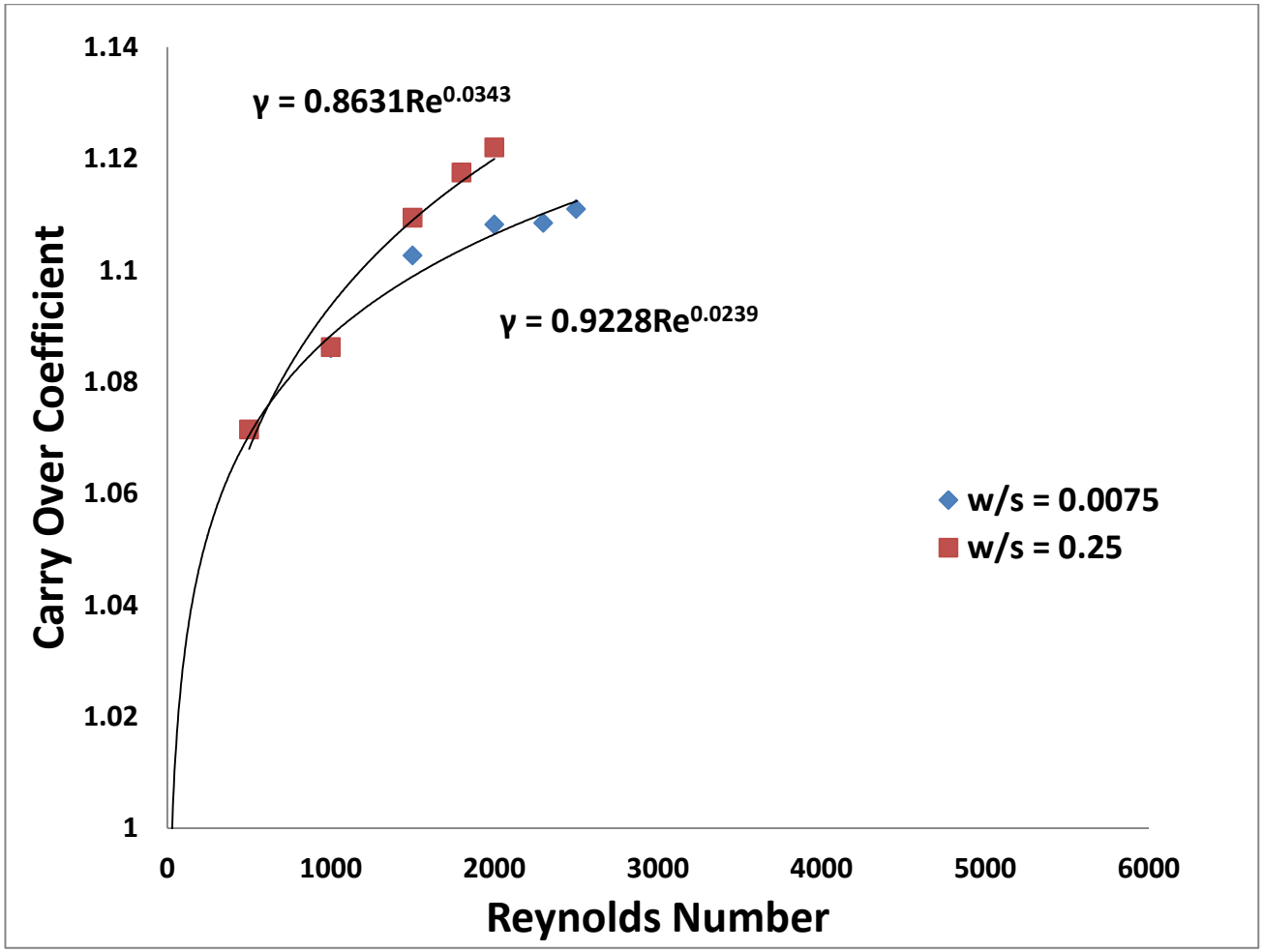

Fig 6.7 Variation of γ with Re for different w/s ratios, water

$$\gamma = \sqrt{\left(\frac{1 + \tan(\beta)\ \left(\frac{s}{c}\right)}{\tan(\beta)\ \left(\frac{s}{c}\right)}\right)}$$

Since the c/s ratio is constant for the above comparison we could replace this factor with a constant k which further simplifies the above equation in the following expression as mentioned below.

$$\gamma = \sqrt{\left(\frac{1}{\tan(\beta)\ k} + 1\right)}$$

Thus from the above expression one can conclude that with increase of beta angle (β) the carry over coefficient decreases. One more quick observation can be made from the above expression is that; ideal flow field should have the angle β value of 90^0 for maximum energy loss to occur.

6.3.3 Effect of Pitch on the Carry over Coefficient

Traditionally, pitch has been chosen to be the factor to non-dimensionlize the geometrical features of a given labyrinth tooth configuration including clearance, tooth width and tooth height. This choice has been validated in many research works including that done recently by Saikishan [21]. Increasing the pitch for the same clearance will

decrease the carry over coefficient. This result should be opposite for increasing of clearance with fixed pitch. Also this change should be more prominent at high Reynolds numbers. The same effect is expected to be observed with the tooth width. The carry over coefficient value should decrease with the increase in the tooth width and this effect should also be more prominent with higher Reynolds number.

6.3.4 Effect of Shaft Speed Variation on Carry over Coefficient

Completing the analysis of observing the effect of flow parameters (i.e. Reynolds Number) and geometrical parameters (non-dimensional) parameters on carry over coefficient we study variation of carry over coefficient with changing speed of rotating boundary condition.

The rotation of shaft creates an additional introduction of swirl velocity. This makes it important to study effect of shaft speed on carry over coefficient. The effect of swirl velocity on the instability of the flow field is also defined by Taylor Number. To compare the effects of shaft speed, the forces involved in the variation of carry over coefficient must be considered.

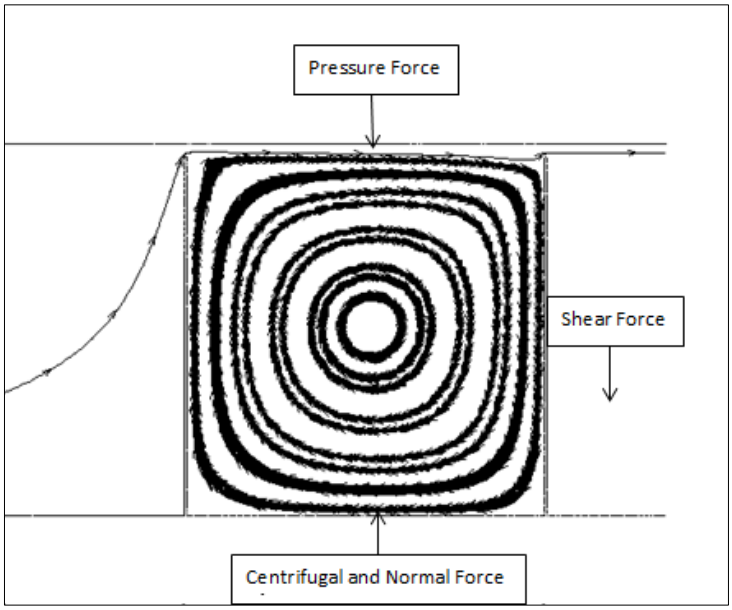

Fig 6.8 Forces on the fluid in the cavity along the radial direction, First cavity

From Figure 6.8 the major forces affecting the angle β which is used in our definition of carry over coefficient can be observed. Effect of these forces on carry over coefficient could be summarized as mentioned in Table 1below.

Table 1 Variation of Cavity Forces

Forces	**Effect on flow angle β**	**Effect on Carry over Coefficient γ**
Centripetal Force	Decreases	Increases
Pressure Force	Increases	Decreases
Shear Force	Increase	Decreases

For the fluid in the cavity (separated from the main flow by mean streamline) to be balanced normal force and centrifugal force should be equal to pressure and shear forces (here it refers to additional shear acting on the fluid in the cavity due to the rotation of the shaft). Since we are changing shaft speed in well-defined intervals, further discussion shifts to variation of pressure and shear forces as compared to centrifugal force. In other words we are comparing the rate of changes of shear and pressure forces effectively as compared to changes in the centrifugal forces. First cavity of geometry G1 will be used to explain the effects for each different RPM. From the Figures (6.9,6.10 &6.11) it can observed that for a low Reynolds number, changes in pressure force and shear forces are initially more than the increment in the centrifugal forces for low shaft RPM as indicated by carry over coefficient till their increment is same as the centrifugal forces.

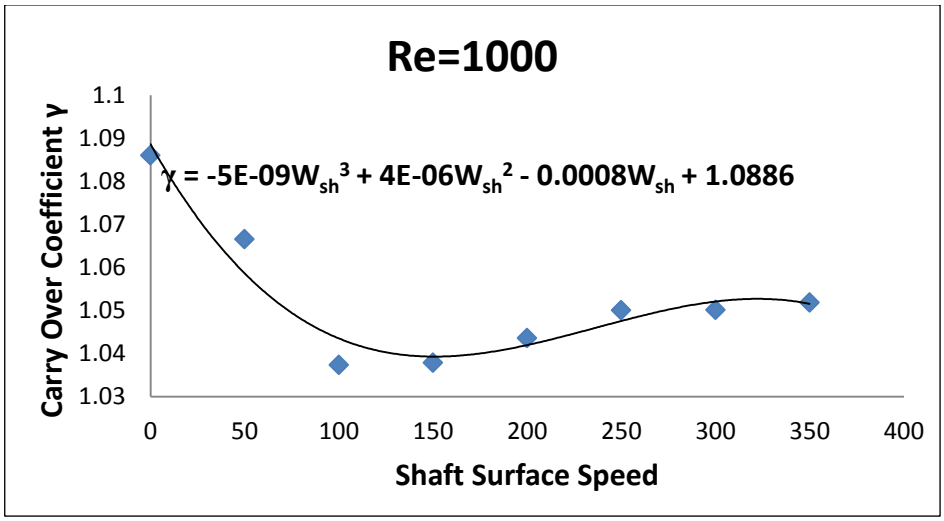

Fig 6.9 Variation of γ for cavity 1 with shaft surface speed at Re=1000

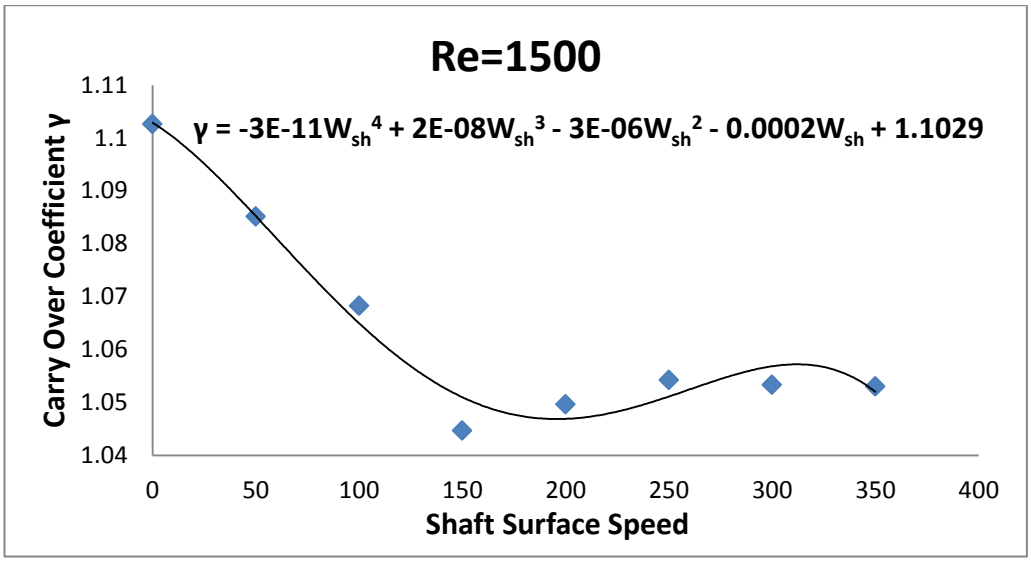

Fig 6.10 Variation of γ for cavity 1 with shaft surface speed at Re=1500

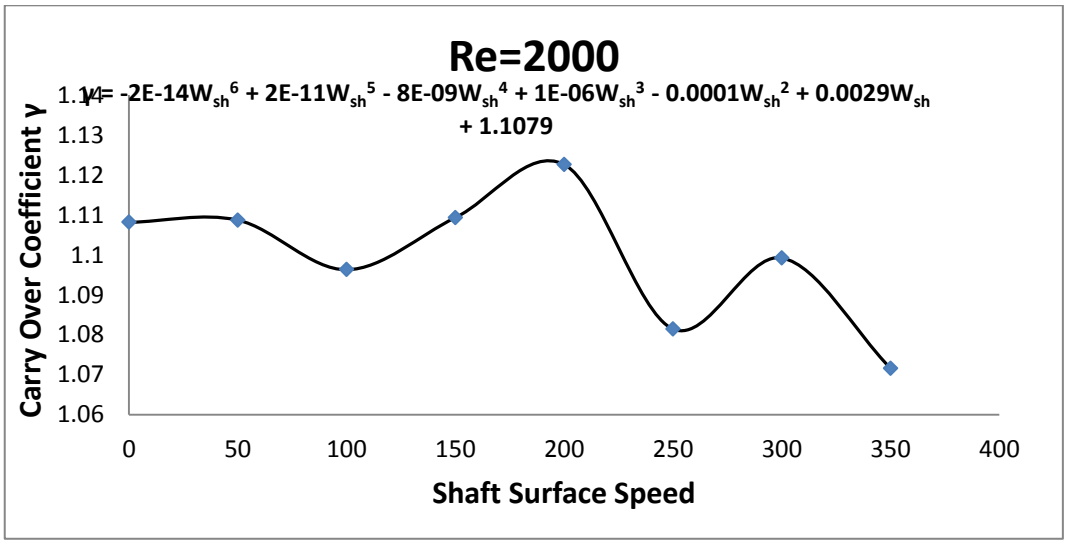

Fig 6.11 Variation of γ for cavity 1 with shaft surface speed at Re=2000

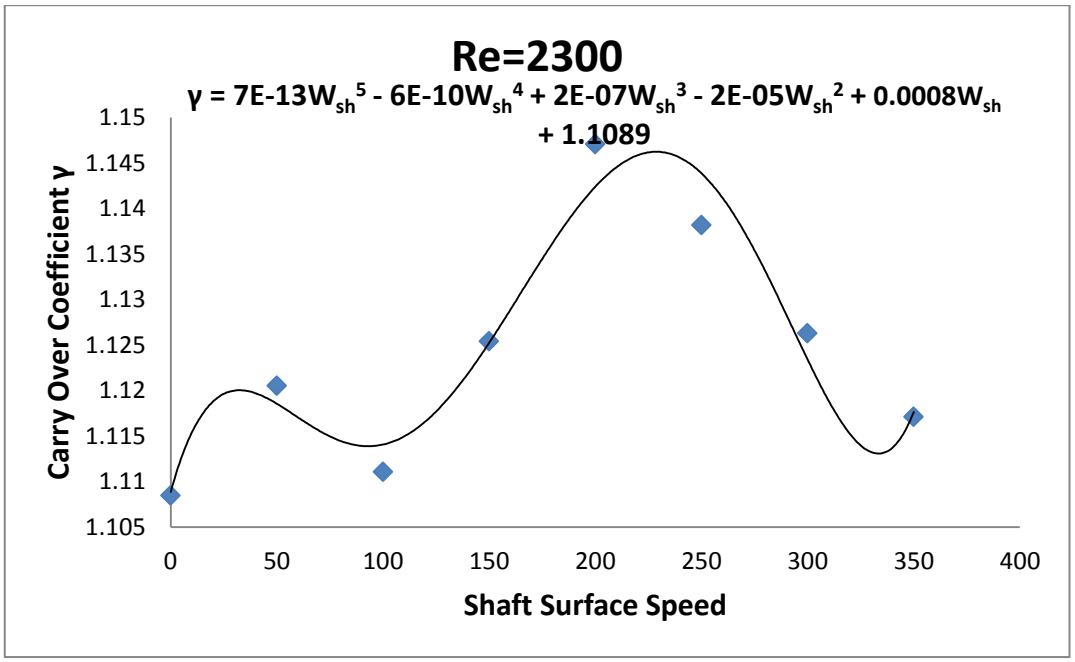

Fig 6.12 Variation of γ for cavity 1 with shaft surface speed at Re=2300

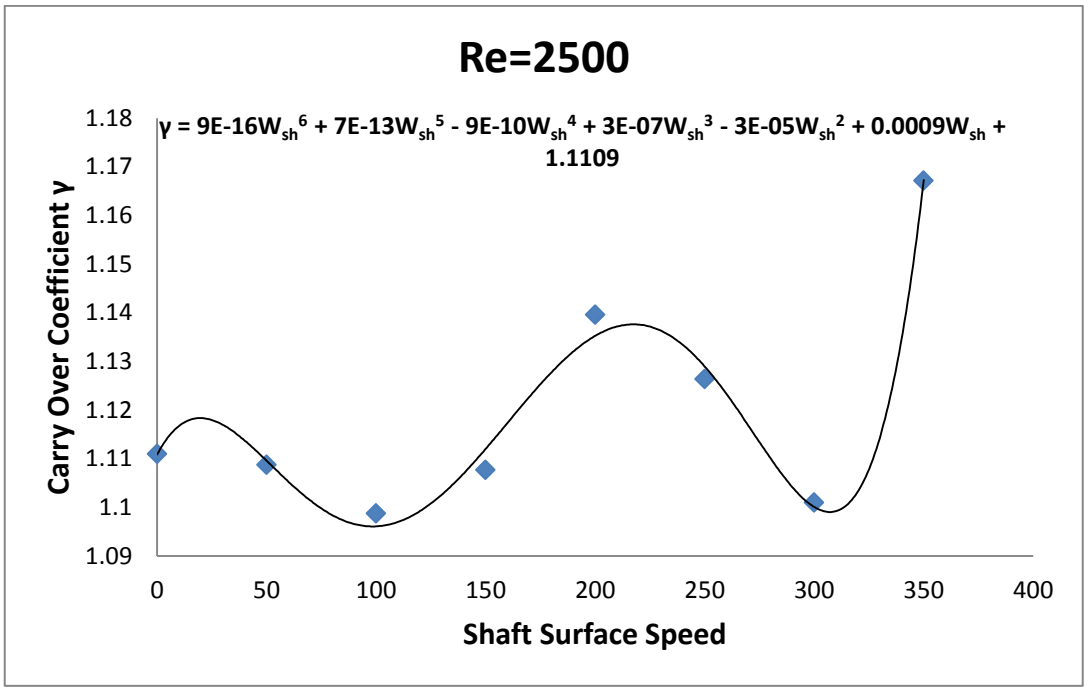

Fig 6.13 Variation of γ for cavity 1 with shaft surface speed at Re=2500

Same is observed for Figures (6.12 & 6.13) This trend is observed in both the case with Re=1000 & Re=1500. For Re=2000 the increment is same till the shaft surface speed reaches 50 m/s. After that the increment in pressure force and shear forces is less than in centrifugal forces and this continues till shaft surface speed reaches 200m/s above which it becomes same as for low Re.

From the above discussion it can be concluded that the variation of shear force and pressure forces are varying with shaft RPM. But the variation of pressure with shaft RPM is linear (for constant Reynolds number) as shown in the Figure 6.14 below.

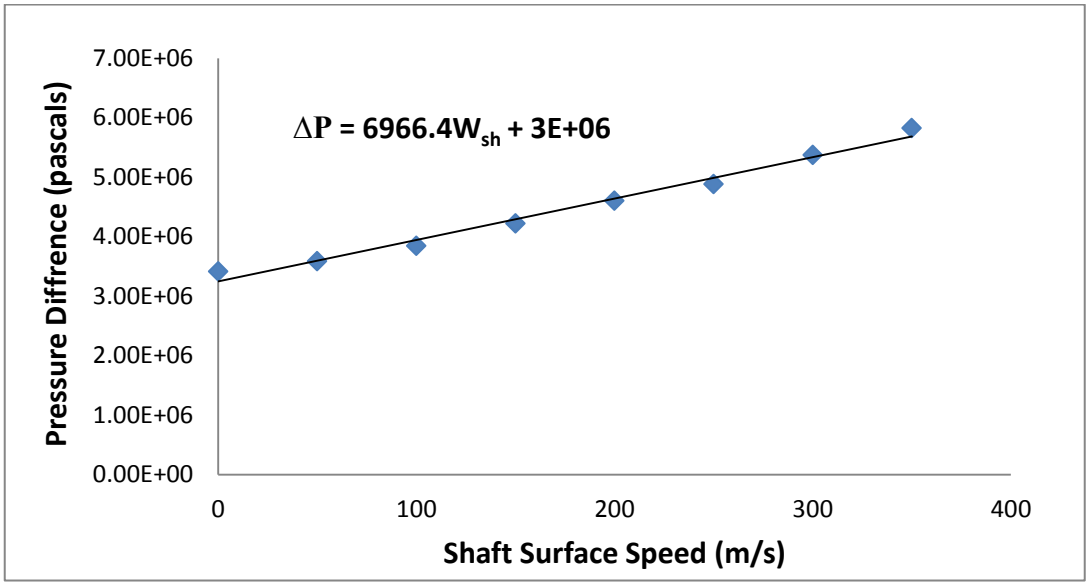

Fig 6.14 Pressure difference variation with shaft speed (G1& Re=1000)

Assuming the shear force to vary linearly with shaft speed because the increment in shaft speed is proportional to the increase in shear forces provided the area of fluid to

surface contact remains same (neglecting the change of vortices at high Taylor Number), quantitatively the variation of these forces could be summarized as:

1. Centrifugal Force ~ W_{sh}^2
2. Pressure Force ~ W_{sh}
3. Shear Force ~ W_{sh}

This shows how forces are changing with shaft speed. So we could expect a situation as shown in the Figure 6.15 below (drawn not from the cases simulated but used another set of data to draw it):

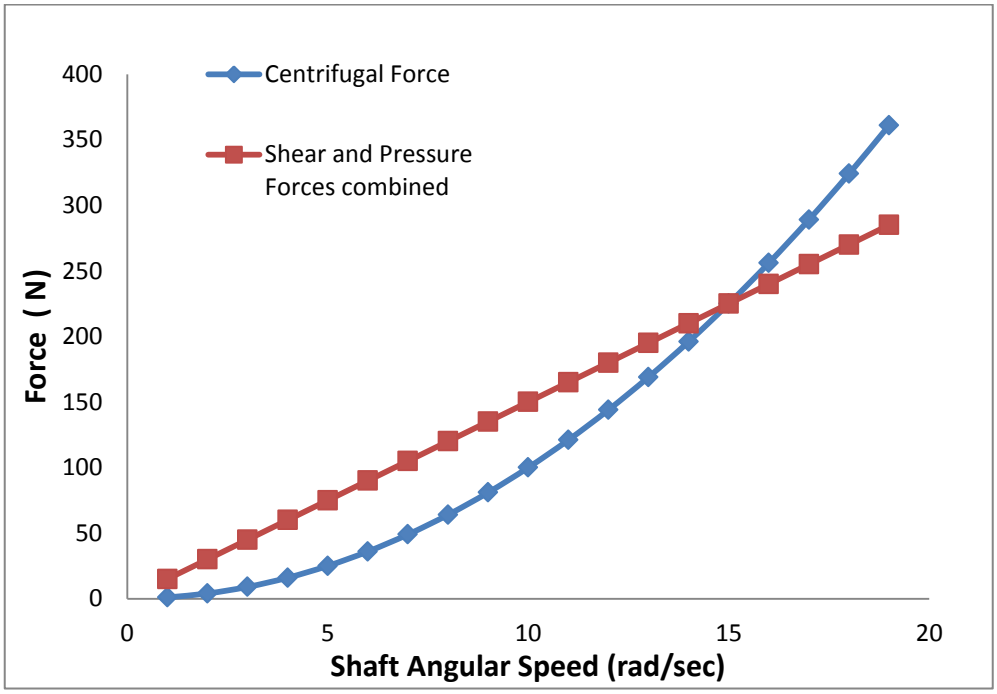

Fig 6.15 Variation of forces with shaft speed (Not to scale)

From here, understanding of the variation of carry over coefficient for different cases is achieved. It may be explained as, for different Reynolds number the slope of the pressure force and shear force will be different from centrifugal forces which change the crossing points of two graphs. Also if we further consider the variation of vortex formation in cavity at high Taylor Number there can be more variation in this graph by changing the slope of straight line at different shaft speed. This will lead to more points of intersections which correspond to ups and downs in the carry over coefficient graph for a given geometry and Reynolds number. Also for high clearance geometries this variation in forces is comparatively less as shown in the Figures (6.16, 6.17, 6.18, 6.19 & 6.20) below.

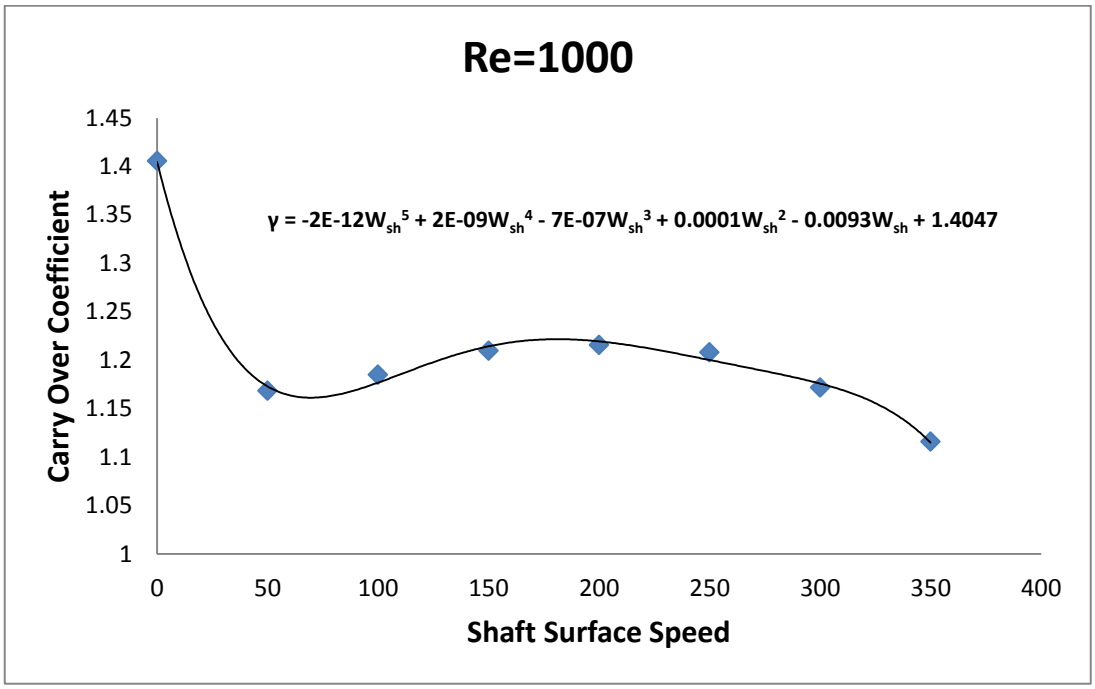

Fig 6.16 Variation of γ for cavity 1 with shaft surface speed for G4

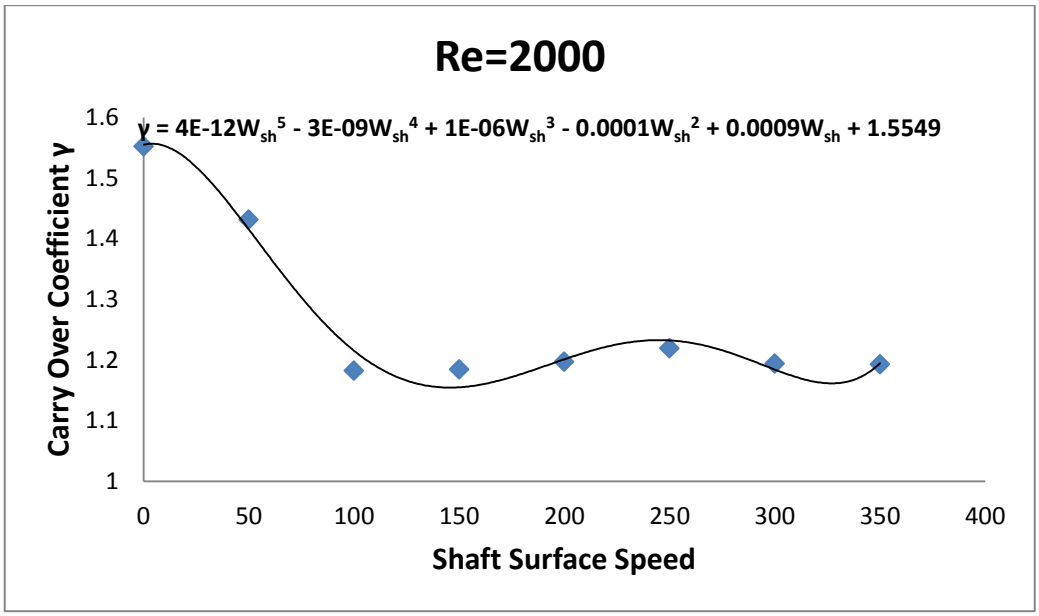

Fig 6.17 Variation of γ for cavity 1 with shaft surface speed for G4

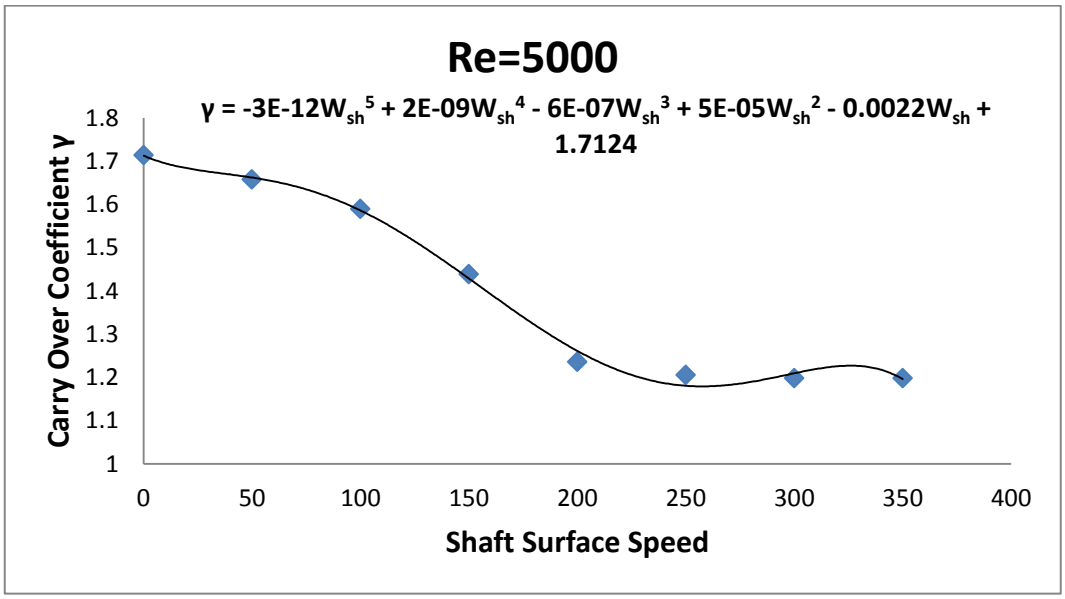

Fig 6.18 Variation of γ for cavity 1 with shaft surface speed for G4

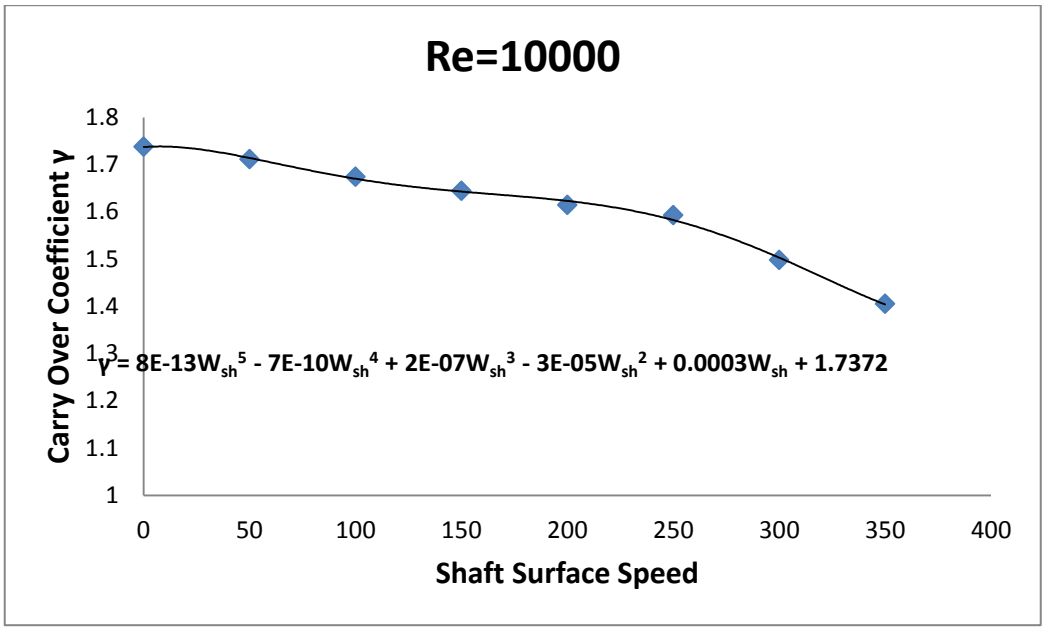

Fig 6.19 Variation of γ for cavity 1 with shaft surface speed for G4

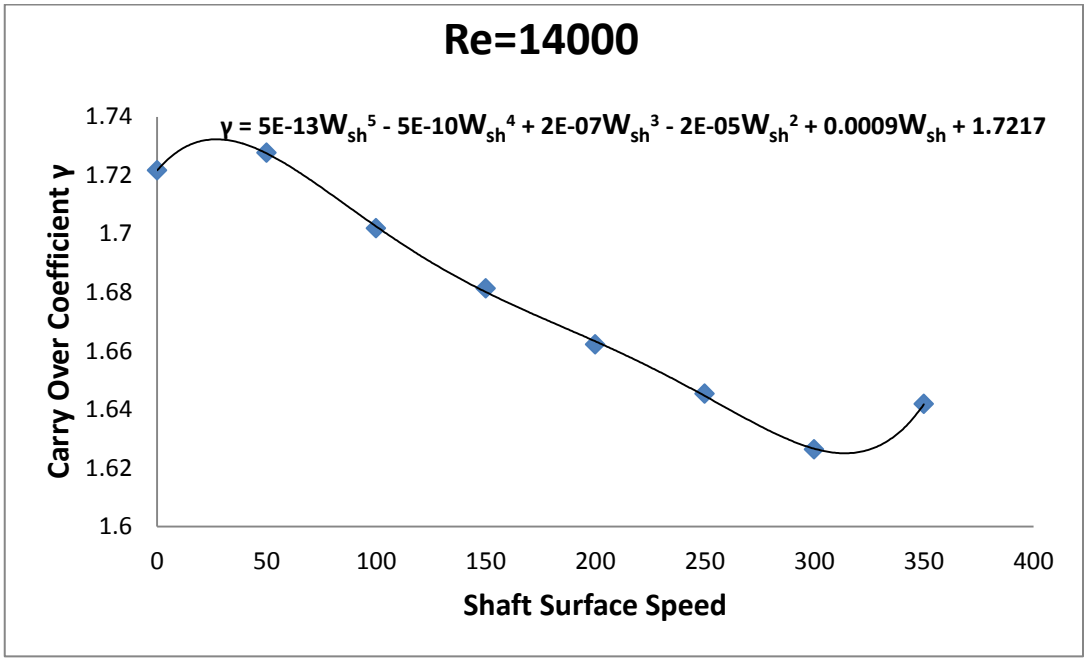

Fig 6.20 Variation of γ for cavity 1 with shaft surface speed for G4

6.4 Cumulative Effect of Changing Various Factors on Carry over Coefficient

Finally we are going to analyze the cumulative effect of various parameters affecting the carry over coefficient all together. For this analysis, the complete data set has been divided in two main categories based on the tooth width to pitch ratio (w/s), one for (w/s= 0.25) and another for (w/s= 0.0075). Further for each (w/s) we have different clearance to pitch ratios. Figure 6.21 shows there is very little variation in the carry over coefficient value for low c/s value of 0.0075. The maximum value of carry over coefficient is below 1.2 which implies a cavity effectively decreases the kinetic energy carried over into the next cavity. For c/s= 0.015 the variation similarly is not much with the maximum value of carry over coefficient limited to 1.4. As the c/s ratio is increased to 0.0375 there is more variation in carry over coefficient from 1.2 to up 1.8. The two largest c/s values show the general trend of carry over coefficient increasing with Reynolds number and decreasing with Taylor Number. Hence the cavity for a tooth on rotor seal is more effective at dissipating kinetic energy for a large shaft speeds and low Reynolds numbers (low pressure differentials across the seal).

Figure 6.22 shows the same results for w/s=0.0075. Almost the same observation can be made for that of w/s = 0.25. The variation of carry over coefficient with Taylor Number and Reynolds number is less for c/s =0.0075 as compared to the variation for c/s = 0.0375. The variation of carry over coefficient of c/s 0.0075 is limited by 1.2 and for c/s=0.0375 there is a larger variation in carry over coefficient up to 1.7. From the rest of figures in Appendix we also conclude that this trend is followed irrespective of cavity location in the labyrinth seal.

Cavity 1

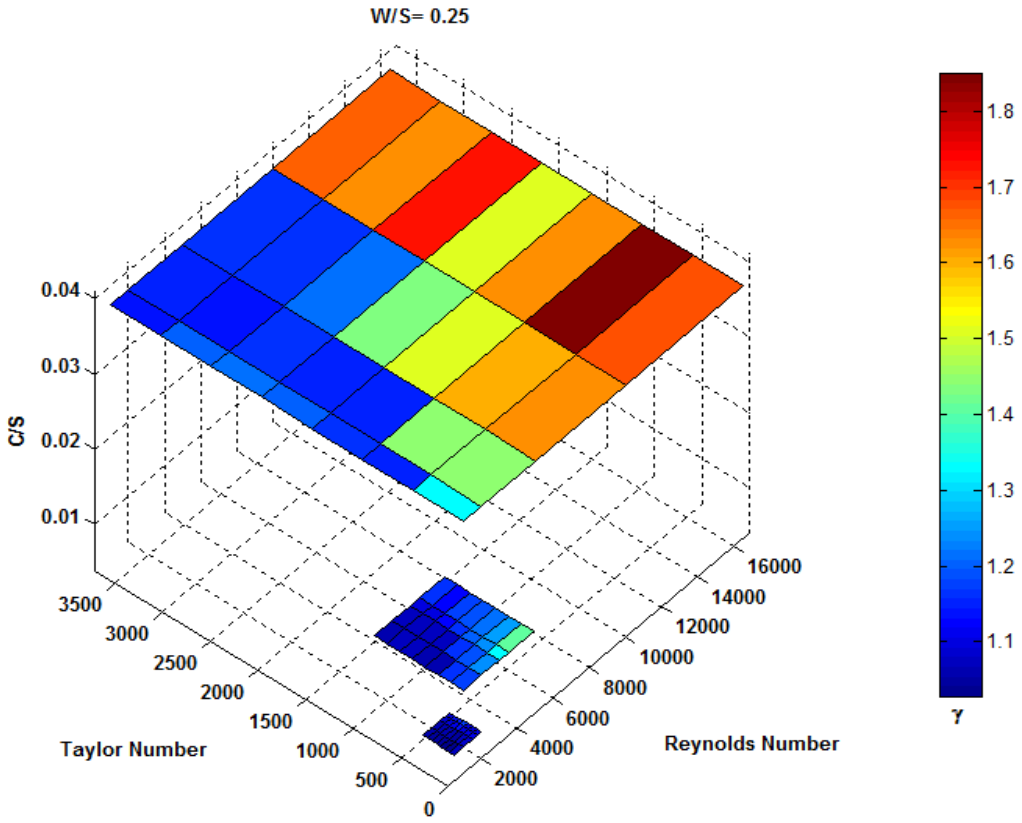

Fig 6.21 γ changes with Ta, Re and C/S for W/S =0.25 (G2, G3 & G5)

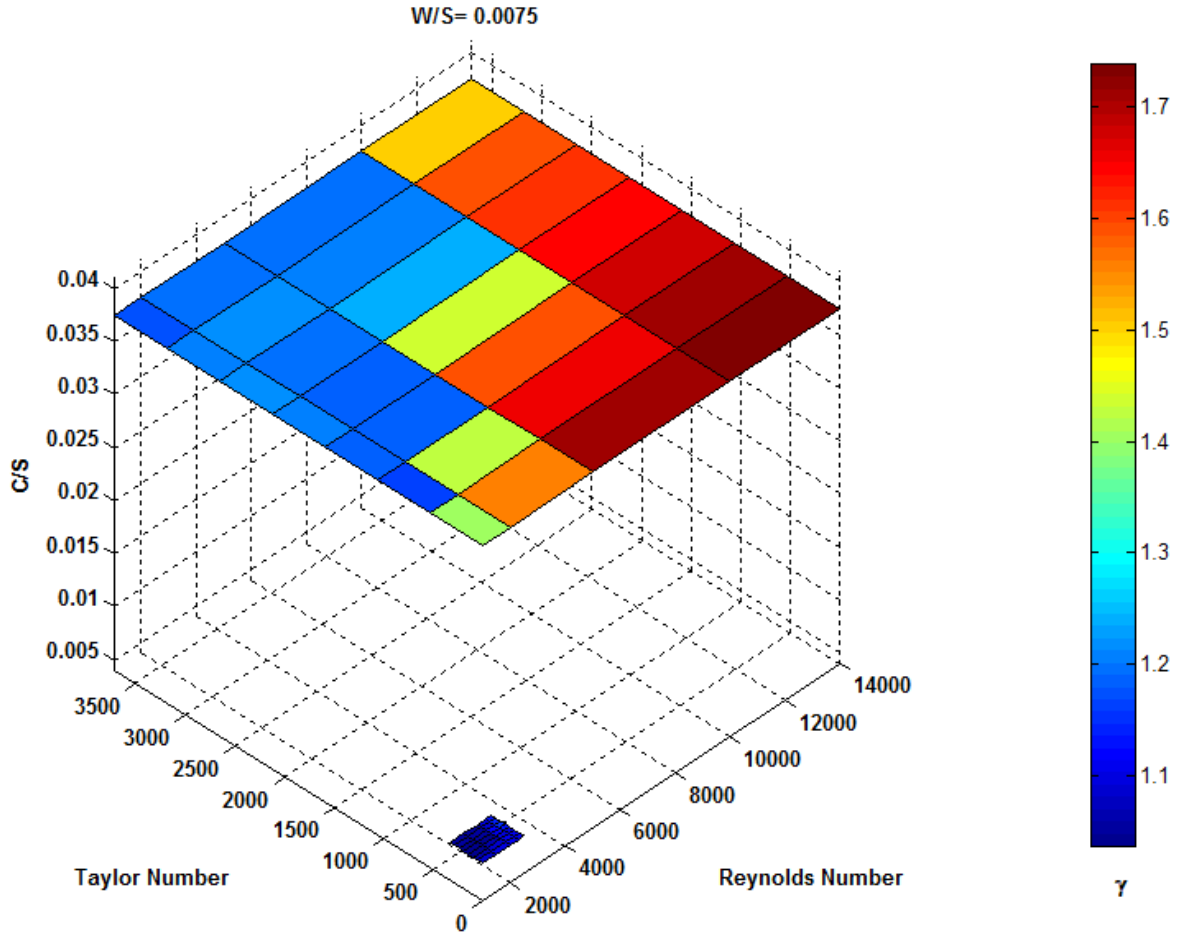

Fig 6.22 γ changes with Ta, Re and C/S for W/S =0.0075 (G1 & G4)

Figures 6.23 and 6.24 show the streamlines inside the seal cavity for geometry G4, Re=10,000, W_{sh}= 0 and W_{sh} =350 m/s. As observed by Demko [25], at the higher shaft speeds (Taylor number) a secondary recirculation zone appears due to the centrifugal forces generated by the induced tangential velocity. This is what causes the carry over coefficient to decrease with increasing Taylor Number. This shows that increasing shaft speed increases the efficiency of seals with high Reynolds number while the change for the low Reynolds number is not significant. Further these changes are more important for seals with high clearance to pitch ratios only. This observation is explained by seeing the streamlines below for low c/s ratio at different shaft RPM's.

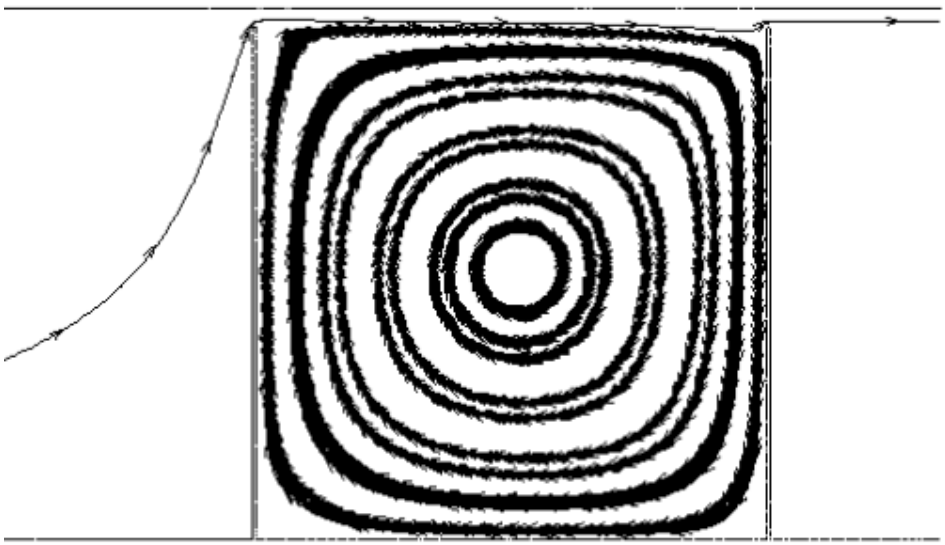

Fig 6.23 Mean flow streamlines for Re=10000 at W_{sh} =0 for G4

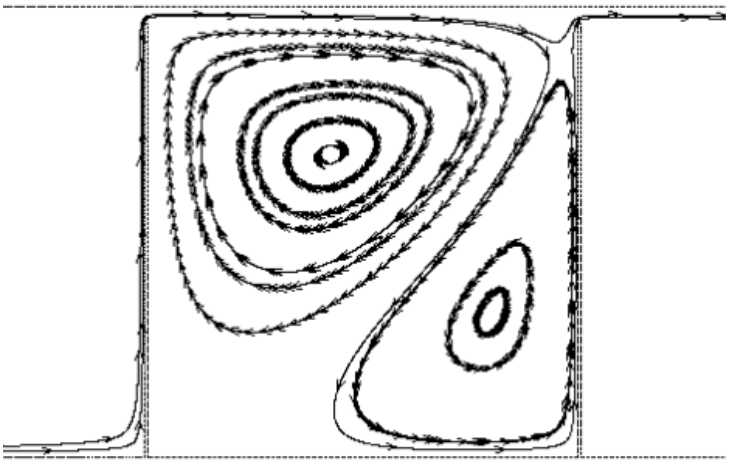

Fig 6.24 Mean flow streamlines for Re=10000 at W_{sh} =350m/s for G4

Comparing Figure 6.23 and Figure 6.24 it is observable that the carry over coefficient for Figure 6.23 is less than for Figure 6.24 because there is additional throttling occurring in the second case due to presence of two recirculation zones. This leads to additional head loss. So from the above discussion we came to the conclusion that for a given Shaft RPM and Reynolds Number increment in will increase carry over coefficient. The results are mentioned in Table 2 below and data used for Figures 6.21 and 6.22 is shown in Table 3 underneath.

Table 2 Effect of Tooth Width and c/s on Carry over Coefficient

	Tooth width (w)	**Carry over coefficient (γ)**
Large (c/s=0.0375) G4 & G5	**Increases**	**Increases**
Small (c/s= 0.0075) G1 &G2	**Increases**	**Increases**

Table 3 Reynolds Number and Shaft RPM used for simulation

Geometry	Reynolds Number	Shaft RPM							
2	500	0	1666.65	3333.33	5000	6666.66	8333.35	9999.99	11666.65
1,2,3,4,5	1000	0	1666.65	3333.33	5000	6666.66	8333.35	9999.99	11666.65
1,2	1500	0	1666.65	3333.33	5000	6666.66	8333.35	9999.99	11666.65
2	1800	0	1666.65	3333.33	5000	6666.66	8333.35	9999.99	11666.65
1,2,3,4,5	2000	0	1666.65	3333.33	5000	6666.66	8333.35	9999.99	11666.65
1	2300	0	1666.65	3333.33	5000	6666.66	8333.35	9999.99	11666.65
1	2500	0	1666.65	3333.33	5000	6666.66	8333.35	9999.99	11666.65
3	3000	0	1666.65	3333.33	5000	6666.66	8333.35	9999.99	11666.65
3	3500	0	1666.65	3333.33	5000	6666.66	8333.35	9999.99	11666.65
3	4900	0	1666.65	3333.33	5000	6666.66	8333.35	9999.99	11666.65
4,5	5000	0	1666.65	3333.33	5000	6666.66	8333.35	9999.99	11666.65
4,5	10000	0	1666.65	3333.33	5000	6666.66	8333.35	9999.99	11666.65
4	14000	0	1666.65	3333.33	5000	6666.66	8333.35	9999.99	11666.65
5	16000	0	1666.65	3333.33	5000	6666.66	8333.35	9999.99	11666.65

7. DISCHARGE COEFFICIENT

After obtaining an understanding about the carry over coefficient which describes the percentage kinetic energy being dissipated in a cavity, the next step is to define another coefficient used to calculate the total pressure loss in a labyrinth seal. In this work, these losses are represented with the symbol C_d and call it the discharge coefficient. This coefficient is used to represent both the losses under the tooth and in the cavity combined. The formulae for this coefficient is as mentioned below:

$$C_d = \frac{\dot{m}}{A\sqrt{2\,\rho\,(P_i - P_e)}}$$

where $\dot{m}$ is used to denote the mass flow rate through the labyrinth seal, while P_i and P_e represent the inlet and exit pressures across the tooth and ρ defines the density of the fluid (which is variable for compressible fluid such as air and constant for water). Both these pressures are supposed to be calculated from the center of the cavity to the center of the next cavity as shown in the Figure 7.1 below by the points P1 and P2. For compressible flow density ρ is the value where pressure value P_i is measured.

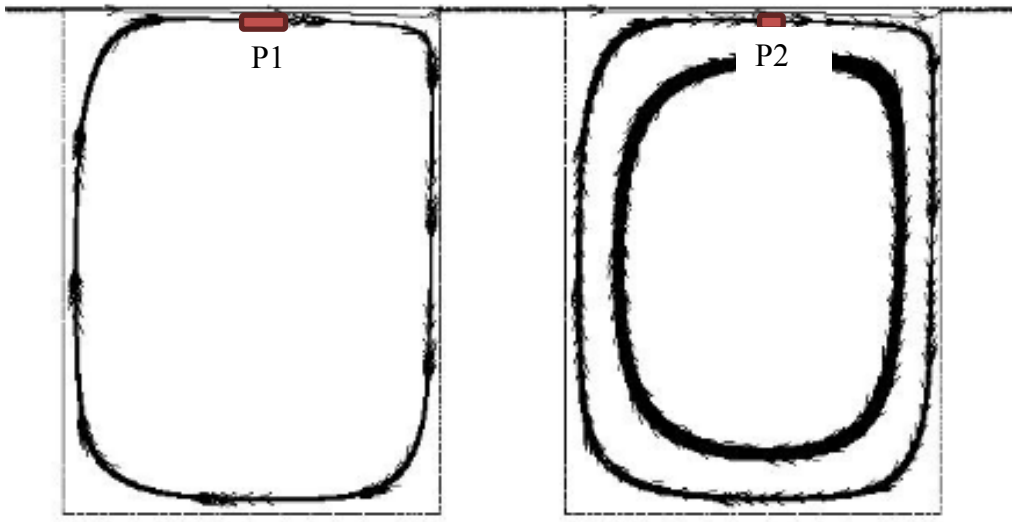

Fig 7.1 Carry over coefficient calculation points

Once the value of the discharge coefficient and the external pressure field distribution is known, they can readily be used in the calculation of the mass flow leakage through the labyrinth seals. This has a great advantage in the loss estimation in the design of new turbo machinery or changing the worn out seals of a running turbine during its overhaul. It can also save time for the manufacturer and experimental persons involved in the design of these machines. Furthermore it can even be used to simulate the flow through turbines, compressors and pumps. Also it would be beneficial in rotor dynamic calculations where the accuracy of the damping coefficients for labyrinth seals entirely depends upon the correct prediction of the flow through the labyrinth seals.

In many of the previous investigations it has been shown that the discharge coefficient significantly varies for the first tooth from subsequent teeth. This change

could be attributed to the carry over coefficient of the previous cavity which substantially changes the discharge coefficient of the intermediate teeth. This effect is not present for the first tooth so the change in the behavior of the discharge coefficient is obvious. The Figure 7.2 shown below further supports this statement.

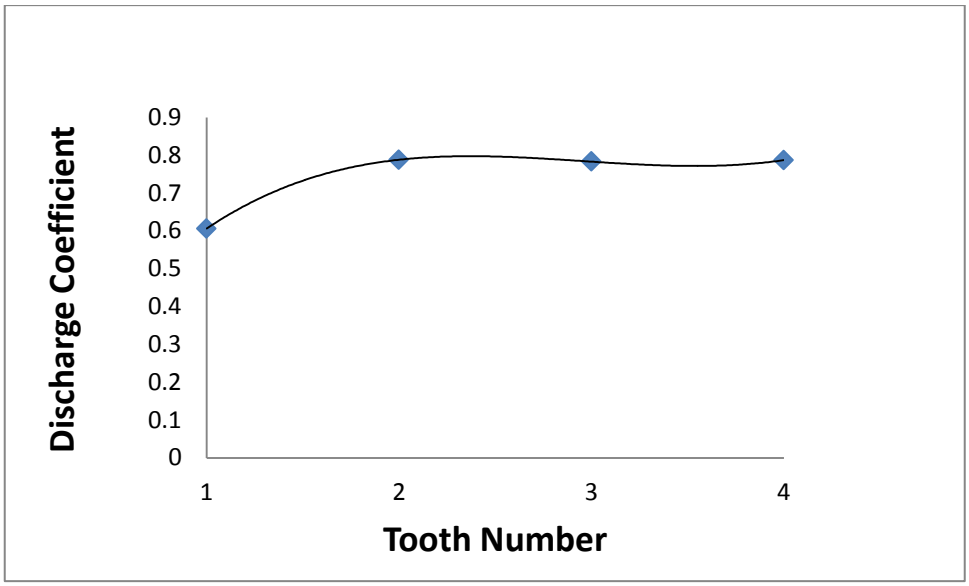

Fig 7.2 Variation of C_d with tooth (Water, G4, Re=2000,W_{sh} =0)

In this current research work all the geometries have 4 teeth. Therefore the effects of various geometrical and flow parameters on the first tooth C_d^{1tooth} are considered separately from that on the multiple downstream teeth. The first tooth will be analyzed first and the intermediate teeth later.

7.1 First Tooth

7.1.1 Effect of Reynolds Number on Coefficient of Discharge

In this subsection the effect of Reynolds number on the discharge coefficient of the first tooth of water seals is analyzed. For this study, the geometry chosen is G3 (s=4, h=4, c=0.06, w=1) (all dimensions in mm) where the Reynolds number varies from 1000 to 4900.

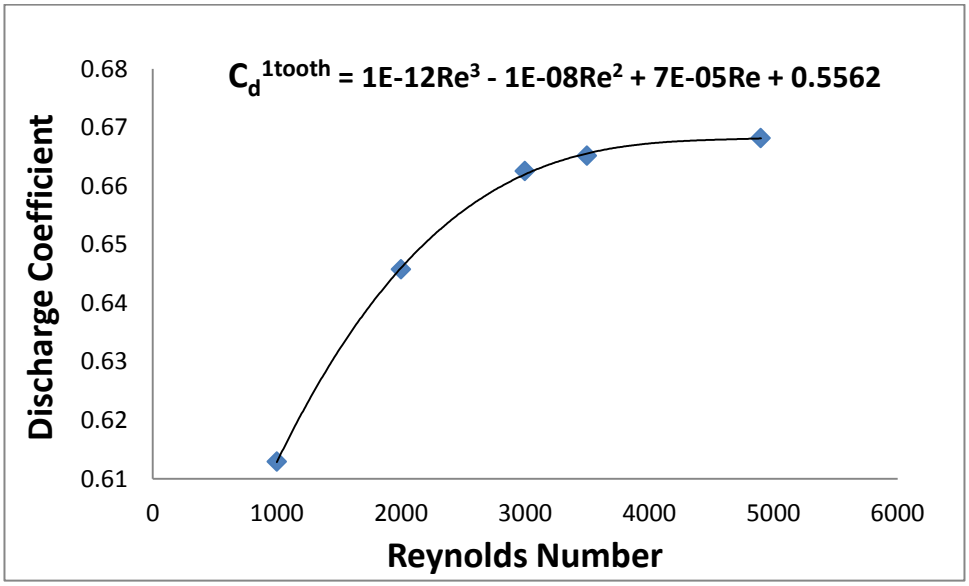

Fig 7.3 Variation of C_d^{1tooth} with Re (Water, G3, 0 RPM)

From the above Figure 7.3, it can be observed that the discharge coefficient is increasing with Reynolds number. This implies that the seal becomes less effective to fluid flow losses by decreasing its friction to fluid flow. This can be explained as follows. The value of carry over coefficient increases with increasing Reynolds Number, so

kinetic energy loss goes down. This implies there is less total pressure head loss. The values of Cd1tooth follow the same trend as carry over coefficient. Also the value of coefficient of discharge for first tooth (C_d^{1tooth}) is limited by 1 (Bernoulli's flow no loss).

7.1.2 Effect of the Clearance Ratio on Coefficient of Discharge

The effect of the major geometrical parameter clearance on the coefficient of discharge is analyzed next. The dimensionless parameter, clearance to pitch ratio (c/s) is used to present the results in terms of non-dimensional numbers. This ratio used is the same as used for the subsection on carry over coefficient. This had been done intentionally to compare the effects of other losses parallel to the carry over coefficient while observing the trend for discharge coefficient variation on various parameters.

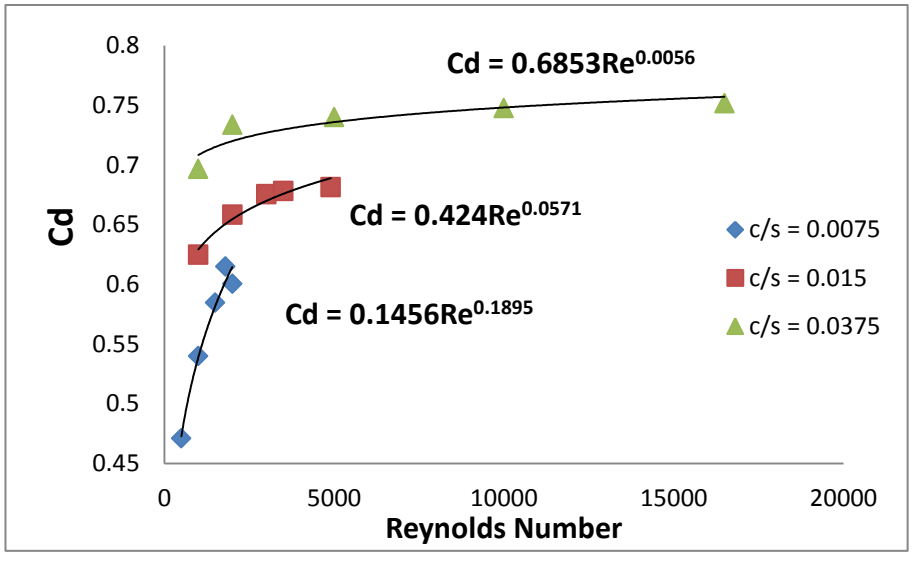

Fig 7.4 Variation of coefficient of discharge with Re for different c/s ratio

From the above Figure 7.4 it is observed that the Coefficient of Discharge asymptotically approaches the value of 1 while increasing the Reynolds number. This physically signifies no losses or the incapability of the seal to stop flow losses. On the other hand it decreases drastically with the decreasing clearance to pitch ratio. This follows the trend for the carry over coefficient becoming lower as c/s decreases which indicates more kinetic energy being dissipated which reduces the pressure recovery in the cavity which decreases the Coefficient of discharge .There is a decrease of 14% in the discharge coefficient with the decrease of the clearance to pitch ratio by 2.5 times (from 0.0375 to 0.015). Increasing the clearance by a factor of 5 (from 0.03 to 0.15) increases the discharge coefficient by 33%. Also we could observe that higher Reynolds number and clearances have more deviation from the curve than the lower Reynolds number and clearances.

7.1.3 Effect of Tooth Width on Coefficient of Discharge

In the previous subsection it was observed that both the discharge coefficient and carry over coefficient increases with increasing clearance to pitch (c/s) ratio. But those results are valid for a fixed tooth size. The effect of changing the tooth width to pitch ratio (w/s) parameter upon the variation of the discharge coefficient will be addressed now. In this comparison, geometry G1 and G2 with the same clearances but different tooth size (increment from 0.03mm to 1 mm, 97%) will be used.

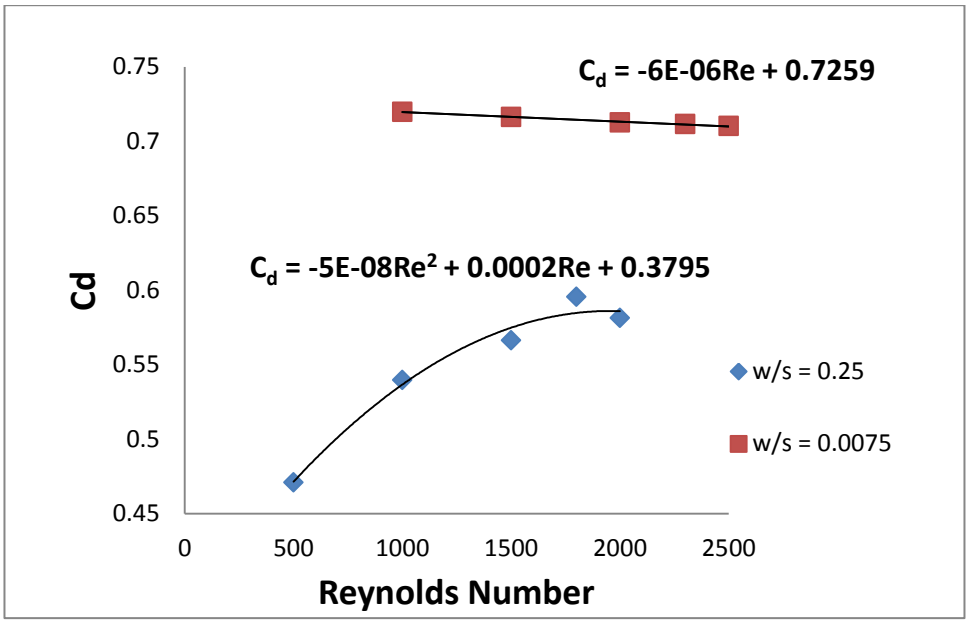

Fig 7.5 Variation of coefficient of discharge with Re for different w/s ratio

From the Figure 7.5 it can be noted that the changes in the coefficient are more gradual for the small tooth width seals than for wide tooth seal geometry at the same Reynolds number. Also contrastingly while the change for the small tooth is opposite to that of the larger tooth. This is an interesting fact which reveals the contrasting different effect of tooth width on coefficient of discharge as compared to carry over coefficient. The reason for smaller tooth decreasing discharge coefficient with increasing Reynolds number could be attributed to that fact that recirculation above the tooth flushes away with the increasing inertia of fluid. For the wider tooth geometry G2, the main parameter affecting the discharge coefficient is the shear stress loss which increases with the increase of Reynolds number due to increasing velocity gradients. Both the above reasons could be better understood by seeing the streamlines for the two geometries below in Figure 7.6 and Figure 7.7 respectively.

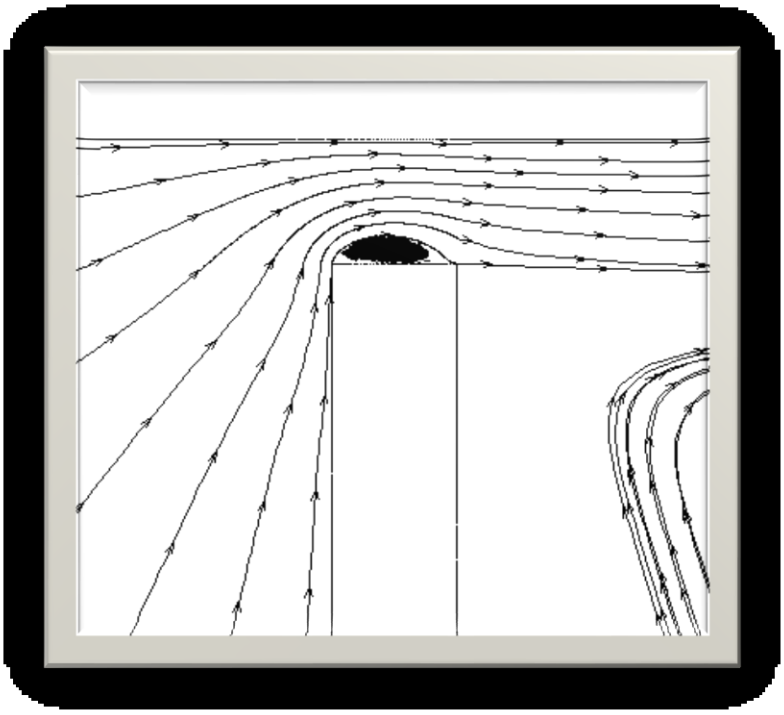

Fig 7.6 Streamlines for G1 (W_{sh} =0 & Re=2000)

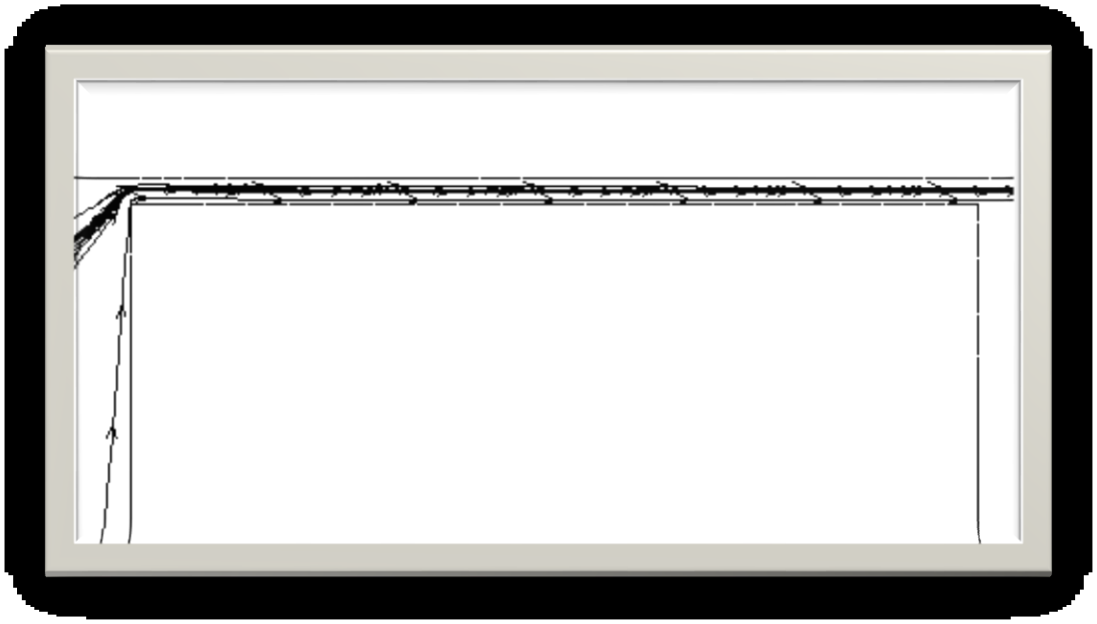

Fig 7.7 Streamlines for G2 (W_{sh} =0 & Re=2000)

7.1.4 Effect of Shaft Rotation on Coefficient of Discharge

In previous subsections the effects of the main geometrical parameters i.e. tooth width to pitch ratio (w/s) and clearance to pitch (c/s) ratio on the discharge coefficient were presented. The effect on shaft rotation on the discharge coefficient will be presented next. For this subsection the Reynolds number is fixed for a chosen geometry.

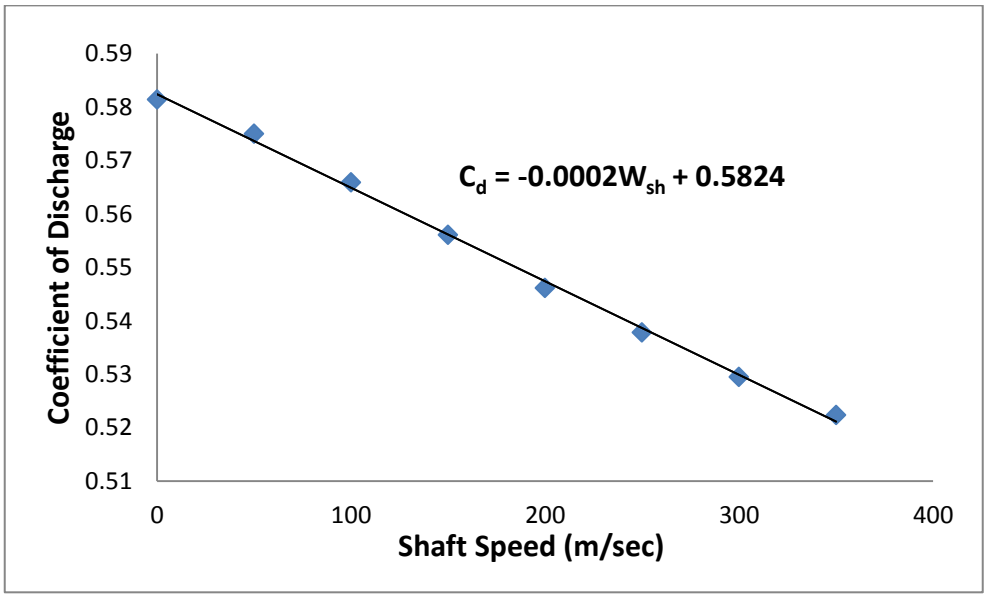

Fig 7.8 Variation coefficient of discharge for different shaft surface speeds

The geometry G2 (s=4, h=4, c=0.03, w=1) and a Reynolds number value at 2000 were chosen. It is clear from Figure 7.8 that there is a linear relation between discharge coefficient and shaft speed. This result can be explained by the fact that a recirculation zone is formed before the entrance of the tooth as the Taylor Number increases. The

intensity of the vortex formed upstream of the first tooth increases with the shaft speed. This increases resistance to the flow at the entrance of the first tooth. Additionally the occurrence of secondary vortex at high shaft speed also increases the flow losses by creating throttling of the fluid in the cavity. The shear stress losses also increase as the shaft RPM increases due to higher velocity gradients at the boundary layer and increased pressure gradient throughout the fluid which increases the forced vortex strength in the cavity. The above explanation is more evident from the Figures 7.9 & 7.10 below.

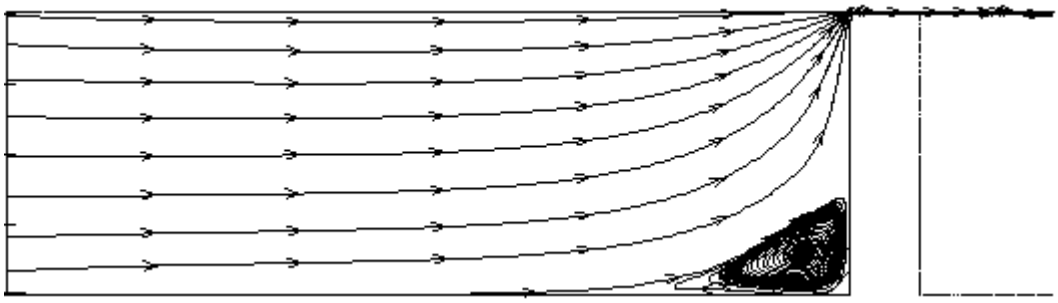

Fig 7.9 Streamlines upstream of first tooth for W_{sh} =0 for G2 and Re=2000

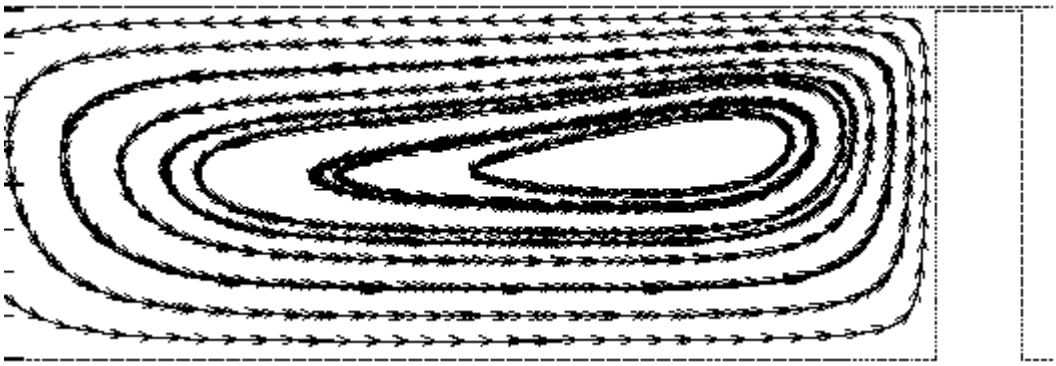

Fig 7.10 Streamlines upstream of first tooth for W_{sh} =350 for G2 and Re=2000

7.2 Intermediate Tooth of a Multiple Tooth Labyrinth Seal

7.2.1 Effect of Reynolds Number on Coefficient of Discharge

In this subsection the variation of discharge coefficient for intermediate teeth with Reynolds number will be analyzed. This study is for the water seals with compressible effect being considered in the next section on compressibility factor. For better comparison of this study, second tooth of geometry G3 (s=4, h=4, c=0.06, w=1) is being used (same as used for the first tooth coefficient of discharge study). The Reynolds number varies from 1000 to 4900.

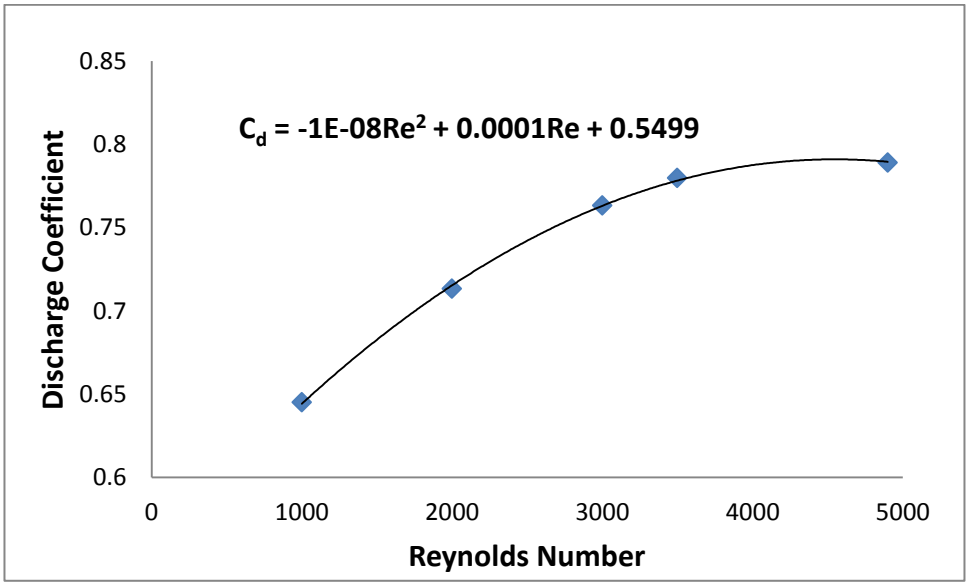

Fig 7.11 Variation of C_d with Re, G3 (tooth2, water)

The Figure 7.11 shows that the discharge coefficient increases with Reynolds Number. This trend is same as the carry over coefficient which increases with Reynolds Number. Other losses at the tooth also increase due to increasing pressure difference and velocity gradients which causes more losses. Also to note, this change is similar to the first tooth discharge coefficient variation only the C_d is larger. Thus the upstream tooth channeling the through flow to the region upstream of the next tooth increases the C_d for the downstream tooth.

7.2.2 Effect of the Clearance Ratio on Coefficient of Discharge

The effects of the geometry on labyrinth seal flow are investigated next. This is done using the dimensionless parameter clearance to pitch ratio (c/s) for the ease of comparing different results.

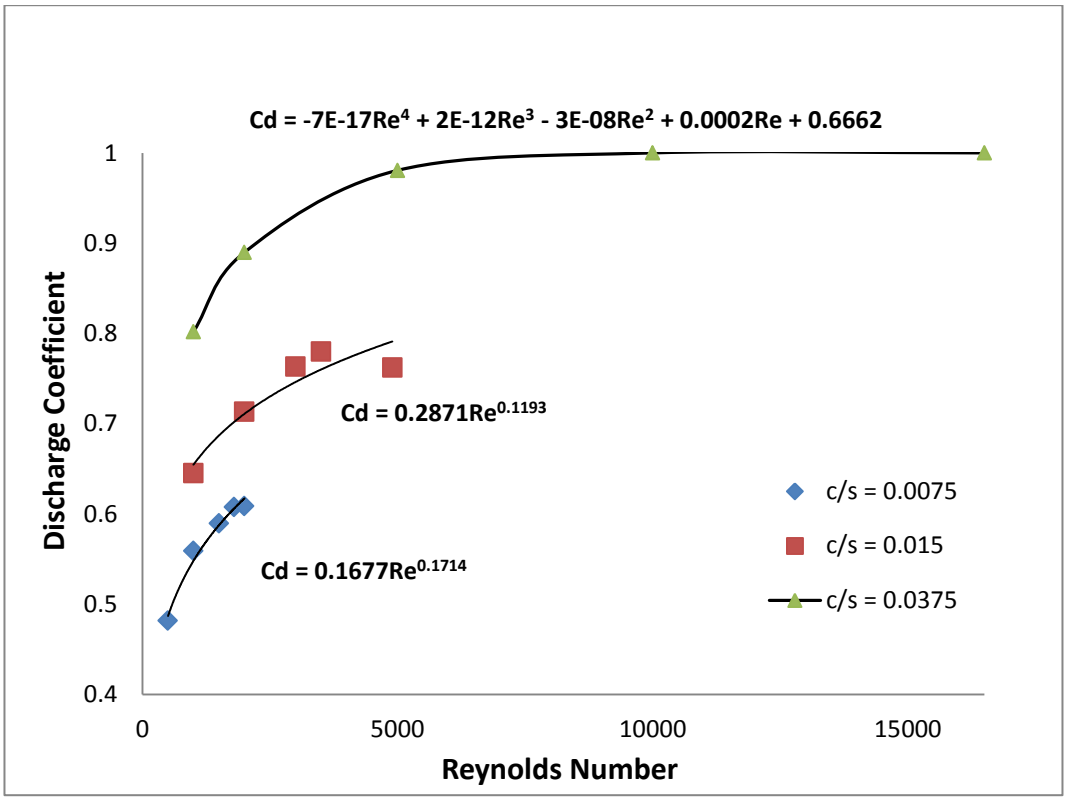

Fig 7.12 Variation of C_d with Re for different c/s ratio (tooth2, water)

From the Figure 7.12 it can be seen that the Coefficient of Discharge approaches the value of 1 with increasing Reynolds Number and increasing c/s where the seal ceases working. For the lower Reynolds number it decreases drastically with the decreasing clearance to pitch ratio. This implies for higher Reynolds number small clearances are required while large clearances (undesirable performance but economic to manufacture) could perform well for small Reynolds numbers. There is a decrease of 11% in the discharge coefficient with the decrease of the clearance to pitch ratio by 2.5 times (from 0.0375 to 0.015) at Re=10000. Further increasing the clearance by a factor of 5 (from 0.03 to 0.15) increases the discharge coefficient by 27% at Re=10000. It is also

observable that at higher Reynolds number and clearances there is more deviation from the curve than the lower Reynolds number and clearances which could be attributed to the fact of increasing demand for computational accuracy as the mesh nodes requirement increases significantly at high Re.

7.2.3 Effect of Tooth Width on Discharge Coefficient

In the previous subsection we observed that the discharge coefficient and carry over coefficient increases with increasing clearance to pitch (c/s) ratio. But those results are true only for fixed tooth size. The effect of changing the tooth width to pitch (w/s) ratio on the discharge coefficient will be considered now. In this comparison the geometry used to study the variation of the first tooth will be used for easy comparison (with water as working fluid). G1 and G2 with the same clearances but different tooth sizes (from 0.25 to 0.03 mm (88%) will be used.

From Figure 7.13 it can be noted that the coefficient of discharge is less for the tooth with higher w/s ratio. This behavior is opposite to that suggested by the carry over coefficient. While the flow losses in the cavity decreases with increasing tooth width at the same time the total head loss increases as indicated by discharge coefficient. It can be concluded that there should be an optimum tooth width for a given pitch where the flow losses (seal performance) are maximized. A more detailed investigation in this area is required.

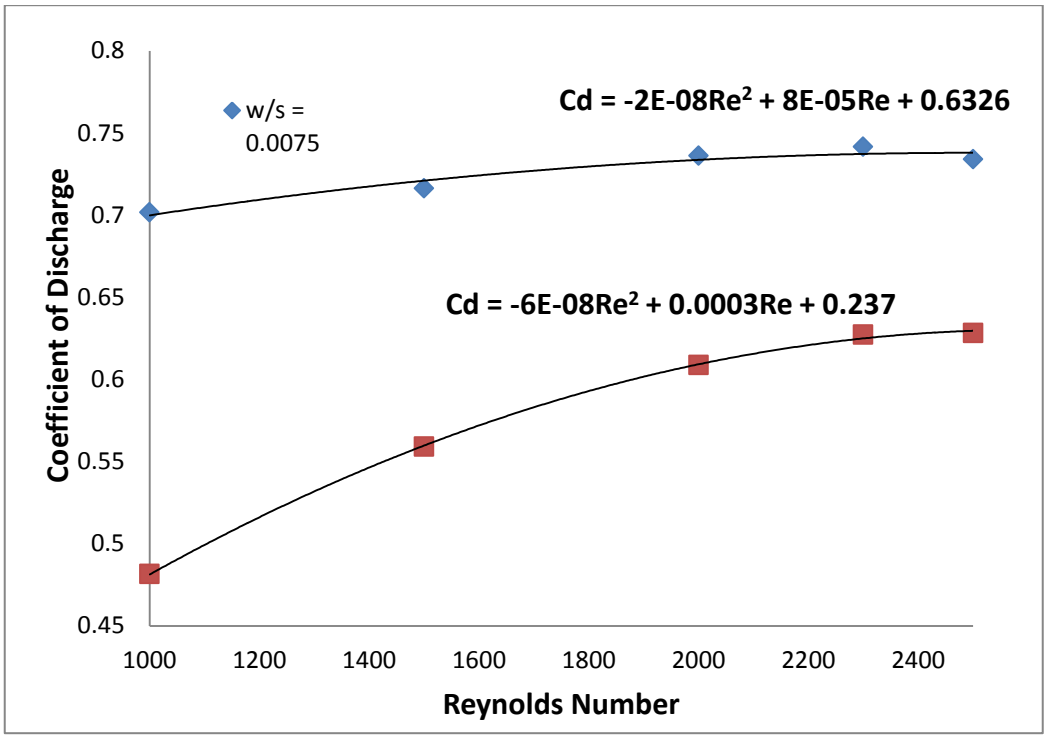

Fig 7.13 Variation of C_d with Re for different w/s ratio (tooth2, water)

7.2.4 Effect of Shaft Rotation on Discharge Coefficient

In the two previous subsections the effect of geometrical parameters (i.e. tooth width to pitch ratio (w/s) and clearance to pitch (c/s) ratio) upon the value of the discharge coefficient were investigated. Now the effect of shaft rotation on the discharge coefficient will be presented. For this subsection the Reynolds number and geometry are fixed.

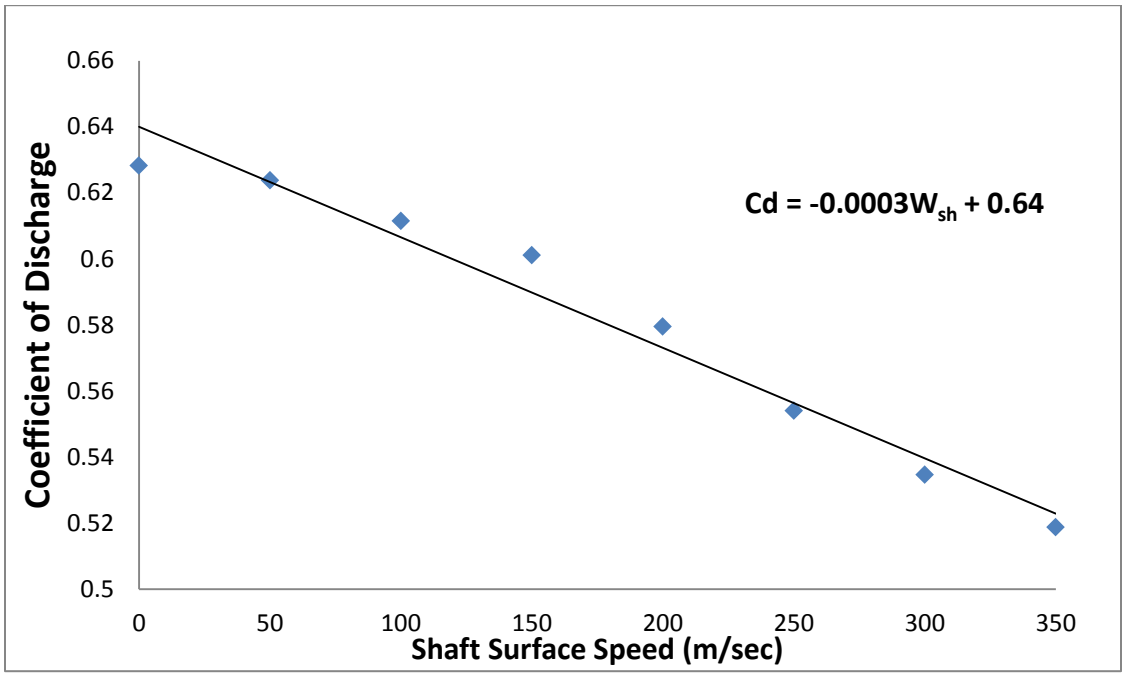

Fig 7.14 Variation C_d for different shaft speed, G2 (tooth2, water, Re=2000)

The geometry G2 (s=4, h=4, c=0.03, w=1) and Reynolds number value at 2000 were chosen with fluid as water for Figure 7.15. It is clear that there is a linear relation between the discharge coefficient and the shaft speed. This result could be explained by the occurrence of secondary vortex (reducing the size of the eddy containing most of the energy) in the cavity at high shaft rotation speeds which suggests the lower energy content being dissipated through turbulence eddy viscosity. Comparing the results for the second to the first tooth it is observable that coefficient of discharge is larger for the second tooth than for the first tooth at zero RPM but decreases in value 50% faster with increasing shaft speed than for the first tooth. Eventually coefficient of discharge for the second tooth is lower than for the first tooth at high shaft speed. This leads us to suspect there are other losses which increase with shaft RPM. From further studying of the

streamlines of this flow field in the cavity it is concluded that there is an additional throttling occurring for the partial flow going below the second vortex formed at high shaft RPM as shown in Figures 7.15 and 7.16 below.

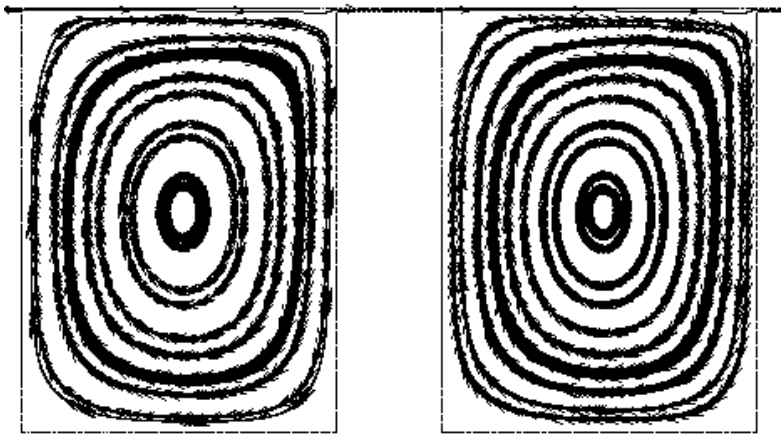

Fig 7.15 Mean flow streamlines for Re=2000 at W_{sh} =0 for G2, tooth 2

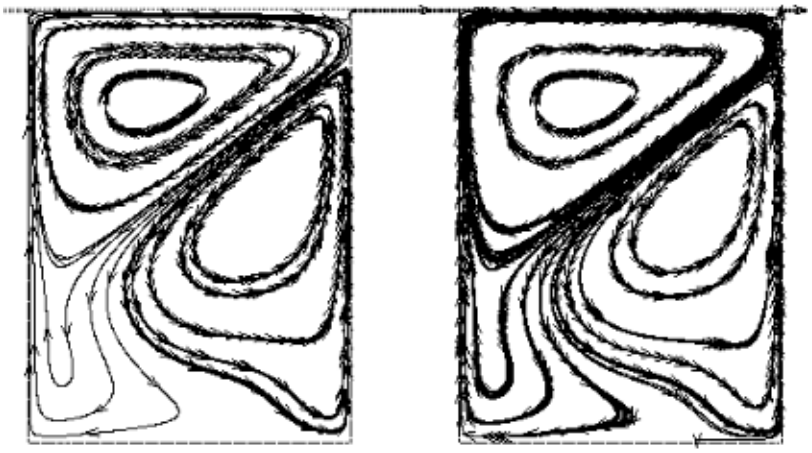

Fig 7.16 Mean flow streamlines for Re=2000 at W_{sh} =350m/s for G2, tooth 2

7.3 Discharge Coefficient Dependence upon Tooth Position, W/S, C/S, Ta and Re

In this subsection we will study the effect on discharge coefficient for all different flow and geometric conditions considered. This study is done by dividing the simulations used for the current study into two categories based on the tooth width to the pitch ratio.

Figures 7.17 and 7.18 present the discharge coefficients for all cases considered using water as the working fluid. The range of Taylor Number decreases with decreasing c/s due to the definition of the Taylor number even though the shaft speeds are the same. The Reynolds numbers decrease with decreasing c/s since a maximum pressure drop of 200atm was considered for all the cases. Thus the Reynolds number for small c/s is lower since the smaller clearance reduces the mass flow rate.

The discharge coefficient for the first tooth decreases with increasing Reynolds number and decreasing Taylor number for both w/s values. The opposite is true for all the interior teeth. The interior teeth all possess very similar discharge coefficient distributions. Discharge coefficient is very low (0.2) for low Reynolds number, high Taylor number flows. This is due to the centrifugal forces causing the secondary recirculation zone which causes most of the through flow to travel a path deep into the cavity. This enhances kinetic energy dissipation and lowers the value of discharge coefficient. As the Reynolds number increases, the value of discharge coefficient increases for all Taylor numbers. At the highest Reynolds number, the effect of shaft speed is reduced, appearing only at the maximum value Taylor number for the largest c/s. As c/s decreases, the range of discharge coefficient variation decreases. The smaller

Tooth 1

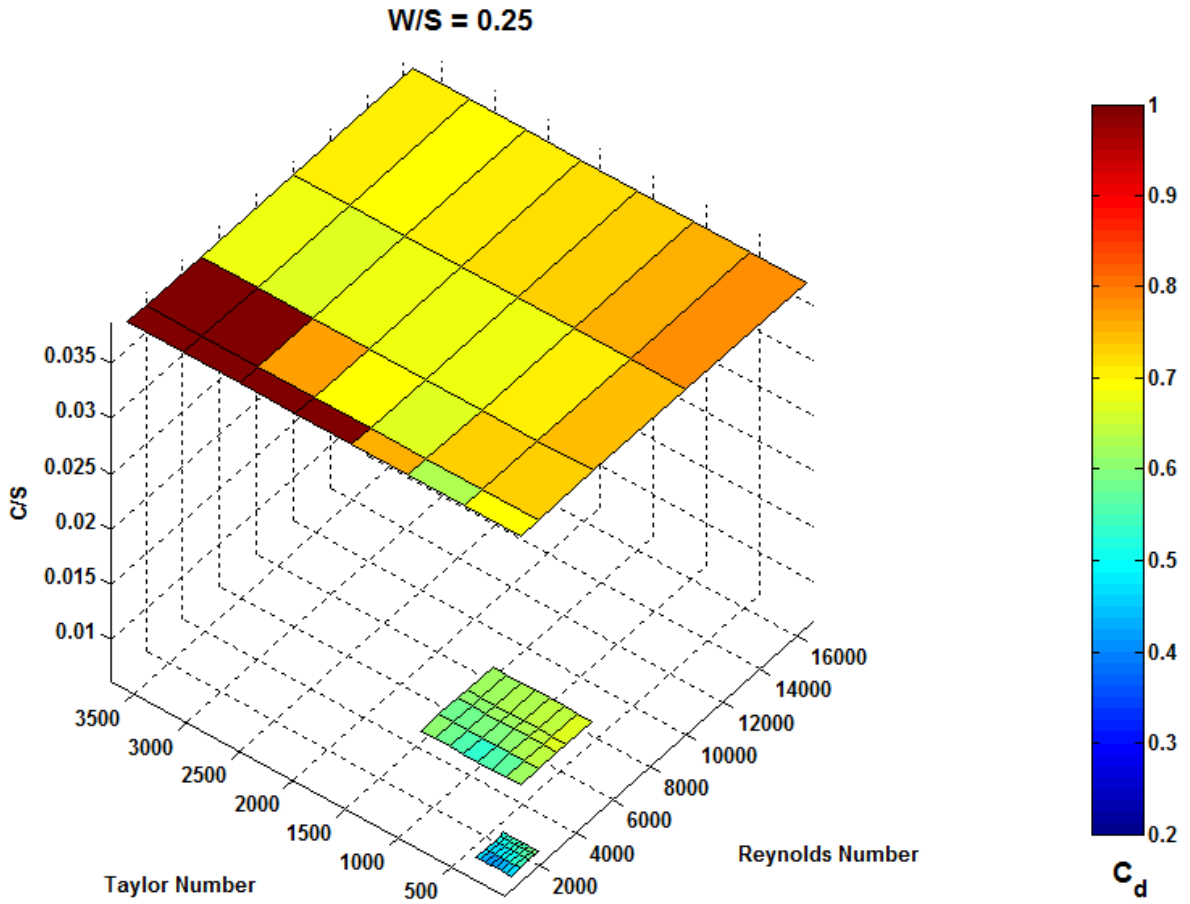

Fig 7.17 C_d changes for Ta, Re and C/S for W/S =0.25 (G2, G3 & G5)

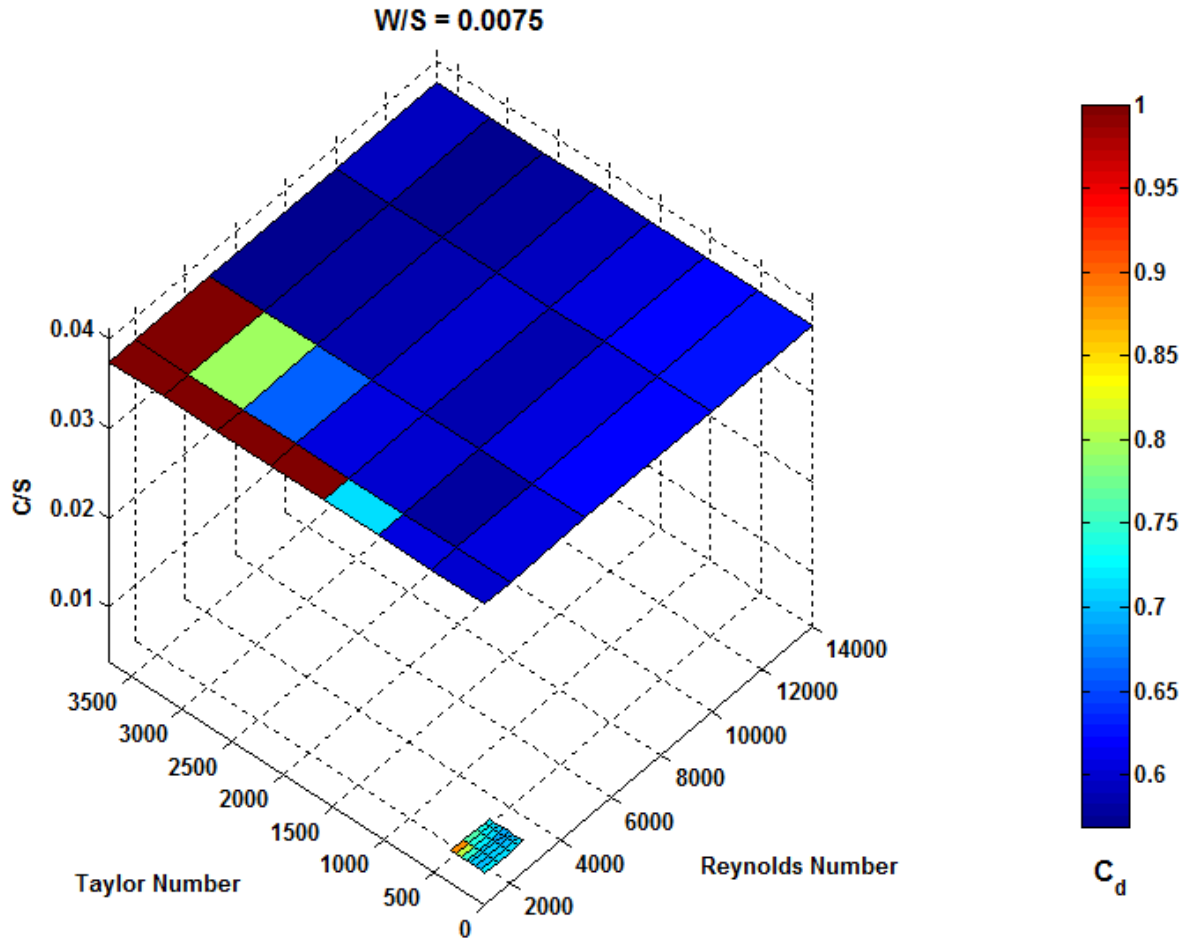

Fig 7.18 C_d changes for Ta, Re and C/S for W/S =0.0075 (G1 & G4)

values of c/s have lower values of discharge coefficient indicating the release more effective with smaller values of c/s. The larger tooth width (w/s) reduces the value of discharge coefficient for the lower values of c/s. Thus for an optimal tooth on rotor seal design smaller clearances and larger tooth widths are desired. The above effect of tooth width for a given shaft RPM and Reynolds Number can be concluded as shown in the Table 4 below:

Table 4 γ variation with C/S and tooth width

	Tooth width (w)	Carry over coefficient (γ)	Discharge Coefficient T1	Discharge Coefficient T2
Large (c/s=0.0375) G4 & G5	**Increases**	**Increases**	**Increases**	**Increases**
Small (c/s= 0.0075) G1 &G2	**Increases**	**Increases**	**Decreases**	**Decreases**

From the above table we conclude that the tooth width could be useful only clearance to pitch ratio is low or for low clearance seals but for high clearance seals this effect is reversed. This phenomenon could be explained using the fact that for the same Reynolds number throttling is very less for high clearance geometries and the corresponding conversion of pressure to kinetic energy (to be dissipated) is negligible however, for the small clearance geometries we have high conversion of pressure energy to kinetic energy whose dissipation in the tooth clearance and boundary plays a major role in deciding the value for discharge coefficient.

8. COMPRESSIBILITY FACTOR

The earlier subsections basically dealt with water as the working fluid to determine the various effects of seal geometry and flow parameters on carry over coefficient and discharge coefficient. All the empirical relations mentioned in the graphs were basically used to define the variance of the primary factors i.e. carry over coefficient and discharge coefficient with different boundary conditions. This was done specifically because mathematically the problem is an elliptic problem defined by the Navier-Stokes equation. However, in the industry gas seals in Gas Turbines and Compressors are also as common as water seals in pumps. Therefore the study cannot be completed without understanding the effect of the compressibility on the various other factors studied. As Saikishan [21] said in his study that the compressibility factors need to be considered only when the pressure difference across the teeth goes below the factor of 0.7. To verify this pressure limit we will study the variation of the discharge coefficients when pressure across the gas seals goes below 0.7 and also the water seals at the same Reynolds Number and Geometry.

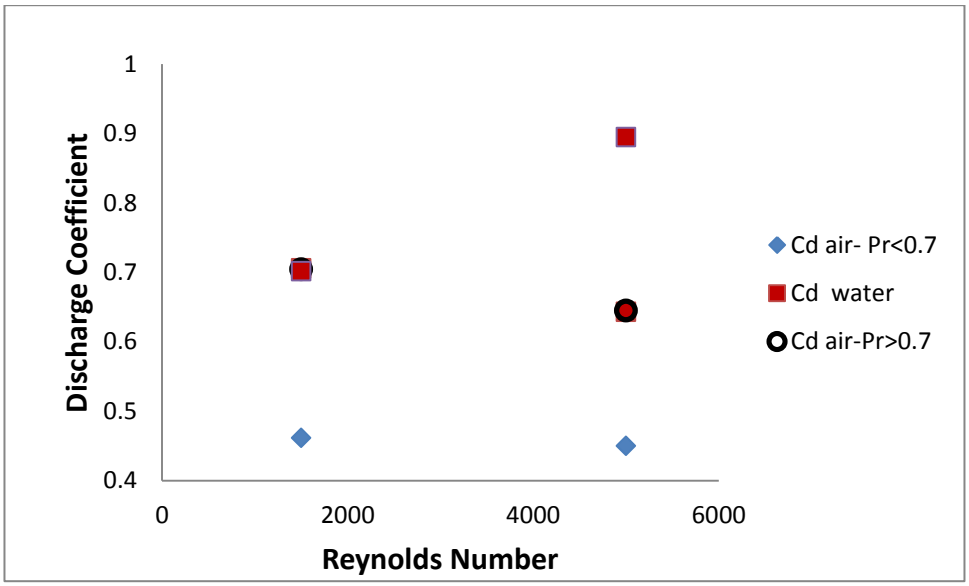

Fig 8.1 Variation of discharge coefficients at different pressure ratios

From the Figure 8.1 it is validated that the assumption of the pressure ratio of limit 0.7 is correct. From the Figure 8.1 it is visible that the dark black circles of air with Pressure ratio greater 0.7 coincide with the corresponding discharge coefficient of water, while the blue hexagonal symbol of air coefficient for pressure ratio less than 0.7 does not.

In this work the effect of compressible fluid is defining by the compressibility factor ψ, as was defined by Saikishan in his work. So following the same definition the compressibility for the current work is defined as the ratio of the discharge coefficient of air vs. the discharge coefficient of water.

$$\psi = \frac{C_{d_{air}}}{C_{d_{water}}}$$

This definition by itself considers the effect on compressibility on carry over coefficient because we have included that in the definition of the discharge coefficient. In many other previous works we do find the definition of compressibility following the same trend as including here by Hodkinson [3], Vermes [18]. All the people who used the Martin's basic equation added different coefficients to determine the compressibility factor either empirically or on the basis of some hypothesis. Truly none of them accurately defined the compressibility factor earlier because either the assumptions made were wrong and also the disability to correctly solve the turbulent flow regime whose accuracy cannot be more than the CFD solver code used to solve them. Further we are going to analyze the effects of various non- dimensional fluid and geometrical parameters on the compressibility factor as we did for the carry over and discharge coefficients earlier.

8.1 Effect of Position of Tooth on the Compressibility Factor

Figure 8.2 shows the effect of compressibility for both the first tooth and the second tooth. The need for this study arises after coming across the difference in the value of the discharge coefficient. Also, as the absolute pressure in each seal cavity decreases in the downstream direction, the pressure ratio increases. The minimum value usually occurs at the last tooth where the flow may be choked.

.

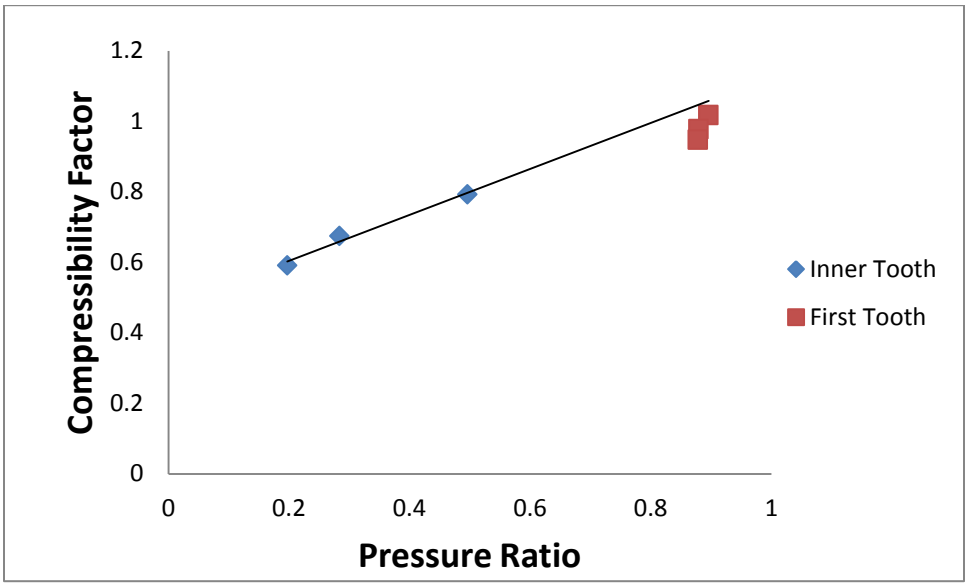

Fig 8.2 Variation of compressibility factor with tooth position

From the above Figure 8.2 it is clearly visible that the compressibility factor variation is negligible with the tooth position so it becomes valid that the relations that would be found between flow parameters and geometrical parameters on compressibility will be valid for the entire teeth series similarly. So this eliminates the need to separately analyze the first tooth from the other teeth on the labyrinth seals for all the parameters suspected to change it.

8.2 Effect of Flow Parameters on Compressibility Factor

As stated in all the earlier studies, compressibility has been shown to be a major function of pressure ratio (here we refer to the absolute pressure ratio across the tooth rather than across the whole seal).

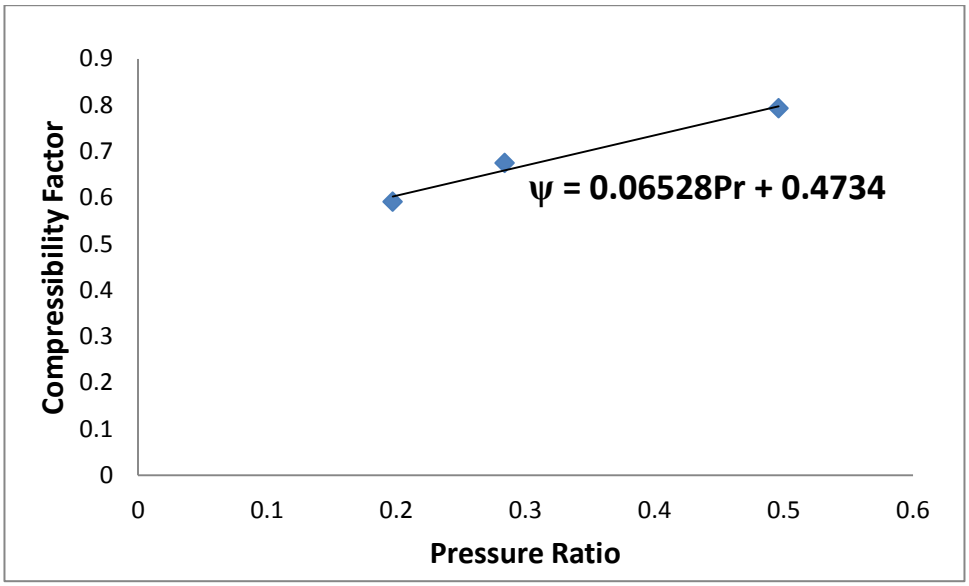

Fig 8.3 Variation of compressibility factor with pressure ratio

For the Figure 8.3 geometry, G2 has been chosen due to the similar Reynolds number simulation for air and water cases as compared to that for the other geometries. For the current graph, the pressure ratio across the last tooth has been chosen because of the pressure ratio increases across the tooth as the flow progresses from upstream to downstream as known from Gas Dynamics. From the above graph it is clear that there exists a linear relation between Pressure Ratio and Compressibility Factor. This fact is exactly the same as in the case of tooth on rotor cases except that it is more prominent for the tooth on rotor case than the tooth on stator labyrinth arrangement. This is because increasing Reynolds number increases the pressure ratio more in case of tooth on rotor than the tooth on stator. This fact can be attributed to the reason that the boundary layer area moving is different in the two arrangements. In the case of tooth on stator about 20% of the wet seal area is moving with the shaft while in tooth on rotor about 70% of the wet

seal area is rotating along with the shaft. So there is more energy transfer to increase the pressure ratio of the fluid flowing through the latter case. In other words we could say that for same geometry of both the teeth arrangement, tooth on rotor has more pressure difference across the seal so the compressibility is more prominent here.

8.3 Effect of Clearance on Compressibility Factor

Three different clearances to pitch ratios will be examined to determine clearance effect upon the compressibility factor. This change is studied by considering geometries with same geometrical features apart from clearances. For this reason, the geometries G2, G3 and G5 qualify for this test.

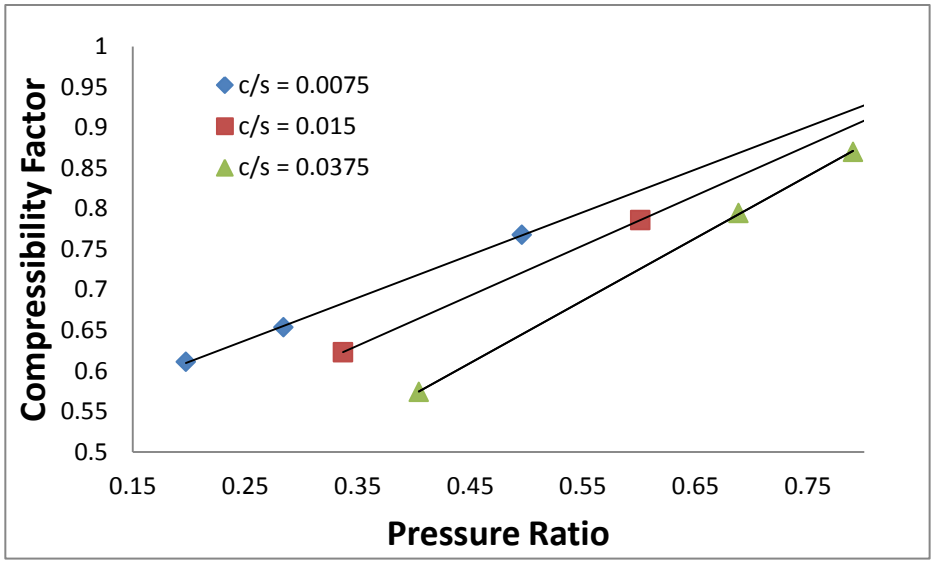

Fig 8.4 Variation of compressibility factor with c/s ratio

From the above Figure 8.4 it is seen that the compressibility factor does not varies much with the clearance to pitch ratio. This implies there is negligible change with this factor on compressibility.

8.4 Effect of Tooth Width on Compressibility Factor

In this subsection the effect of changing the tooth width to pitch ratios on the compressibility factor will be examined. This change is studied by considering geometries with same geometrical features and apart from tooth width will be considered. For this reason the geometries G1and G2 qualify for this test. Figure 8.5 shows that

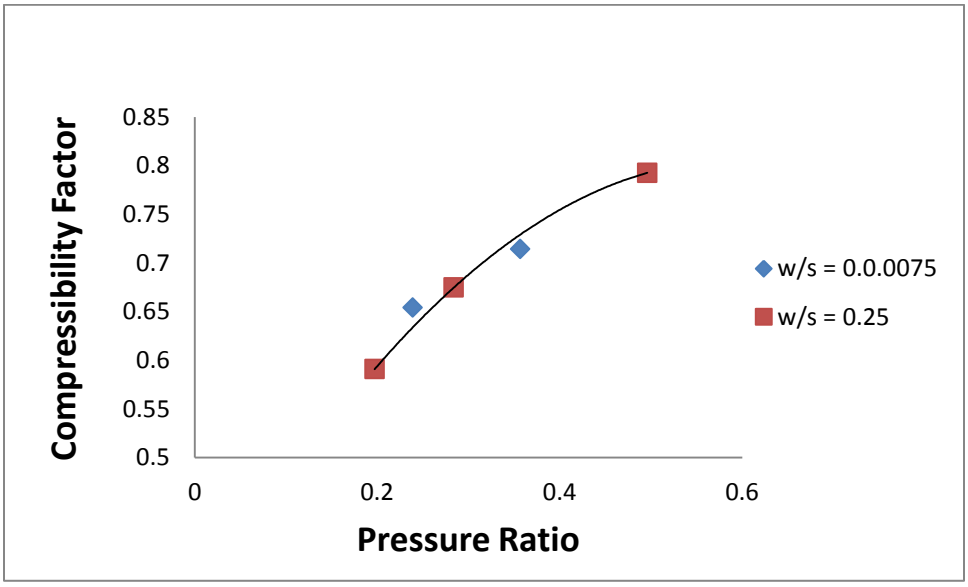

Fig 8.5 Effect of compressibility factor with w/s ratio

there is no major variation of the discharge coefficient from changing the tooth width which implies it is independent of this factor.

8.5 Effect of Shaft Rotation on Compressibility Factor

The effect of changing the shaft surface speed on the compressibility factor will be analyzed next. This change is studied by considering various shaft speeds without varying the Reynolds number or geometry. For this study geometry G1 and a Reynolds number of 1000 were chosen. This choice of geometry and Reynolds number is purely arbitrary and comparison could be done using other geometries as well.

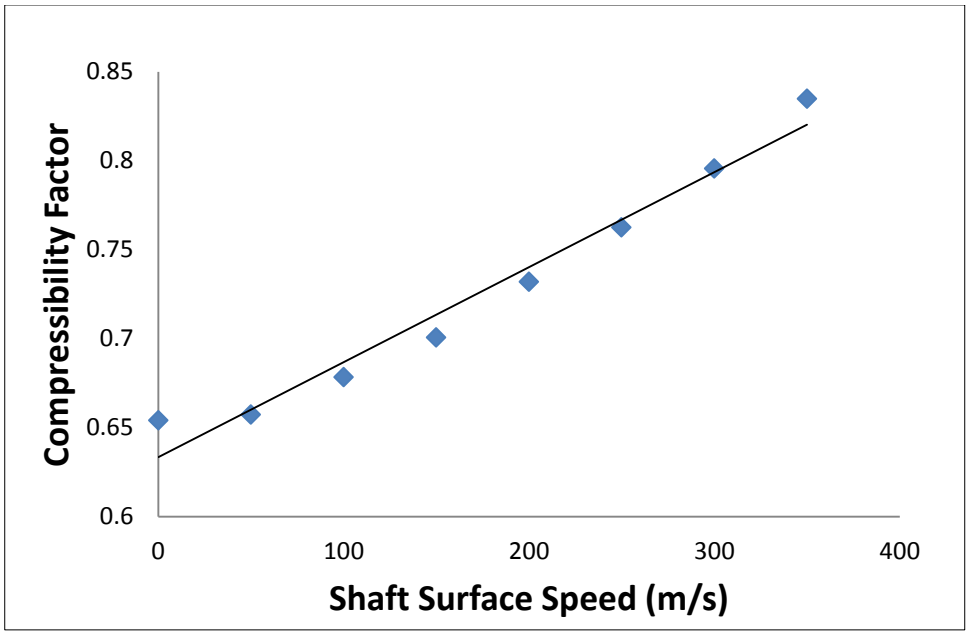

Fig 8.6 Effect on compressibility factor with shaft speed

Figure 8.6 shows that compressibility factor increases with increasing shaft speed. Also we know that the pressure difference across the tooth increases with the increasing shaft rotation speed. So we conclude that the behavior of Coefficient of Discharge of

water and air are same for same Reynolds Number and Geometry are same for increasing RPM.

8.6 Contours of Compressibility Factor

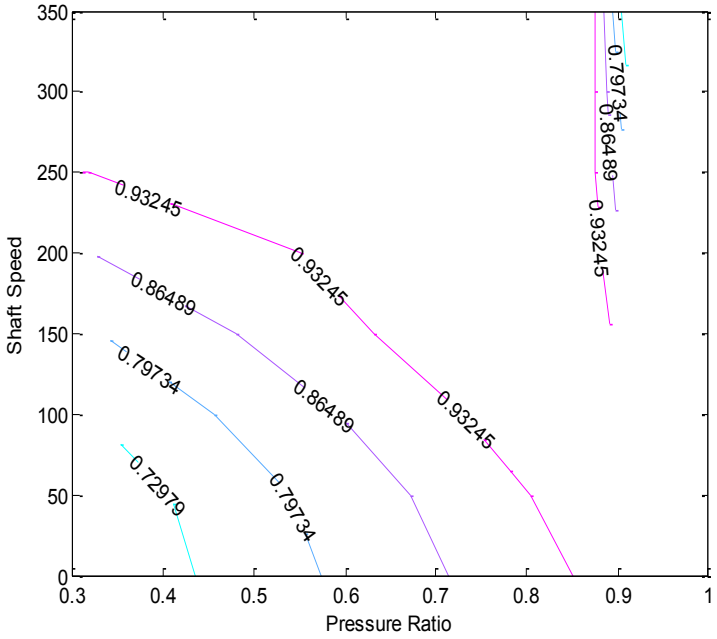

Fig 8.7 Contour of ψ for Re=1000, G1

The Figures (8.7, 8.8, 8 9, 8.10 &8.11) gives an illustration of the variation of compressibility factor by varying tooth geometry and shaft speed.

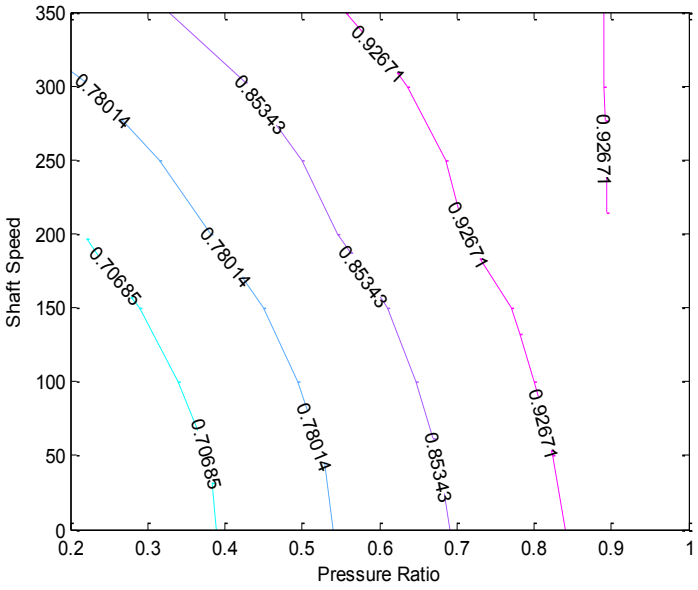

Fig 8.8 Contour of ψ for Re=1500, G1

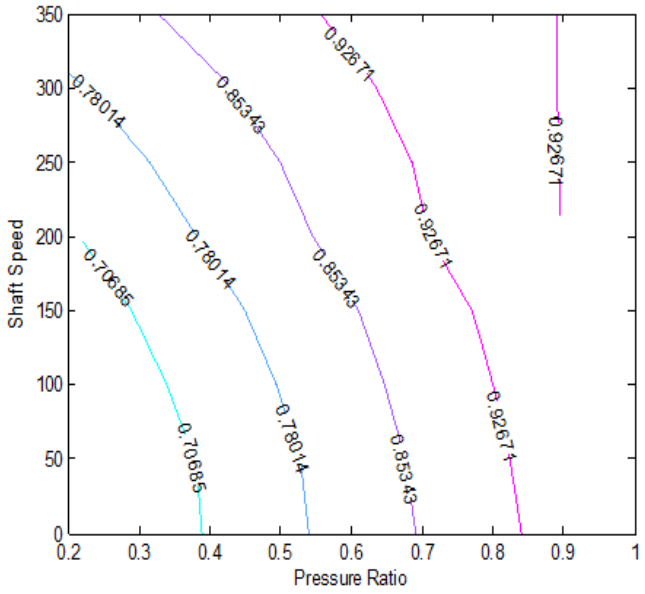

Fig 8.9 Contour of ψ for Re=2000, G1

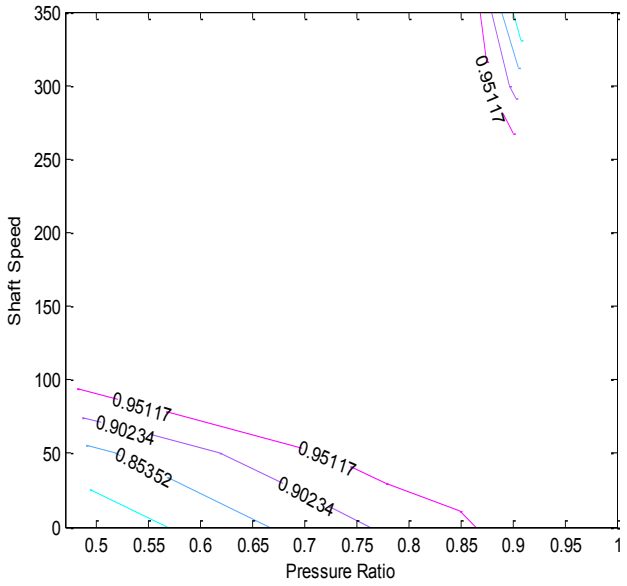

Fig 8.10 Contour of ψ for Re=500, G2

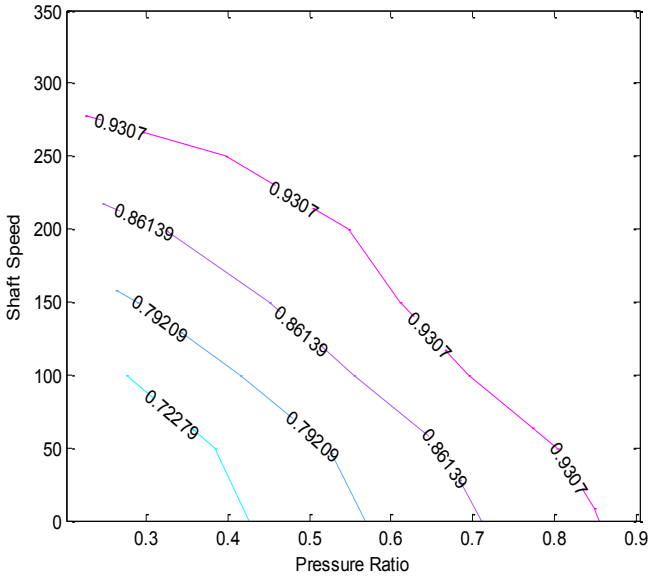

Fig 8.11 Contour of ψ for Re=1000, G2

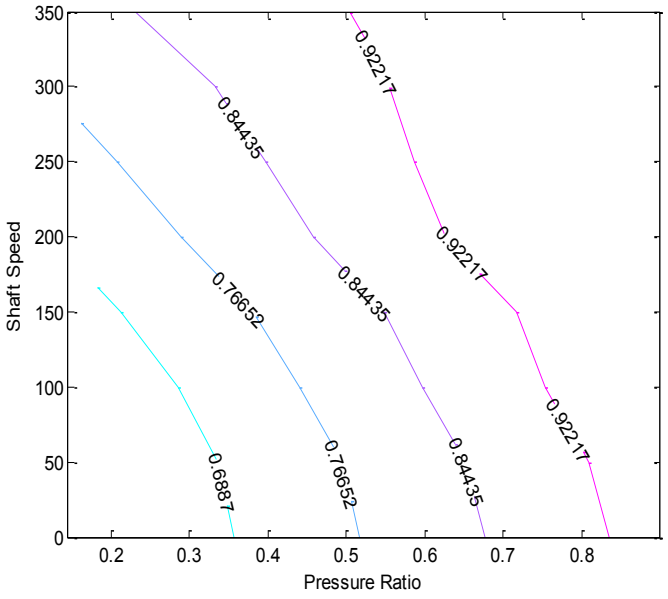

Fig 8.12 Contour of ψ for Re=1500, G2

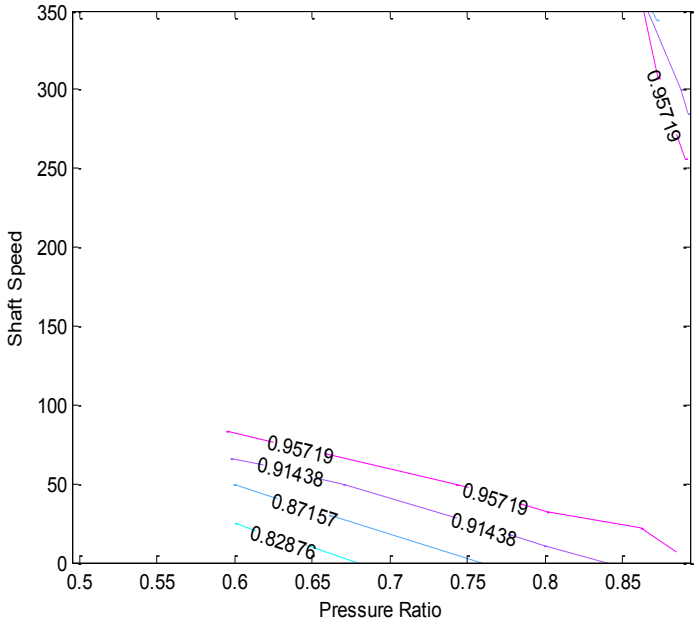

Fig 8.13 Contour of ψ for Re=1000, G3

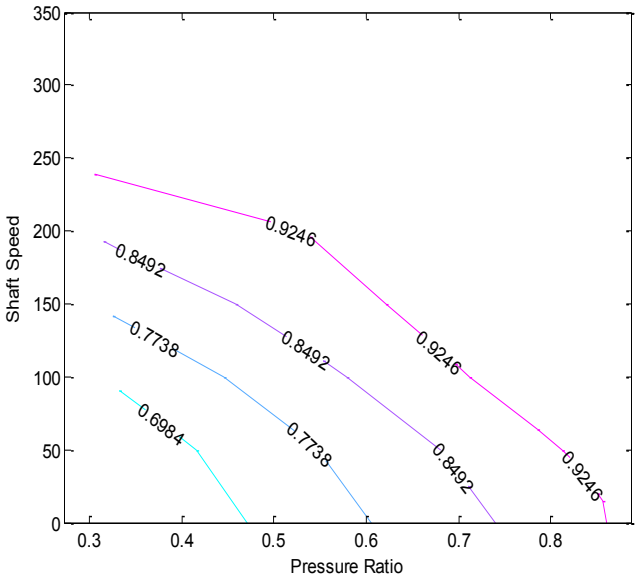

Fig 8.14 Contour of ψ for Re=2000, G3

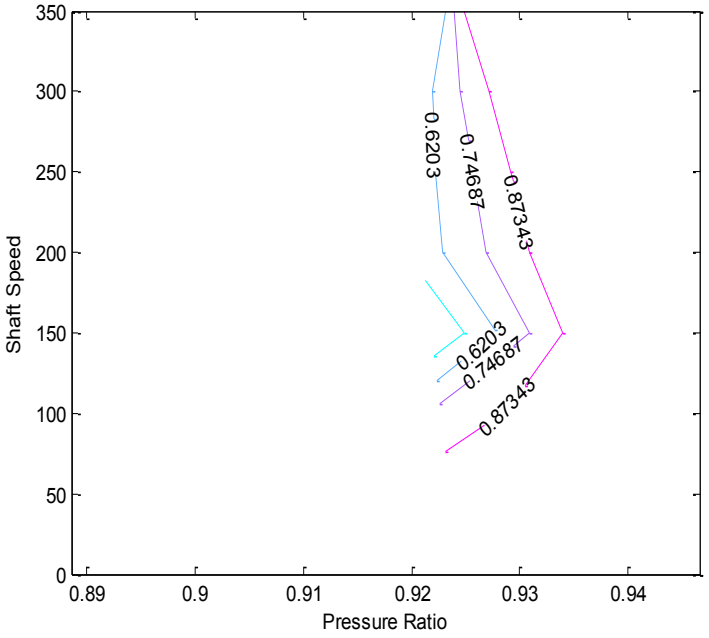

Fig 8.15 Contour of ψ for Re=1000, G4

Similarly Figures (8.12, 8.13, 8.14, 8.15, 8.16, 8.19 & 8.20) shows variation of compressibility factor by varying tooth geometry and shaft speed.

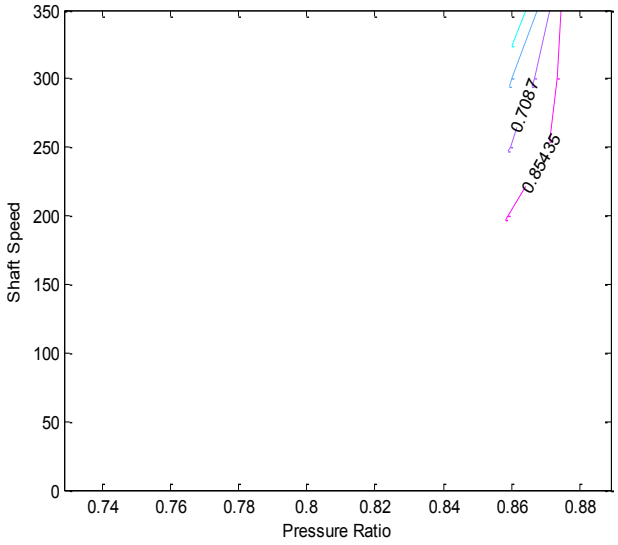

Fig 8.16 Contour of ψ for Re=2000, G4

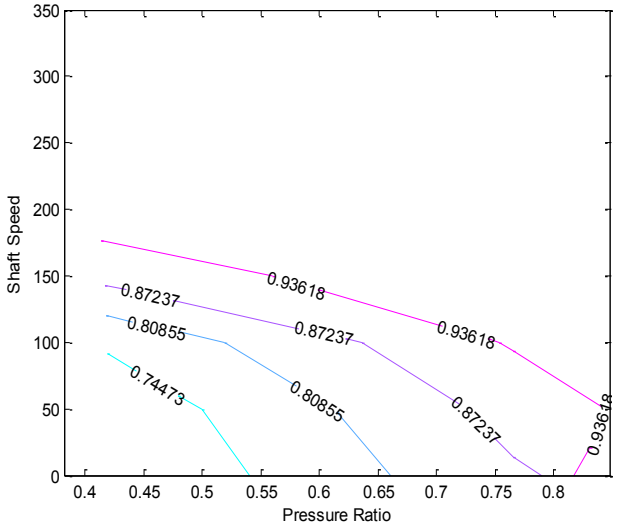

Fig 8.17 Contour of ψ for Re=5000, G4

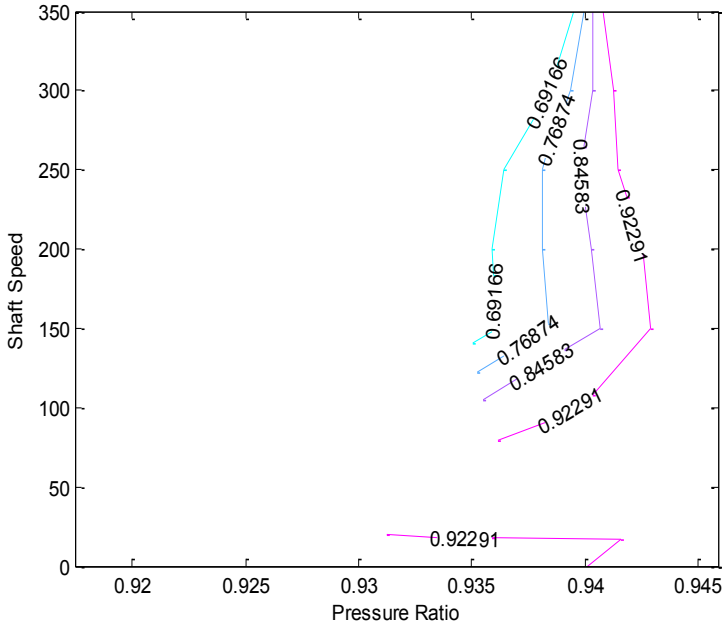

Fig 8.18 Contour of ψ for Re=1000, G5

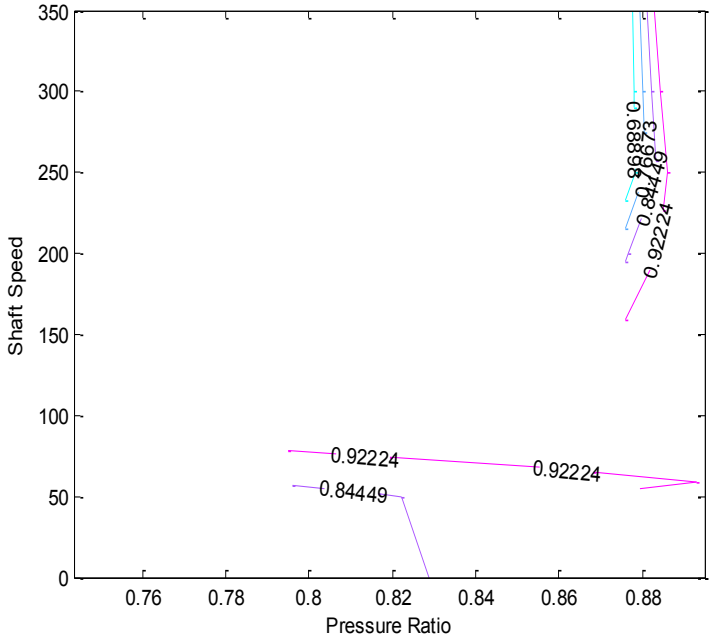

Fig 8.19 Contour of ψ for Re=2000, G5

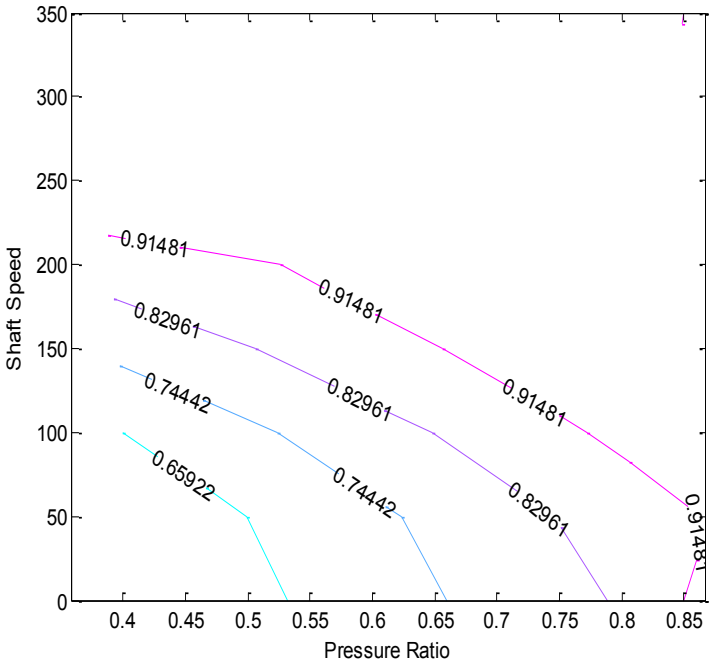

Fig 8.20 Contour of ψ for Re=5000, G5

For the geometry G1(smallest c/s and w/s) Figures 8.7 and 8.8 show how compressibility factor decreases as the Reynolds number increases, the Taylor number decreases and the pressure ratio decreases. Saikishan had showed for tooth on stator seals that compressibility factor decreases with decreasing pressure ratio. The present study shows how increasing shaft speed (Taylor number) decreases the effects of compressibility. Since the value of coefficient of discharge is highly dependent upon Reynolds number and Taylor number, these data also indicate some Reynolds number

dependence. This is due to the changing nature of the recirculation zone with the value of Reynolds number and Taylor number.

Increasing the tooth width to pitch ratio to 0.25 (G2, Figures 8.10 to 8.12) at same pressure ratio does not change the effects of compressibility (larger compressibility factor values) tremendously. The effect of Taylor Number is also decreased with this much wider tooth width. There is still a significant increase in compressibility factor as Reynolds number increases. This further confirms that the pressure ratio is the only governing factor which changes the compressibility.

Maintaining the large tooth width and increasing the seal clearance to pitch ratio (G3, w/s =0.25 and c/s=0.015) compressibility factors is decreases slightly. This implies an increment in compressibility. Taylor number dependence is further reduced.

The two geometries with largest clearance to pitch ratio cases G4 (w/s =0.0075 and c/s=0.0375) and G5 (w/s =0.25 and c/s=0.0375) had minimized data obtained at lower Reynolds numbers as indicated by the small regions of contours. The compressibility factor is also changing at a comparatively slower pace than that from the geometries with smaller clearance to pitch ratio cases G1 (w/s =0.0075 and c/s=0.0075) and G2 (w/s =0.25 and c/s=0.0075). Also to note that the effect of changing clearance to pitch (c/s) is more pronounced than by changing tooth width to pitch (w/s) as visible from Figures 8.7 and 8.15 for G1and G4 for Re=1000.

From the above discussions we conclude that compressibility is *only* a function of pressure ratio which change by varying Taylor Number and Reynolds Number for a flow field. Any change in geometry and boundary condition keeping pressure ratio

constant across tooth will not change the compressibility factor. This agrees well with definition of compressibility factor which has been defined to take care of changing fluid density (only a function of pressure and temperature for a given ideal working fluid. Further it has been also confirmed that density ratios and pressure ratios across a tooth are fairly same. This further supports the results obtained.

9. SUMMARY

9.1 Carry over Coefficient

The carry over coefficient was calculated using the divergence angle of the seal. The definition given by Hodkinson was used to calculate the carry over coefficient. It was found that it depends upon flow conditions, geometry of the seal and the changing boundary conditions. It was found that for cases with water as working fluid carry over coefficient does increase with Reynolds number. This increase is same in nature for the case on stator arrangement. The tooth clearance to pitch (c/s) was determined to be the major geometrical parameter to determine the carry over coefficient. It was observed that the tooth width to pitch ratio (w/s) cannot be neglected at higher Reynolds number flow where its effect is a major consideration. Shaft RPM effect was very complex which suggests to study about the changing shear forces with changing flow field in the cavity from one vortex to the complete generation of secondary vortex at high Taylor number. By comparing all the factors it was concluded that Taylor number decreases at higher carry over coefficient.

9.2 Discharge Coefficient

It is defined to calculate the total pressure loss in a labyrinth seal. This coefficient was found to vary with the position of the teeth on the shaft. While the first tooth was found to have more losses than the intermediate teeth as was for the teeth on stator

configuration. The discharge coefficient was found to increase with the Reynolds number for a given geometry and shaft speed. Among the geometrical factors relation of discharge coefficient with tooth clearance to pitch (c/s) was found at lower Reynolds number which dies away with the increasing flow inertia. Tooth width to pitch ratio (w/s) was also found to change discharge coefficient at low Reynolds number. Taylor number increment also found to change discharge coefficient in the opposite direction.

9.3 Compressibility Factor

This factor is defined to correlate the flow losses of compressible fluid to incompressible flow. It is calculated using the ratio of discharge coefficient for air to that of water at the same Reynolds number for a given geometry and tooth. It was found to be mainly dependent on shaft RPM and pressure ratio. While for the tooth width to clearance ratio (w/s) and tooth width to clearance ratio (w/c) affects the compressibility factor negligibly less. It is also found that tooth position also does not effect this value but increases linearly with the shaft RPM.

9.4 Suggestible Tooth Configuration

So from this study we conclude that the most efficient tooth geometry is decided by the shaft RPM in the following way. For stationary shaft we need to have small c/s and low Reynolds Number. Further it could be divided into two cases using the Table 5 below:

Table 5 C_d and γ variation with c/s ratio

	Tooth width (w)	Carry over coefficient (γ)	Discharge Coefficient T1	Discharge Coefficient T2
Large (c/s=0.0375) G4 & G5	**Increases**	**Increases**	**Increases**	**Increases**
Small (c/s= 0.0075) G1 &G2	**Increases**	**Increases**	**Decreases**	**Decreases**

For the lower clearance to pitch ratio (c/s) we need to have large tooth width but for the larger clearance to pitch ratio (c/s) we need to have small tooth width. For the rotating shaft we need low Reynolds number for better performance of intermediate tooth and high Reynolds for first tooth (other ratios being same as earlier). This implies we need to adjust the shaft speed for a given mass flow rate to maximize the pressure difference across the seal. Additionally we also need more tooth width for small clearance to pitch ratio (c/s) but for the larger clearance to pitch ratio we need to have small tooth width.

10. RECOMMENDED FUTURE WORK AND CONCLUSION

The current research work has been done within few limitations and simplifications. So there is a need of study the effects of these additional factors on the flow field defining so that we could have a more versatile formulae for the application.

1. This study involves the study of tooth on the same shaft diameter. So we need to further study the effect of changing the shaft diameter for the configuration of tooth on rotor.
2. The current work involves the study of various teeth with different flow and geometric limitations. So there is a need to explore the same effect with the increasing tooth clearances and tooth width. This would help to understand more about the different seals used in the industry which are not limited by the geometric and flow criteria of this study.
3. The current study uses ideal air as the compressible fluid for the study so we need to explore the effect of the different real gases on the losses through the seals. This should be incorporated with real gas equation where more accurate leakage results could be derived for the real gas in application in various turbines and the compressors.
4. This study is limited to the straight through rectangular tooth on rotor. So there is a need to explore the seals with different tooth geometries and different arrangements. This includes staggered and stepped seals.
5. Different papers have done the fluid analysis work using various CFD turbulence models. So there is a need to explore the changes in the results made by these different

turbulence models and compare them with the experimental results where shaft speed goes higher than Mach 1. This might suggest a change in turbulence models with the increasing shaft speed.

6. The viscosity of the fluid under high pressures such as 200 atm for water has been considered to be constant. So an effort could also be made to see the variance in the mass flow leakages with the variation of the fluid viscosity.

REFERENCES

[1] "The Labyrinth Packing" *Engineer* Vol. **165**, 4280, Jan21, 1938, pp. 23-84.

[2] Manish, T., 2009, "Impact of Rotor Surface Velocity, Leakage Models and Real Gas Properties on Rotor dynamic Force Predictions of Gas Labyrinth Seals," M.S. dissertation. Texas A&M University, College Station.

[3] Hodkinson, B., 1939, "Estimation of the Leakage Through a Labyrinth Gland," Proceedings of the Institution of Mechanical Engineers **141**, pp. 283–288

[4] Becker, E. "Stromungsvergange in Ringformigen Spalten," V.D.I., **51**, 1907, pp.1133-1141.

[5] Martin, H.M., Jan 19, 1908 , "Labyrinth Packings,"Engineering, pp 35-36.

[6] Stodola, A., 1927, *Steam and Gas Turbines*, 6th ed., The McGraw-Hill Book Company, New York.

[7] Dollin, F. and Brown, W.S., 'Flow of Fluids Through Opening in Series," Engineer, 164, 4259, Aug 27, 1937, pp. 223-224.

[8] Gercke, M., 1934, "Flow Through Labyrinth Packing," *Mechanical Engineer*, **56,** pp. 678-680.

[9] Elgi, A., 1935, "The Leakage of Steam Through Labyrinth Seals," Trans. ASME, **57**, pp. 115-122.

[10] Keller, C., 1937, "Flow Through Labyrinth Glands", Power Plant Engineering, **41**, 4, pp 243-245.

[11] Bell, K. J. and Bergelin, O.P., 1957(April), "Flow Through Annular Orifices," ASME Transactions, **79**, 3, pp 593-601

[12] Kearton, W. J. and Keh, T. H., 1952, "Leakage of Air Through Labyrinth Glands of Staggered Type," Institution of Mechanical Engineers Proceedings, **166** (2), pp. 180-188.

[13] Zabriske, W. and Sternlicht, B., Sept 1959, "Labyrinth Seal Leakage Analysis", Journal Basic Engineering, **81,** 332-40.

[14] Heffner, F.E., June1960, "A General Method for Correlating Labyrinth Seal Leak-Rate Data", Journal Basic Engineering, 265-75.

[15] Kmotori, H. and Mori T., 1986, "Theoretical and Experimental study of the destabilizing force by Labyrinth Seal", TAMU Instability Workshop.

[16] Rao, V.K. and Narayanamurthi, R.G., 1973, "An Experimental study of the performance characteristics of Labyrinth Seal," Indian Engineering Journal, **56**, pp176-181.

[17] Deych, M. YE., Sept1 1969, "Research on the flow of Moist Vapor in Asymmetrical Laval Nozzles within a broad range of Degrees of moisture", NASA.

[18] Vermes, G., 1961, "A Fluid Mechanics Approach to the Labyrinth Seal Leakage Problem," ASME Transactions - Journal of Engineering for Power, **83** (2), pp. 161-169.

[19] Schlichting, H., Boundary Layer Theory, 8th ed., Springer Publication, New York.

[20] Gamal, A.M., 2007, "Leakage and Rotor-dynamic Effects of Pocket Damper Seals and See-Through Labyrinth Seals," Ph.D. dissertation. Texas A&M University, College Station.

[21] Suryanarayanan Saikishan, 2008, "Labyrinth Seal Leakage Equation", M.S. dissertation. Texas A&M University, College Station.

[22] Morrison, G.L. and Al-Ghasem, A., 2007, "Experimental and Computational Analysis of a Gas Compressor Windback Seal," GT2007-27986, Proceedings of ASME Turbo, Expo 2007, Montreal, Canada, May 14-17.

[23] Johnson M.C., 1989, "Development of a 3-D Laser Doppler Anemometry System with Measurements in Annular and Labyrinth Seals," Ph.D. dissertation. Texas A&M University, College Station

[24] Stoff, H., 1980, "Incompressible Flow in a Labyrinth Seal," ASME Transactions-Journal of Fluid Mechanics, **100** (4), pp. 817-829.

[25] Demko, J. A. 1986, "The Prediction and Measurement of Incompressible Flow in a Labyrinth Seal," Ph.D. dissertation. Texas A&M University, College Station

[26] FLUENT v 12.1 User's Guide, Fluent Inc., Lebanon, NH.

[27] Pope, S.B., 2000, *Turbulent Flows*, Cambridge University Press, Cambridge, U.K.

APPENDIX

Cavity 2

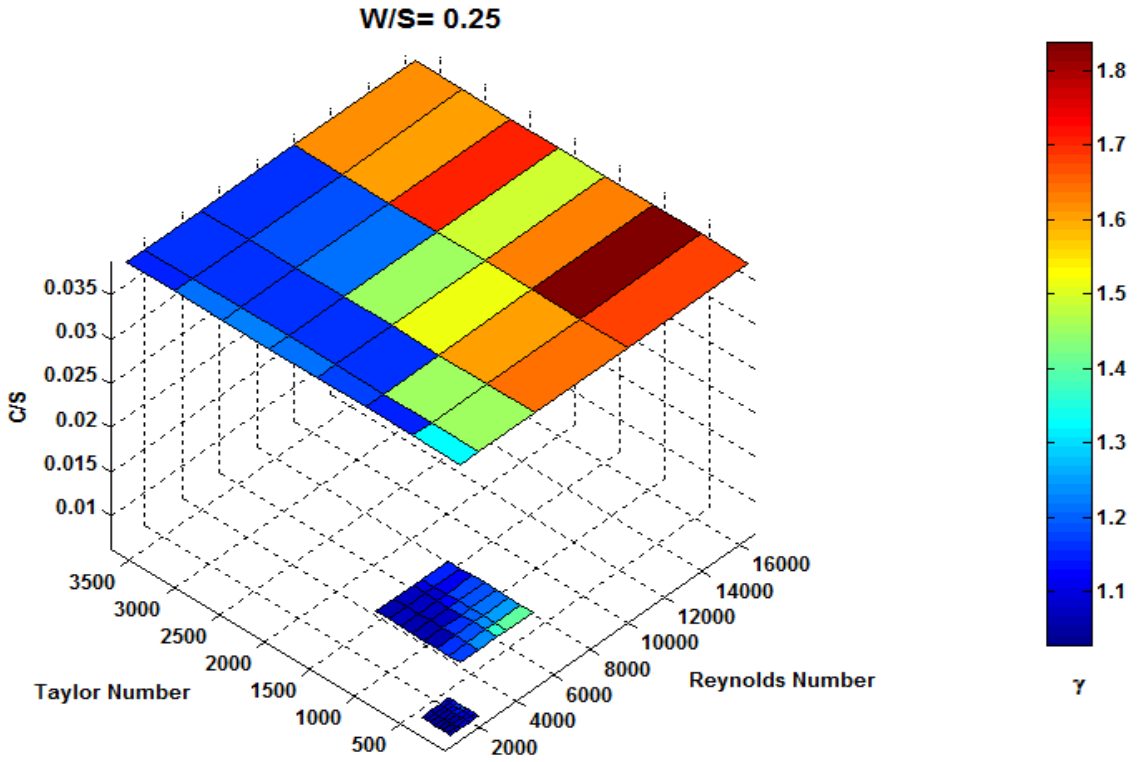

Fig A.1 γ changes with Ta, Re and C/S for W/S =0.25 (G2, G3 & G5)

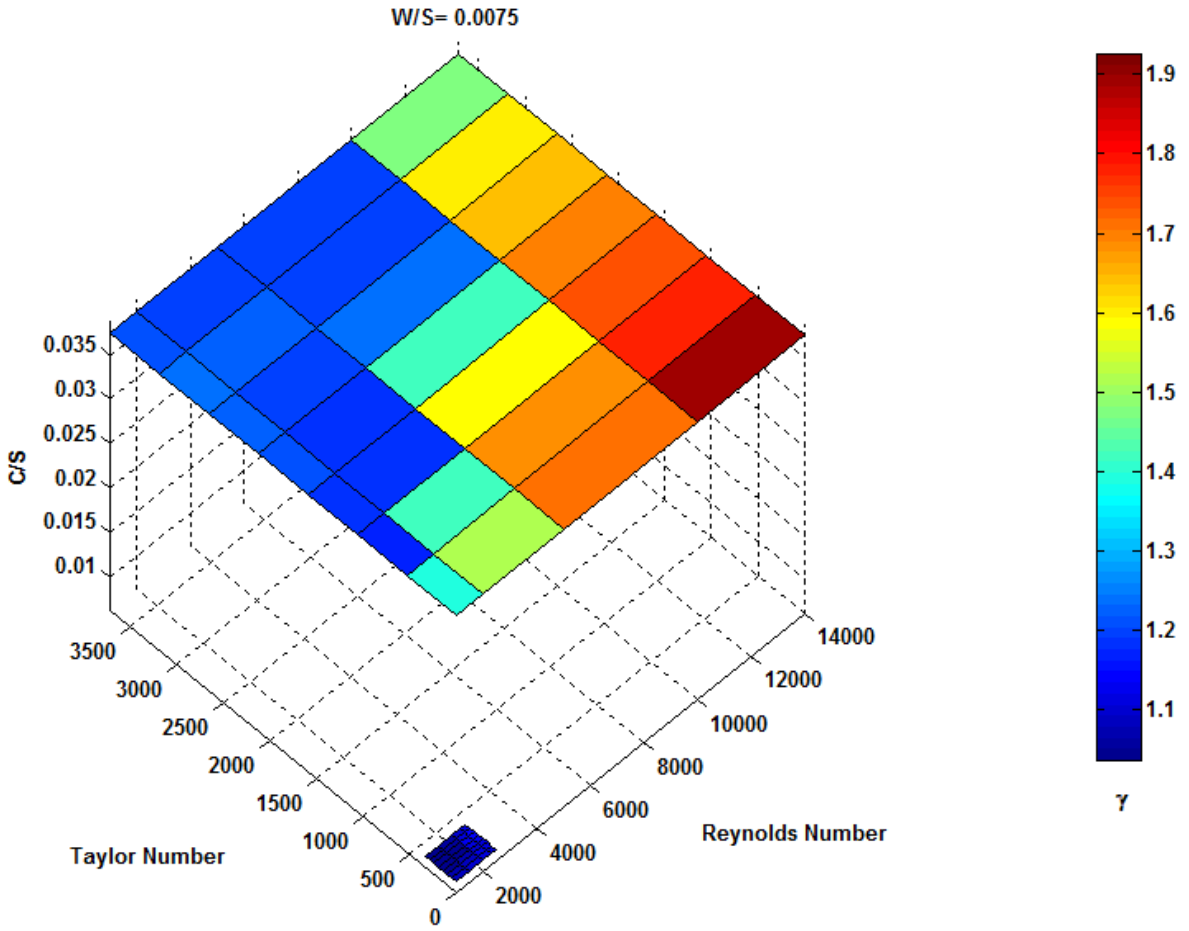

Fig A.2 γ changes with Ta, Re and C/S for W/S =0.0075 (G1 & G4)

Cavity 3

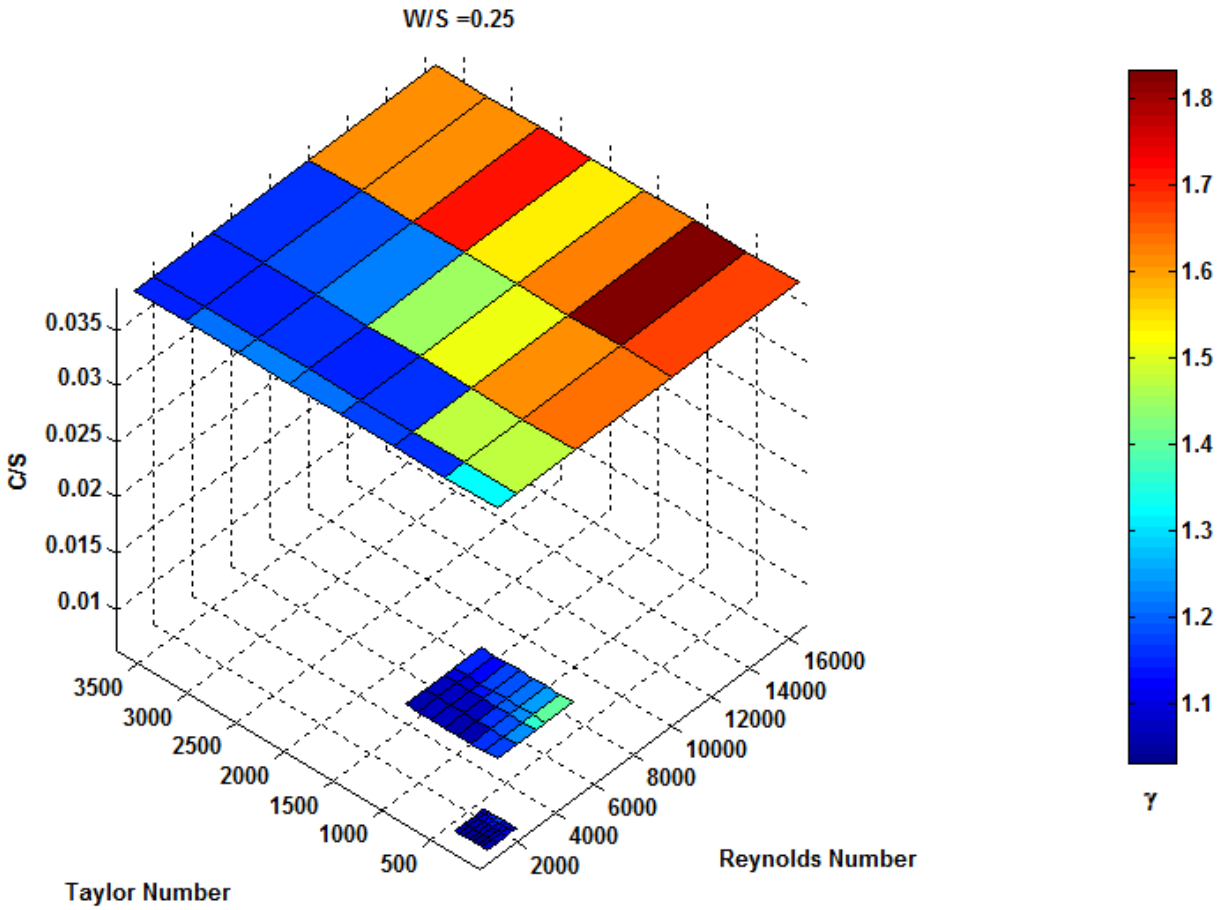

Fig A.3 γ changes with Ta, Re and C/S for W/S =0.25 (G2, G3 & G5)

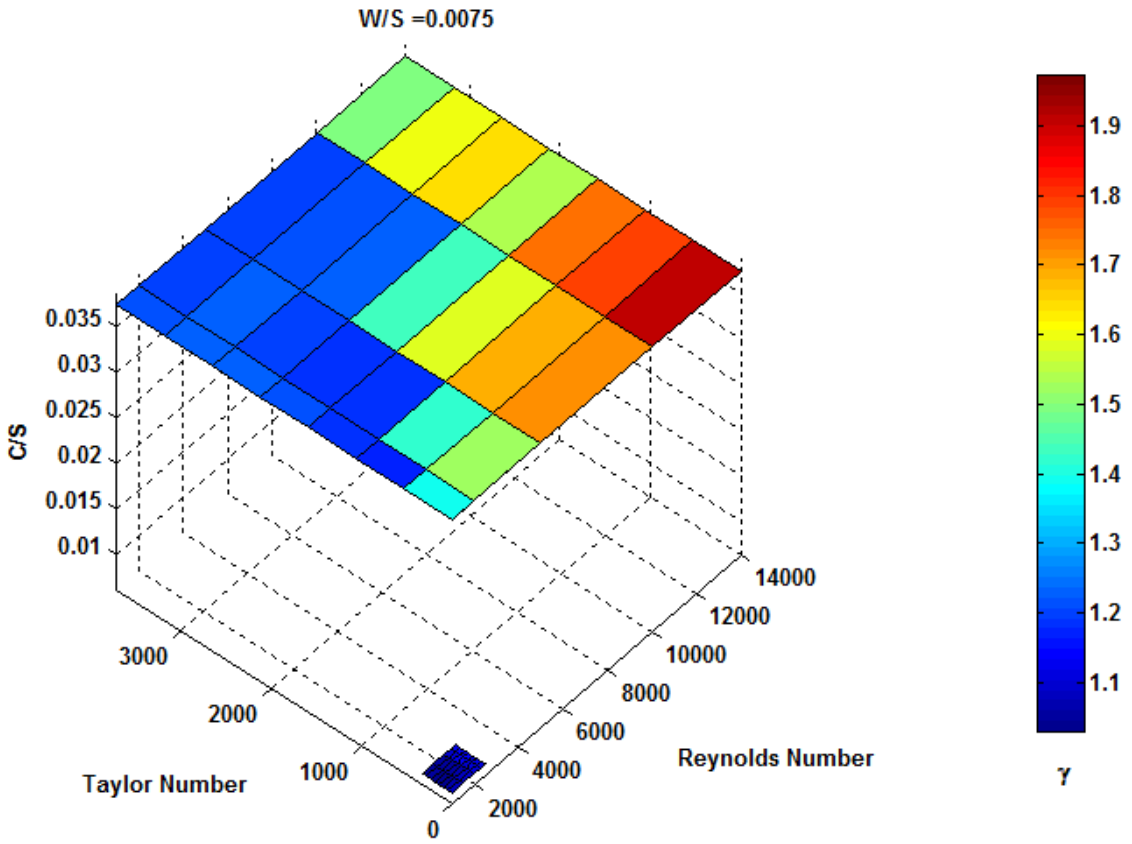

Fig A.4 γ changes with Ta, Re and C/S for W/S =0.0075 (G1 & G4)

Tooth 2

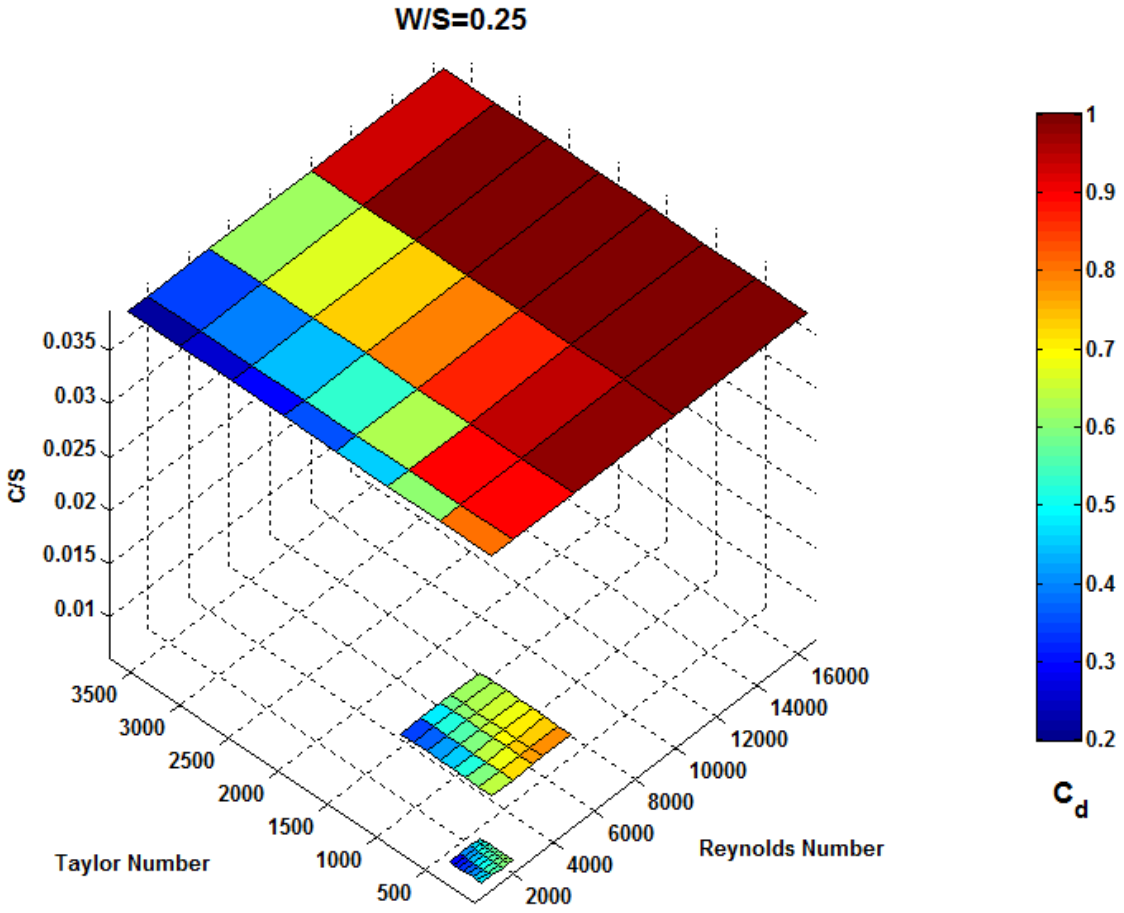

Fig A.5 C_d changes for Ta, Re and C/S for W/S =0.25 (G2, G3 & G5)

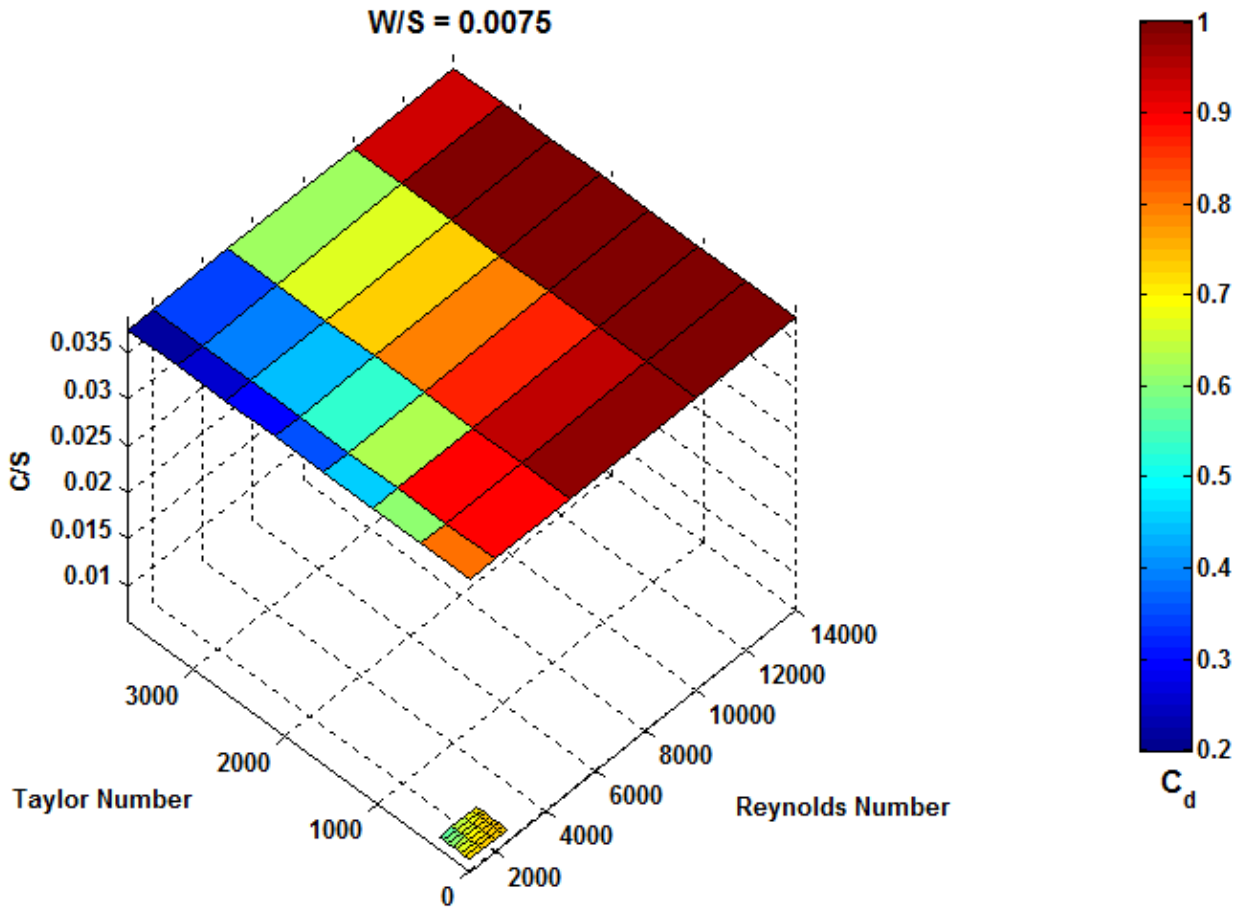

Fig A.6 C_d changes for Ta, Re and C/S for W/S =0.0075 (G1 & G4)

Tooth 3

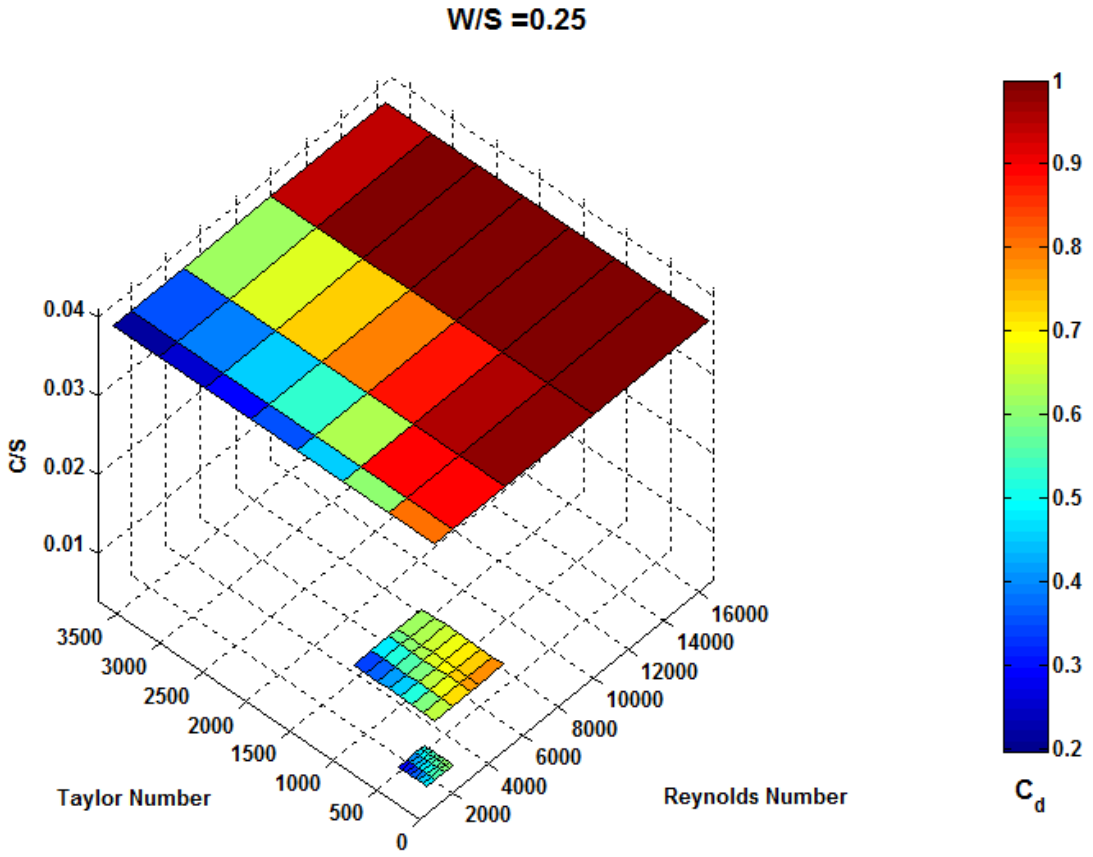

Fig A.7 C_d changes for Ta, Re and C/S for W/S =0.25 (G2, G3 & G5)

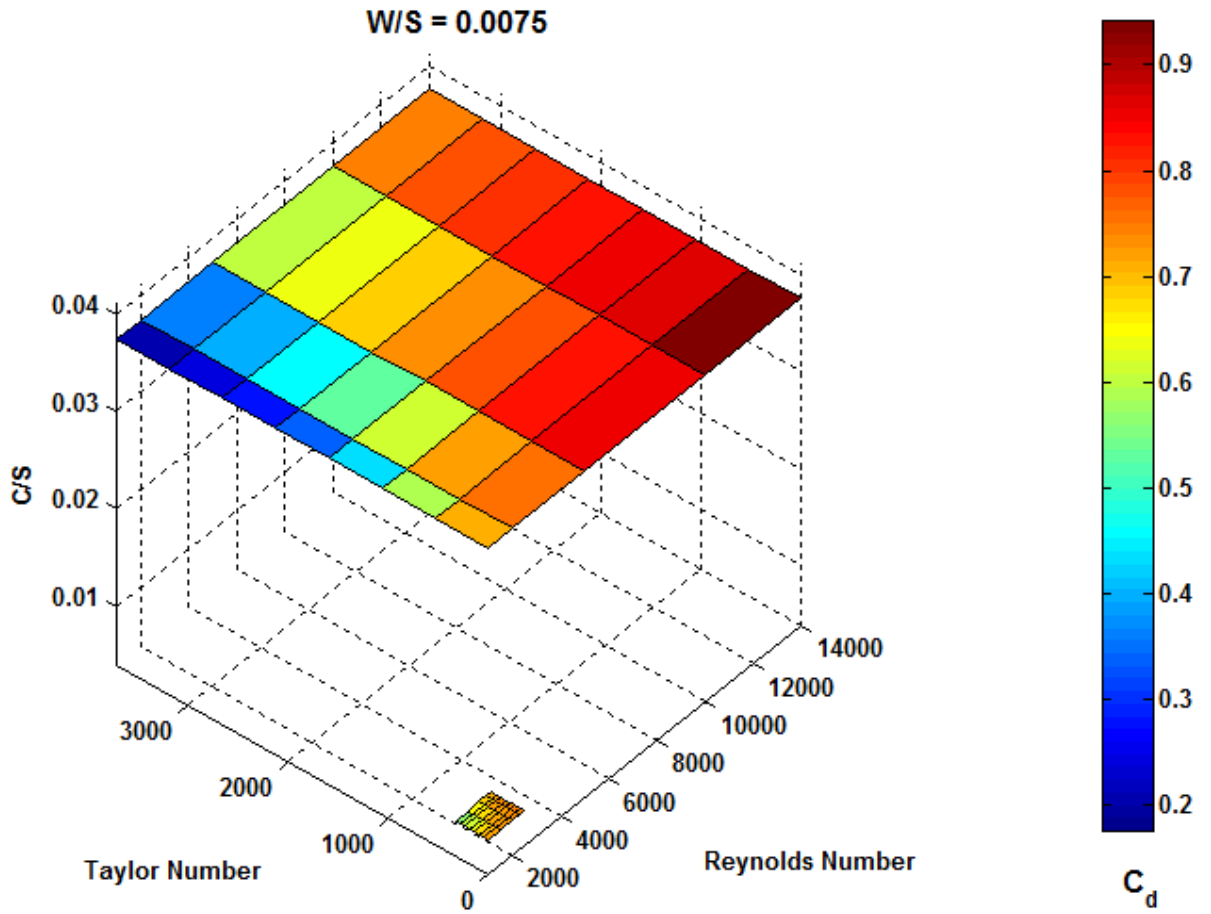

Fig A.8 C_d changes for Ta, Re and C/S for W/S =0.0075 (G1 & G4)

Tooth 4

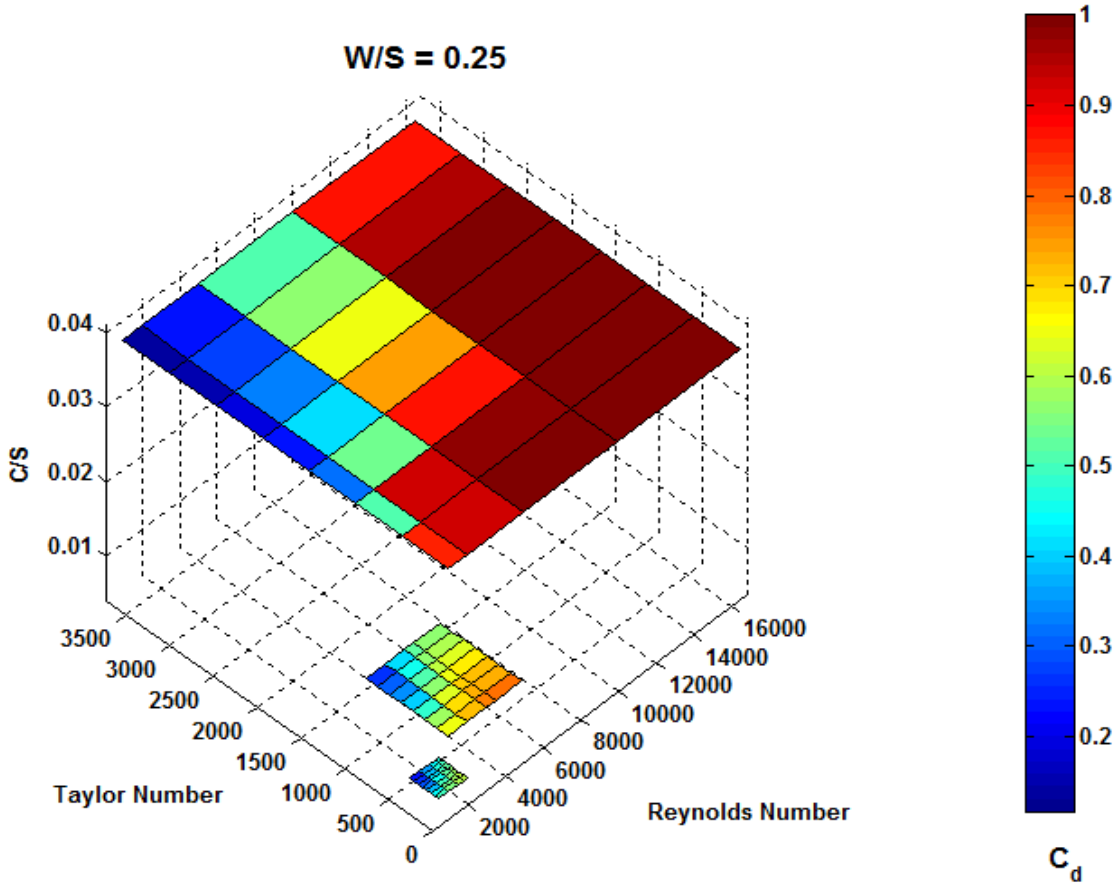

Fig A.9 C_d changes for Ta, Re and C/S for W/S =0.25 (G2, G3 & G5)

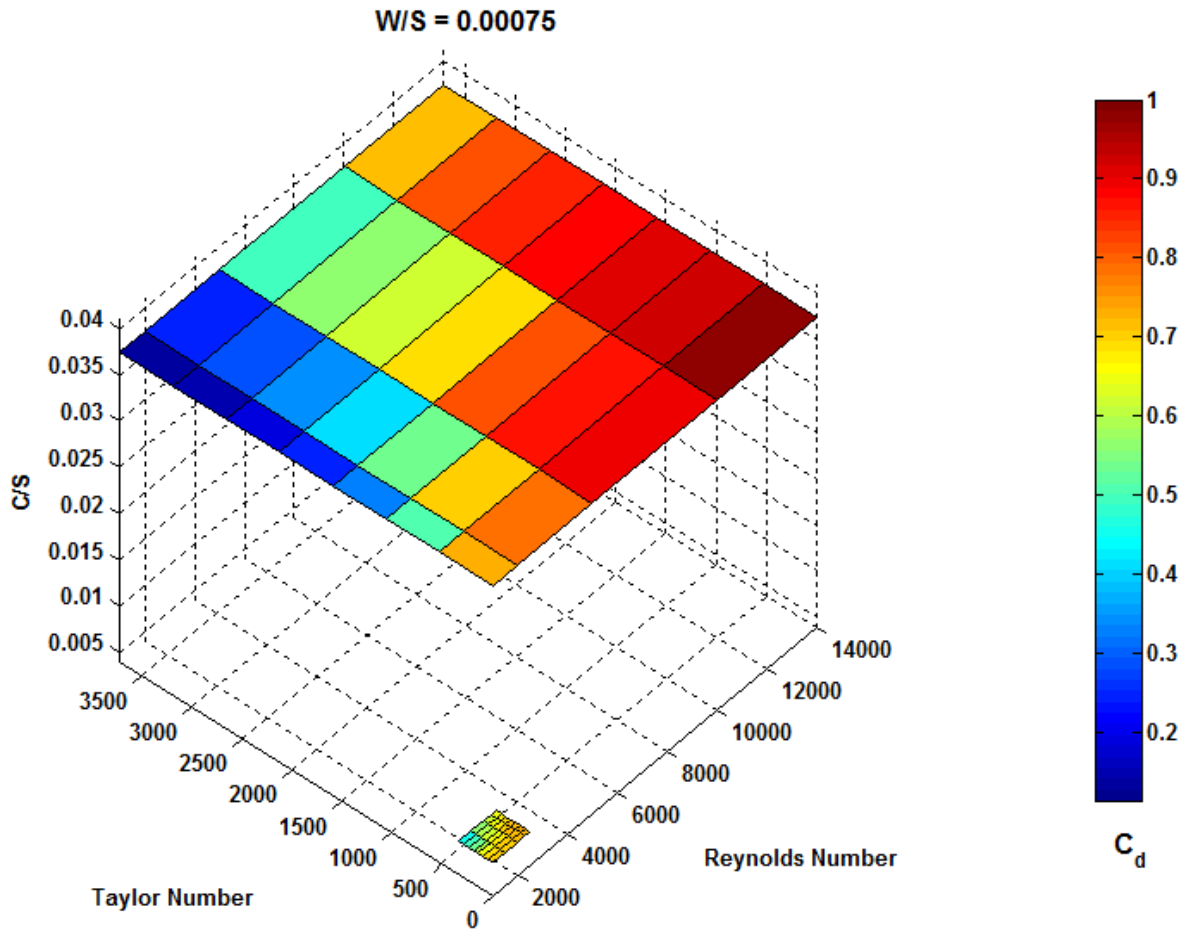

Fig A.10 C_d changes for Ta, Re and C/S for W/S =0.0075 (G1 & G4)

Table 6 Seal geometries used for simulation

Geometry	No. of Teeth	Clearance (mm)	Pitch (mm)	Tooth Width (mm)	Tooth Height (mm)	Shaft Diameter(mm)	c/s Ratio	w/s Ratio
G1	4	0.03	4	0.03	4	60	0.0075	0.0075
G2	4	0.03	4	1	4	60	0.0075	0.25
G3	4	0.06	4	0.03	4	60	0.015	0.25
G4	4	0.15	4	0.03	4	60	0.0375	0.0075
G5	4	0.15	4	1	4	60	0.0375	0.25

Table 7 ΔP (Pascal) variation with shaft surface speed Wsh (m/s)

G1								
	Wsh =0	Wsh =50	Wsh =100	Wsh =150	Wsh =200	Wsh =250	Wsh =300	Wsh =350
Re	ΔP	ΔP	ΔP	ΔP	ΔP	ΔP	ΔP	ΔP
1000	3413788.21	3582087.5	3849660	4220801	4605168	4880281	5367920	5815410
1500	7618018.42	7777858	8046450	8388645	8849893	9120362	9572990	10155160
2000	13335988.9	13339244.7	13645164	13869371	14048082	14725855	15181390	15548790
2300	17609264.4	17521892.8	17883948	17974905	18057876	18507996	19189750	21876750
2500	20732839.8	20930433.7	21319119	21620355	21796696	22344856	22814021	23653760

G2								
	Wsh =0	Wsh =50	Wsh =100	Wsh =150	Wsh =200	Wsh =250	Wsh =300	Wsh =350
Re	ΔP	ΔP	ΔP	ΔP	ΔP	ΔP	ΔP	ΔP
500	1881144.9	2123379.2	2667891	3289486	3925837	4558152	5163120	5865900
1000	5693481.963	6040206.7	6814958	7733857	8693909	9733158	10745950	11870240
1500	11547772.01	11923910.6	12806435	13713841	15112018	1653128	17878620	19309610
1800	15399676.9	15759082.9	17145632	17854036	19401809	21246449	22731680	24397100
2000	19238389.2	19597090.7	20383766	21187060	22732391	24707989	2641720	28063380

Table 5 Continued

G3								
	Wsh =0	Wsh =50	Wsh =100	Wsh =150	Wsh =200	Wsh =250	Wsh =300	Wsh =350
Re	ΔP	ΔP	ΔP	ΔP	ΔP	ΔP	ΔP	ΔP
1000	1067548.37	1278330	1642526	2115101	2550875	3120314	3716227	4266440
2000	3586068.91	3859379.7	4390089	5045910	5762518	6649933	7548140	8552380
3000	7231726	7859460	8485326	9285435	10144409	11083564	12052680	13006010
3500	9551777.9	10662852.1	11239218	11981216	12931873	13946208	14832680	15380760
4900	19190262.1	19560006	20222271	21196067	22281806	23731754	25142440	25887520
G4								
	Wsh =0	Wsh =50	Wsh =100	Wsh =150	Wsh =200	Wsh =250	Wsh =300	Wsh =350
Re	ΔP	ΔP	ΔP	ΔP	ΔP	ΔP	ΔP	ΔP
1000	149714.04	212518.4	372889	602588	895417	1239946	1670890	2190520
2000	531987.14	606639.4	800710	1086246	1422267	1813900	2300910	2867710
5000	2813623.2	3007869.1	3294635	3736807	4201751	4755694	5424090	6162240
10000	10322883	11321274.4	11636887.92	12125717	12801673	13514839	14553730	15443910
14000	2040130.6	21984314	22338780	22819598.2	23477846	24296908	26123339	25677100
G5								
	Wsh =0	Wsh =50	Wsh =100	Wsh =150	Wsh =200	Wsh =250	Wsh =300	Wsh =350
Re	ΔP	ΔP	ΔP	ΔP	ΔP	ΔP	ΔP	ΔP
1000	113718.33	202433.1	378622	577284	819587	1134888	1421010	1785780
2000	385179.69	385179.69	748852	1034987	1448986	1906124	2382180	2917310
5000	2113861.2	2281640.5	2618579	3070863	3588857	4218097	4899893	5736030
10000	5892013	6393635	6912497.4	7491713	8230844	8999607	9777426	10643970
16500	20960605	21063671	21692339	22466386	23437916	24376233	25322270	26468320

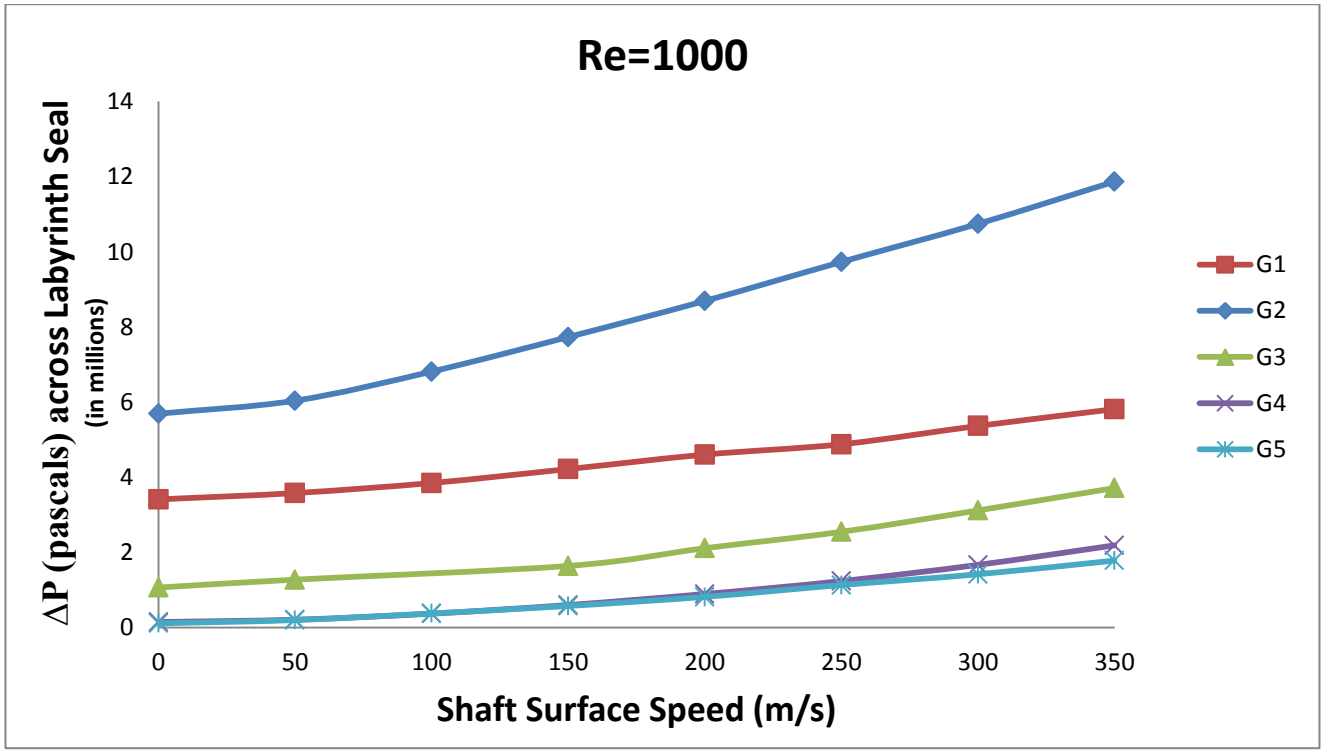

Fig A.11 Variation of pressure ratio across seal

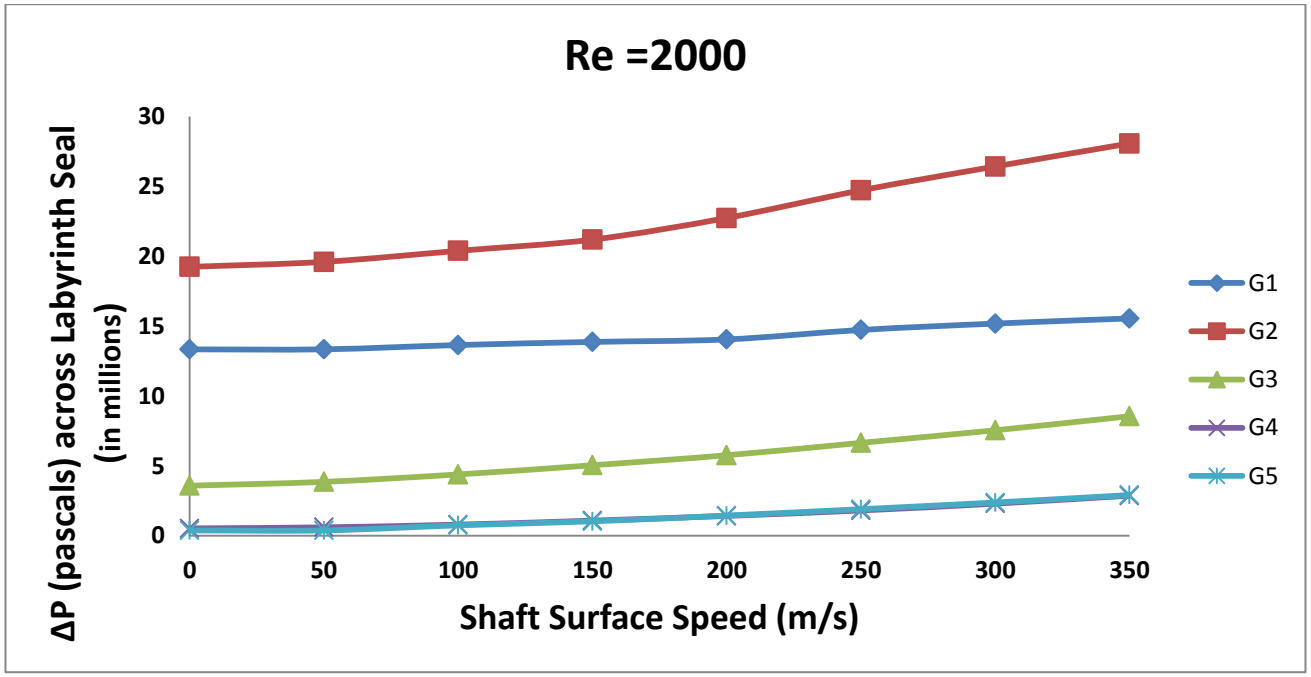

Fig A.12 Variation of pressure ratio across seal

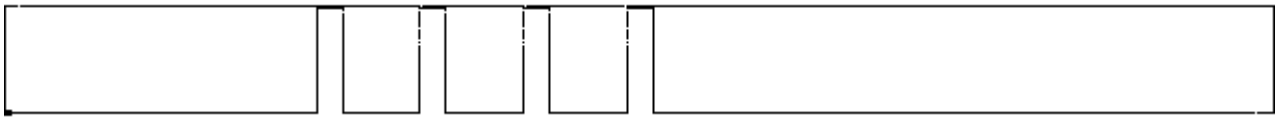

Fig A.13 Large teeth geometry

Fig A.14 Small teeth geometry

The above Figure (A.13 & A.14) shows the variation pressure ratios across different geometries for same Reynolds number/ mass flow rate. We could conclude from the Figure 12.1 that seals with small clearances and larger tooth width (G2) are performing better than the seals with lesser clearance and lower tooth width (G1). Further to notify from Geometries G4 & G5 (same clearance different tooth width) we note that the effect of tooth width is diminishing with increasing clearance where throttling process is not so effective. Figure 12.2 also shows the same result with more diminishing effect of tooth width with Reynolds number increasing where the pressure difference is coinciding each other. Another aspect to be noted is that pressure difference is increasing with shaft speed and the slope of increment does not matter change much with increasing shaft surface speed.

VITA

Gaurav Chaudhary was born in Chitorgarh, India. He completed his high school at BVB's Vidyasharm School, Jaipur, India. In 2004 he entered Panjab University, Chandigarh, India. There, he completed his Bachelor Degree in mechanical engineering with Honors in 2008. In August he entered the graduate school at Texas A&M University and graduated August 2011.

Gaurav Chaudhary may be contacted through Texas A&M University's Department of Mechanical Engineering at the following address:

Texas A&M University

Department of Mechanical Engineering

C/O Dr. Gerald Morrison

3123 TAMU

College Station, TX 77843 – 3123

USA.

Email address: gauravmeel@gmail.com